NASA CR-121242
PWA-4692

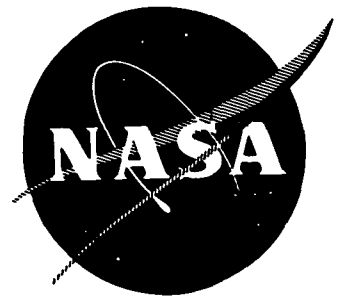

STUDY OF UNCONVENTIONAL PROPULSION SYSTEM CONCEPTS FOR USE IN A LONG RANGE TRANSPORT

by

G. A. Champagne

PRATT & WHITNEY AIRCRAFT
DIVISION OF
UNITED AIRCRAFT CORPORATION

prepared for

NATIONAL AERONAUTICS AND SPACE ADMINISTRATION

NASA Lewis Research Center
Contract NAS3-15550

Robert J. Antl, Project Manager

NOTICE

This report was prepared as an account of Government-sponsored work. Neither the United States, nor the National Aeronautics and Space Administration (NASA), nor any person acting on behalf of NASA:

A.) Makes any warranty or representation, expressed or implied, with respect to the accuracy, completeness, or usefulness of the information contained in this report, or that the use of any information, apparatus, method, or process disclosed in this report may not infringe privately-owned rights; or

B.) Assumes any liabilities with respect to the use of, or for damages resulting from the use of, any information, apparatus, method or process disclosed in this report.

As used above, "person acting on behalf of NASA" includes any employee or contractor of NASA, or employee of such contractor, to the extent that such employee or contractor of NASA or employee of such contractor prepares, disseminates, or provides access to any information pursuant to his employment or contract with NASA, or his employment with such contractor.

Requests for copies of this report should be referred to

National Aeronautics and Space Administration
Scientific and Technical Information Facility
P.O. Box 33
College Park, Md. 20740

1. Report No.	2. Government Accession No.	3. Recipient's Catalog No.
NASA-CR-121242		

4. Title and Subtitle	5. Report Date
Study of Unconventional Propulsion System Concepts for use in a Long Range Transport – Exhibit A, Part II, Task I Final	August, 1973
	6. Performing Organization Code
7. Author(s)	8. Performing Organization Report No.
George A. Champagne	PWA-4692
	10. Work Unit No.
9. Performing Organization Name and Address	
Pratt & Whitney Aircraft Division of United Aircraft Corporation East Hartford, Conn. 06108	11. Contract or Grant No. NAS3-15550
	13. Type of Report and Period Covered
12. Sponsoring Agency Name and Address	Contractor Report
National Aeronautics and Space Administration Washington, D. C. 20546	14. Sponsoring Agency Code

15. Supplementary Notes

Project Manager, Robert J. Antl, V/STOL and Noise Division, NASA – Lewis Research Center, Cleveland, Ohio

16. Abstract

An investigation of unconventional propulsion system concepts for the next generation of subsonic (0.9 Mn) long-range transport aircraft indicates that a noise level of FAR Part 36 minus 20 ePNdB can be achieved by either a fixed geometry, high bypass ratio turbofan with a geared two-stage fan and advanced acoustic treatment; or a moderate bypass ratio turbofan with a variable pitch two-stage fan, variable primary and duct nozzles and advanced acoustic treatment. The geared fan system meets the noise goal with minimum economic penalty. Comparison of the noise footprint areas at take-off and landing in combination with the economic penalties required to achieve lower noise levels at specific noise measuring stations, indicate that both footprint area reduction and current certification procedures should be used to ascertain the point of diminishing returns in establishing future noise goals.

17. Key Words (Suggested by Author(s))	18. Distribution Statement
Variable Geometry Engine Geared Fan Subsonic Aircraft Noise	Unclassified - limited

19. Security Classif. (of this report)	20. Security Classif. (of this page)	21. No. of Pages	22. Price*
Unclassified	Unclassified	104	$3.00

* For sale by the National Technical Information Service, Springfield, Virginia 22151

FOREWORD

The work described herein, which was conducted by the Pratt & Whitney Aircraft Division of United Aircraft Corporation, was performed under NASA Project Manager, Mr. Robert J. Antl, V/STOL and Noise Division, NASA-Lewis Research Center. This report was prepared by G. A. Champagne, with contributions from R. A. Howlett, J. P. Lewis and W. W. Ferguson, under the direction of G. L. Brines, the Pratt & Whitney Aircraft Program Manager.

The provisions of NASA Policy Directive (NPD) 2220.4, dated May 15, 1970, subject: Use of International System of Units (SI) in NASA Publications, have been waived under authority of subparagraph 5.5, NPD 2220.4.

TABLE OF CONTENTS

LIST OF ILLUSTRATIONS

LIST OF ILLUSTRATIONS (Cont'd)

LIST OF ILLUSTRATIONS (Cont'd)

SUMMARY

The primary objective of this study was to investigate concepts other than conventional, fixed-geometry, two-spool turbofans in order to identify the more promising propulsion systems for future subsonic (0.9 M_n) commercial transport aircraft, which might be required to achieve a noise level of FAR Part 36 minus 20 ePNdB.

The concepts evaluated included variable-geometry engines which incorporate variable fan, compressor, turbine and nozzle geometry, plus other concepts such as geared-fan and aft-fan systems. In addition, preliminary design studies were conducted to determine the trades between choked inlets and inlet acoustic rings, internal and external engine accessories and cascade- and umbrella-type reversers.

The results of this study, which was conducted for a 40,000 lb (18,200 Kg) payload - 3000 n. mi. (5550 km) - 0.9 Mn aircraft, indicate that the following two approaches can be used to achieve the FAR minus 20 noise goal:

- *Fixed geometry, high (10) bypass ratio cycle with a geared two-stage fan and advanced acoustic treatment.*

- *Variable geometry, moderate (6.5) bypass ratio cycle with variable pitch two-stage fan, variable primary and duct nozzles and advanced acoustic treatment.*

The geared fan system meets this noise goal with minimum economic penalty. The delta percent change in return on investment (ROI) for a Mach 0.9 aircraft powered by this FAR minus 20 propulsion system is 5 percent lower than that of a Mach 0.9 aircraft powered by an engine which just meets FAR Part 36 noise levels, and 2 percent lower than a FAR minus 15 ePNdB design. This means that if the ROI for the FAR 36 design aircraft is 25 percent, then the FAR minus 20 design would have an ROI of 20 percent. Even one percent reduction in ROI represents a significant economic penalty to the airline.

The variable geometry engine has a higher specific fuel consumption and requires more acoustic treatment than the fixed-geometry geared fan system. This results in an ROI for the variable geometry cycle which is 2 percent lower than that for the geared fan system.

In addition to evaluating the FAR-20 ePNdB concepts, noise and economic studies were conducted with the baseline fixed-geometry STF433 engine (6.5 bypass ratio) design from the original ATT study (NAS3-15550). This permitted a direct comparison, on a consistent technology basis, of the impact of reduced noise goals on both the economic worth and on the community noise exposure for the various concepts evaluated. Summarized below are the significant cycle parameters for the baseline fixed-geometry STF433, variable-geometry version (STF433 VG) and the geared-fan STF456.

	STF433	STF433 VG	STF456
Variable Geometry	No	Yes	No
Geared Fan	No	No	Yes
No. of Fan Stages	2	2	2
Cruise (36,000 ft (10970 m) - Mach 0.9)			
• Bypass Ratio	6.45	6.45	9.9
• Relative Installed TSFC,%	Base	+1.2	−6.3
Max Power Take-Off			
• Bypass Ratio	6.8	8.3	10.6
• Fan Pressure Ratio	1.78	1.64	1.49
• Fan Tip Speed, ft/sec (m/sec)	1120 (341)	1120 (341)	920 (280)
• Total ePNL, treated, α FAR	−14	−19.5	−20

Take-off and approach noise footprints were calculated for the fixed-geometry STF433 propulsion system with various amounts of acoustic treatment added to produce noise levels of FAR, FAR-9 and FAR-15 ePNdB. The FAR-9 system, which utilizes acoustic wall treatment only on an extended inlet and fan exit duct, reduces noise footprint areas to about 25 percent of those achieved with an untreated propulsion system which meets FAR Part 36 noise requirements. This is achieved at the expense of a delta ROI penalty of 1 percent. This wall-treatment-only configuration meets the presently-predicted airframe generated noise floor of FAR minus 8 ePNdB.

The FAR-15 system, which utilizes two inlet rings and a duct splitter in addition to wall treatment, further reduces the footprint areas to 10 percent of the untreated system levels, but at the expense of a delta ROI penalty of 3 percent. The FAR-20 propulsion systems previously described reduce the footprint area to 5 percent of the untreated levels, but produce delta ROI penalties of 5 percent (geared fan) and 7 percent (variable geometry). These results indicate that to achieve noise goals below about FAR-10 ePNdB, severe economic penalties must be paid for relatively small reductions in footprint area. Noise goals should be established to reflect both the footprint area reductions and the absolute noise level in order to provide a more meaningful target for future noise regulations.

Results of the preliminary design study indicated that a nacelle with a choked inlet would provide a significant improvement in ROI over a nacelle incorporating two long inlet rings plus wall treatment. A choked inlet can provide significant improvements in inlet performance and further evaluations of the choked inlet are recommended to determine the weight, cost, complexity, maintainability and reliability of the variable geometry choked inlet and the impact of the inlet support struts on fan generated, aft-propagated noise.

During the landing approach, the propulsion system is operating at low power and low inlet corrected airflow levels. Therefore, to achieve a choked inlet, either the inlet throat area must be reduced or the engine nozzles opened to allow the engine to swallow more airflow. Studies should be conducted to determine the relative amounts of variable inlet and nozzle geometry that are required to produce the best system.

INTRODUCTION

NASA is currently studying the application of advanced technologies to long-range commercial jet transport aircraft. This is being done to assure that future transport aircraft will be responsive to national needs, and that the required technology will be available for application to commercial service.

Under the original NASA Lewis Research Center contract NAS3-15550, Pratt & Whitney Aircraft performed extensive parametric engine cycle studies (ref. 1) to determine the best conventional twin-spool fixed-geometry propulsion system for an advanced technology transport planned for a commercial operation certification date of 1985. This system was designed to meet a noise goal of FAR Part 36 minus 15 ePNdB. The engine cycle selected was a twin-spool turbofan with a low tip speed, widely spaced, two-stage fan that provides both low noise and optimum cycle performance.

It is now appropriate to consider whether extensive use of variable geometry will offer the potential of further noise reductions, or alternatively, whether other cycle concepts may offer a more attractive solution to the requirement for a viable, low noise commercial transport engine for the 1980's.

This report describes propulsion system studies performed under modification 1 of Contract NAS3-15550 with the direction of the Lewis Research Center to support this objective. These studies included:

- Propulsion studies to evaluate concepts other than conventional fixed-geometry, two spool turbofans in order to identify the cycles with the most potential to achieve a noise goal of FAR Part 36 minus 20 ePNdB.

- Aircraft economic studies for the most promising cycles to determine the trades of engine performance, weight, drag and price on the overall system Direct Operating Cost (DOC) and Return on Investment (ROI) of a 40,000 lb. (18,200 Kg) payload - 3000 n. mi (5550 km) - 0.9 Mn aircraft.

CYCLE STUDIES

OBJECTIVE

In Reference 1, studies were conducted to define the optimum fixed-geometry cycle capable of meeting a FAR Part 36 minus 15 ePNdB noise goal for a 1985 certification date, Mach 0.95 aircraft. The resulting cycle, the STF433, was used as the base for the present variable geometry study. Noise estimates for the STF433, presented in Figure 1, show that an average treated noise level of FAR-15 can be attained with extensive wall treatment, two inlet rings and one aft duct acoustic splitter.

The main goals of the study reported herein were to achieve a FAR-20 noise level by reducing the STF433 fan-generated and jet noise by 5 ePNdB at the take-off, 0.25 n. mi. (460 m) sideline, and 3.5 n.mi. (6480 m) cutback conditions and by reducing the approach fan noise by about 3 ePNdB, while maintaining the same amount of acoustic treatment as used in the Reference 1, FAR-15 ePNdB propulsion system.

The aircraft model for this study is a three engine (two on wing, one in tail), Mach 0.9 aircraft with a payload of 40,000 lbs. (18,200 kg) and a range of 3000 n. mi. (5500 km). FAR Part 36 noise requirements for this nominal 300,000 lb. (136100 kg) TOGW aircraft are 106 ePNdB at sideline and approach, and 103 ePNdB at cutback.

The effects of variable fan, turbine and nozzle geometry on the principal noise parameters, i.e., fan pressure ratio, fan tip speed and jet velocities, were individually examined to determine the most effective method to reduce fan and jet noise. The most effective variable geometry components were then incorporated into the STF433 to produce the STF433 VG cycle. Table I summarizes the significant cycle parameters for the baseline fixed-geometry STF433 and the variable-geometry version STF433 VG.

TABLE I
ENGINE CYCLE COMPARISON

	STF433	STF433 VG
Variable Geometry	No	Yes
Geared Fan	No	No
No. of Fan Stages	2	2
Cruise (36,000 ft (10970 m) - Mach 0.9)		
• Bypass Ratio	6.45	6.45
• Relative Installed TSFC,%	Base	+1.2
Max Power Take-Off		
• Bypass Ratio	6.8	8.3
• Fan Pressure Ratio	1.78	1.64
• Fan Tip Speed, ft/sec (m/sec)	1120 (341)	1120 (341)
• Total ePNL, treated, α FAR	−14	−19.5

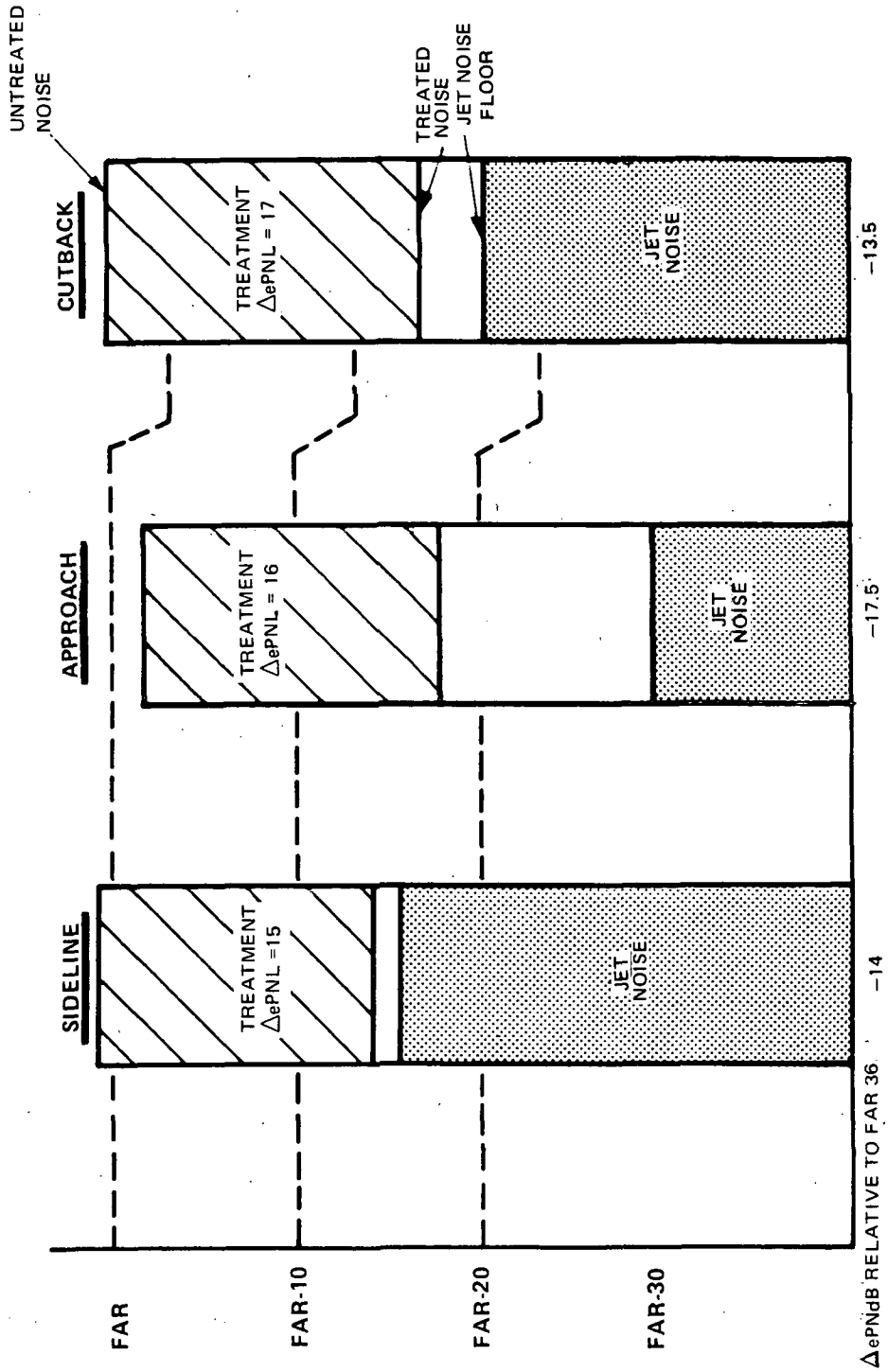

Figure 1 Fixed Geometry STF 433 Noise Levels (FAR-15 Nacelle)

Figures 2, 3, and 4 present a contrast in nacelle configurations required to achieve noise levels from FAR Part 36 down to 20 ePNdB below FAR 36. Figure 2 illustrates an aerodynamically optimum nacelle designed for Mach 0.9 cruise with the fixed-geometry STF433 engine installed. This combination would essentially meet FAR Part 36 noise levels. Figure 3 shows a comparison of the FAR 36 nacelle in the upper portion of the drawing to the nacelle changes necessary to achieve FAR 36 -15 ePNdB with the fixed-geometry STF433. Removing the two inlet rings and fan duct splitter from the long nacelle configuration, but retaining the extensive wall treatment, results in a noise level of FAR 36 -9 ePNdB. Figure 4 presents the dramatic nacelle changes required to achieve FAR 36 -20 ePNdB with the variable geometry STF433 that incorporates variable primary and fan duct nozzles in combination with a variable pitch fan.

FIXED GEOMETRY STF433 CYCLE DESCRIPTION

Subsonic cruise and take-off cycle characteristics and uninstalled (no acoustic treatment) performance characteristics for the two-stage fan STF433 engine are presented in Table II. This engine is sized to produce an uninstalled Sea Level take-off thrust of 31,000 lbs. (138,000N).

TABLE II
STF433 PERFORMANCE SUMMARY

Altitude, ft (m)	38000(11580)	36000(10970)	0
Mach Number	0.95	0.90	0
Bypass Ratio	6.5	6.42	6.7
Cycle Pressure Ratio	25	24.8	22.0
Fan Pressure Ratio	1.95	1.94	1.79
Number of Fan Stages	2	2	2
Fan Tip Speed, ft/sec (m/sec)	1210(369)	1150(351)	1120(341)
Corrected Airflow, lbm/sec (kg/sec)	1006(456)	1021(463)	937(425)
Net Thrust, lbf (N)	6960(30960)	7680(34160)	30920(137500)
TSFC, lbm/hr - lbf (g/sec-N)	0.683(0.0193)	0.664(0.0188)	0.380(0.0108)

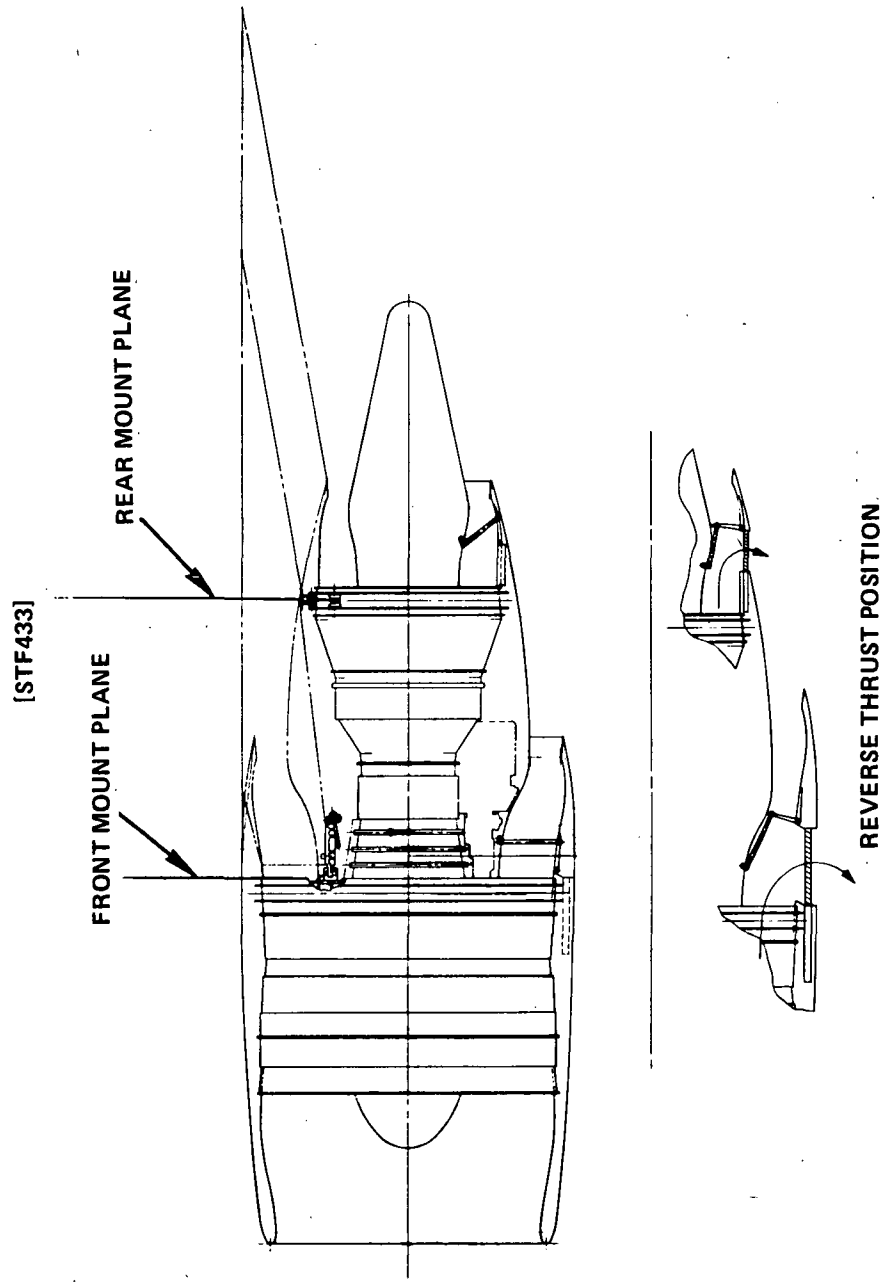

Figure 2 Aerodynamically Optimum Nacelle

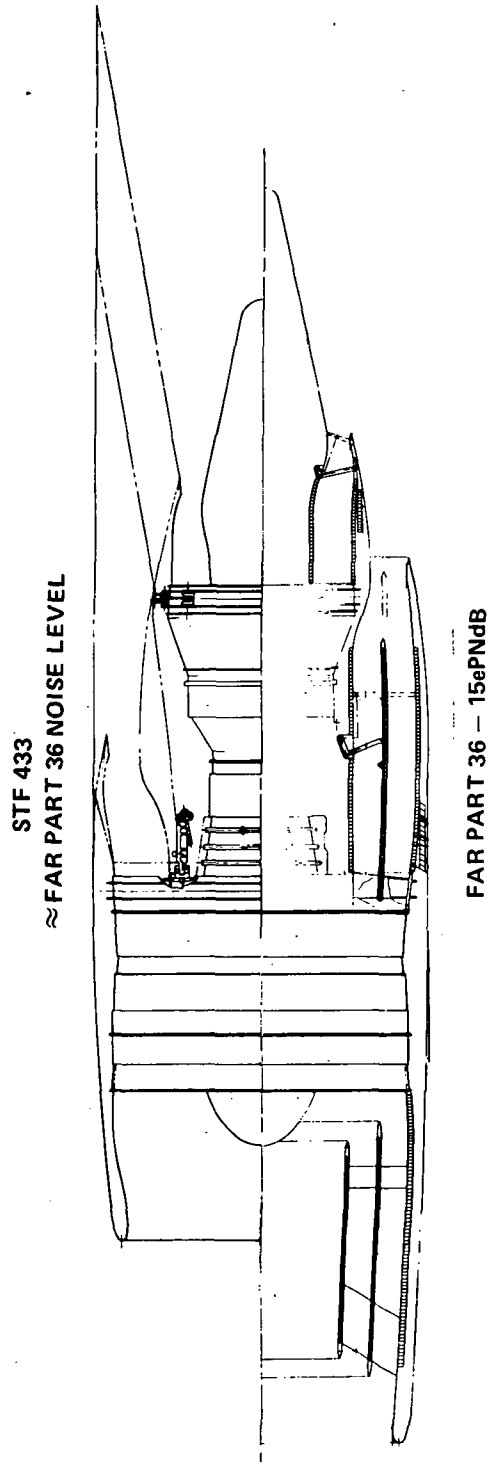

Figure 3 Nacelle Comparison ~ Mach 0.9 Design

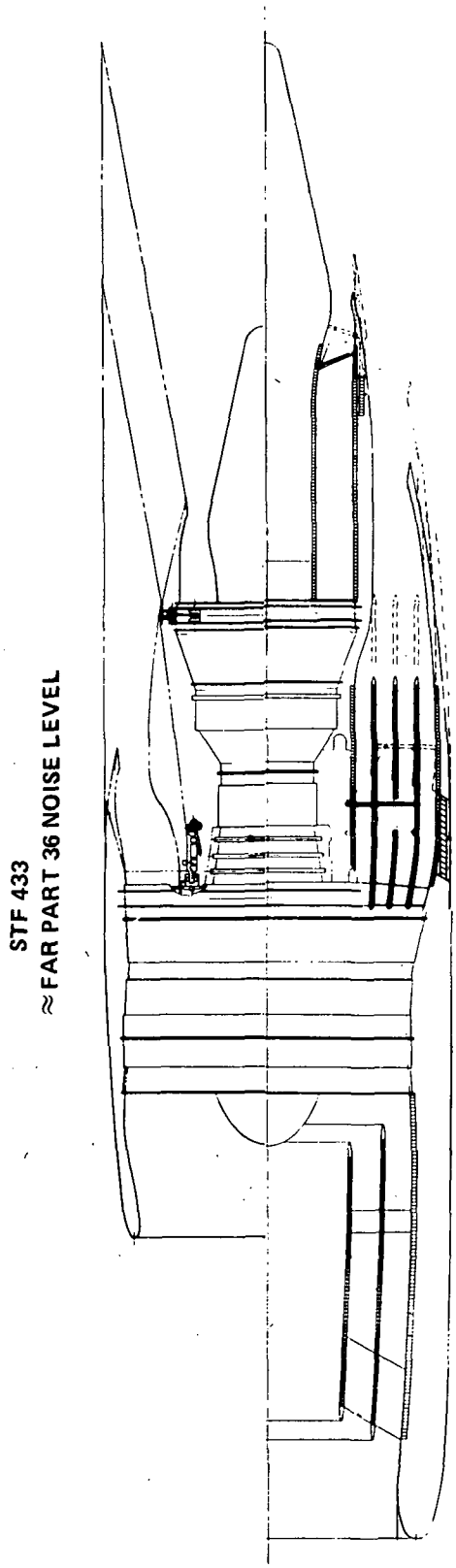

Figure 4 *Nacelle Comparison ~ Mach 0.9 Design*

FIXED GEOMETRY ENGINE NACELLE STUDY

Engine untreated and treated noise levels were calculated for the fixed-geometry STF433 for three nacelle designs:

- Aerodynamically optimum nacelle - no acoustic treatment.
- Nacelle designed to accommodate treatment required to achieve FAR-15 noise - wall treatment plus 2 inlet rings and 1 aft duct splitter.
- Nacelle designed to accommodate FAR-15 acoustic treatment but with inlet rings and aft splitter removed. This configuration produces an average noise level of FAR-9 ePNdB.

Figures 5 through 7 provide detailed outlines of these nacelles, while Table III presents a summary of the engine noise, nacelle weight and dimensions for these three cases. Noise estimates are shown at the take-off 0.25 n.mi. (460 m) sideline, 3.5 n.mi. (6480 m) cutback and 1 n.mi. (1850 m) approach noise reference stations for 3 engines. At the 3.5 n.mi. measuring station, thrust is reduced to 85% of maximum power. Power reduction at this point produces a 1.5 ePNdB reduction in noise relative to full power operation. Engine and nacelle weights and dimensions are single propulsion system values.

TABLE III
FIXED GEOMETRY STF433 SUMMARY

Wall Treatment	No	Yes	Yes
Inlet Rings	No	2	No
Aft Duct Splitter	No	1	No
Sideline Noise α FAR, ΔePNdB	+1	−14.0	−10.0
Cutback Noise α FAR, ΔePNdB	+3	−13.5	−7.5
Approach Noise α FAR, ΔePNdB	−2	−17.5	−10.0
Uninstalled SLTO Thrust, lbf (N)	28440(126500)	31790(141400)	29390(130700)
Bare Engine Weight, lbm(kg)	4770(2170)	5430(2460)	4960(2250)
Nacelle Weight, lbm(kg)	630(287)	1226(556)	1126(511)
Treatment Weight, lbm(kg)	0	915(415)	333(151)
Max. Nacelle Diameter, in(m)	78.6(2.0)	83.1(2.11)	79.9(2.03)
Max. Nacelle Length, in(m)	225(5.71)	315(8.01)	304(7.72)

Table III shows that the untreated STF433 essentially achieves an average noise level required by FAR Part 36, while the wall-treated nacelle meets FAR minus 9 ePNdB. Recent airframe tests with the Boeing 727 and 747 aircraft indicate that the current airframe noise floor for aircraft of the size and type evaluated in this study is around FAR-8 ePNdB at approach.

Noise footprints for a three degree approach and take-off with power reduction at the 3.5 n.mi. (6480m) station are presented in Figures 8, 9 and 10 for the untreated, wall-treated (FAR-9) and fully-treated (FAR-15) propulsion systems.

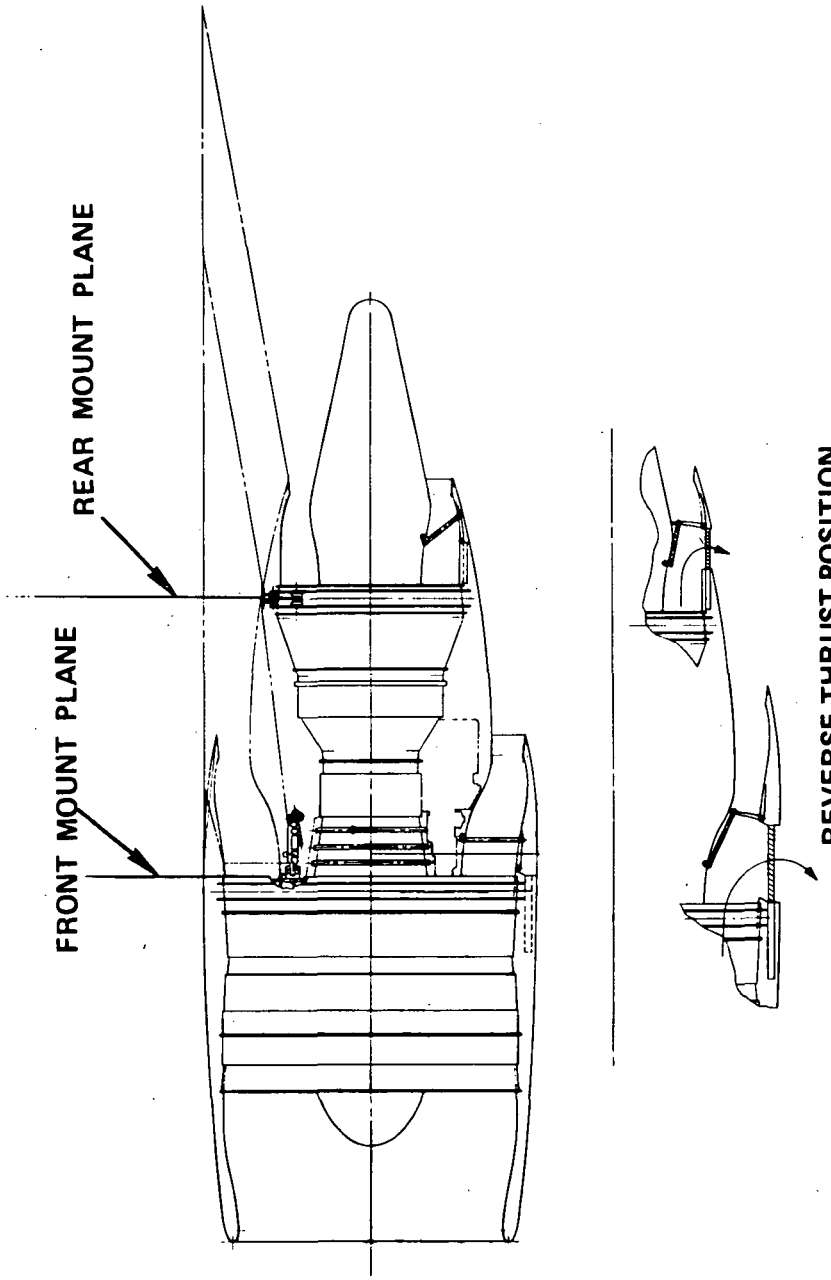

Figure 5 Aerodynamically Optimum Nacelle

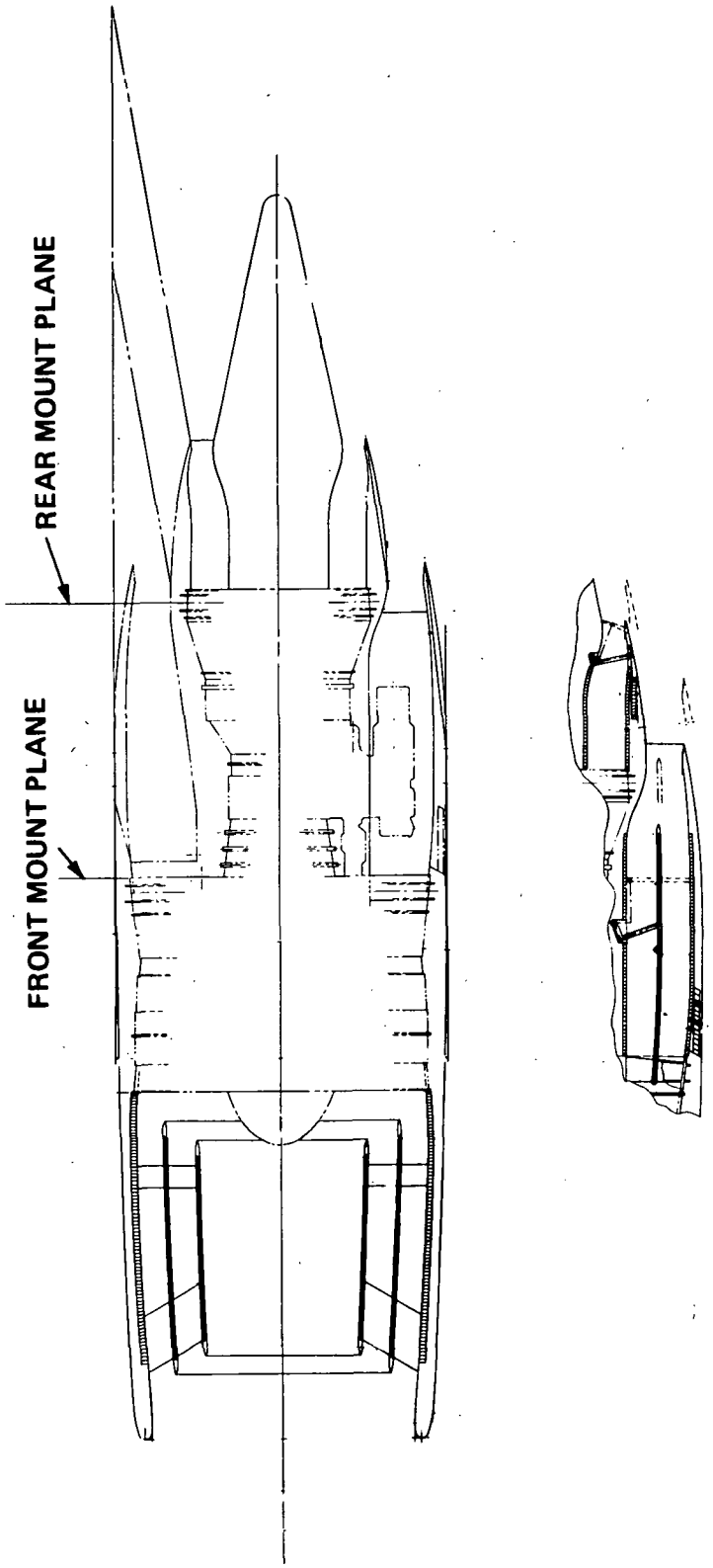

Figure 6 Acoustically Treated (FAR-15) Nacelle

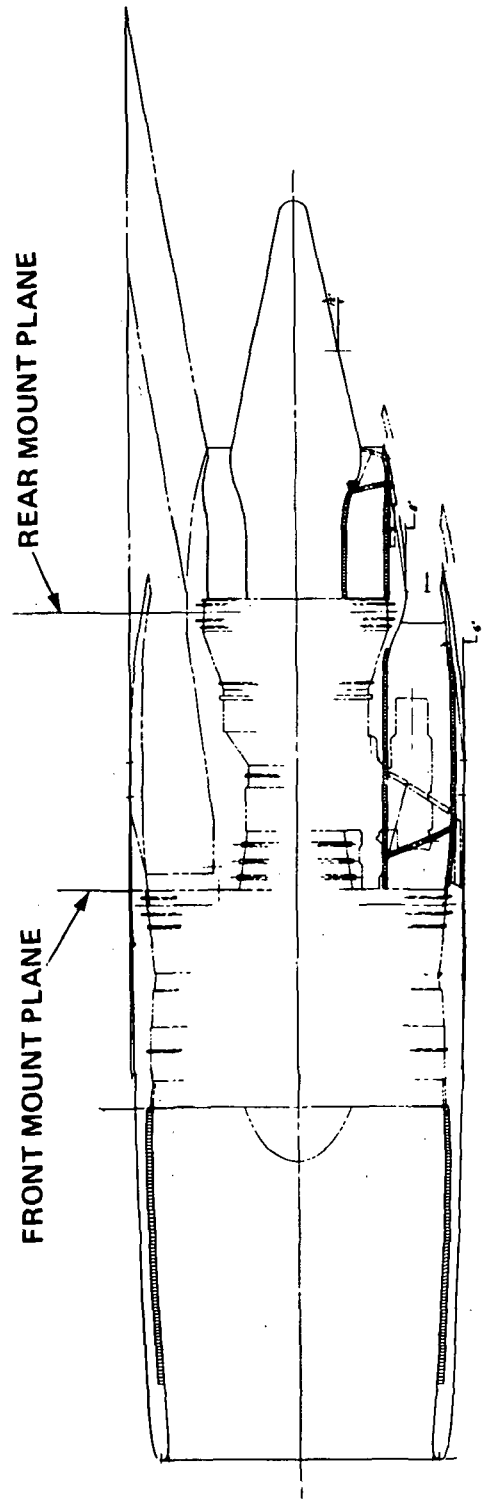

Figure 7 Acoustically Treated (FAR-9) Nacelle

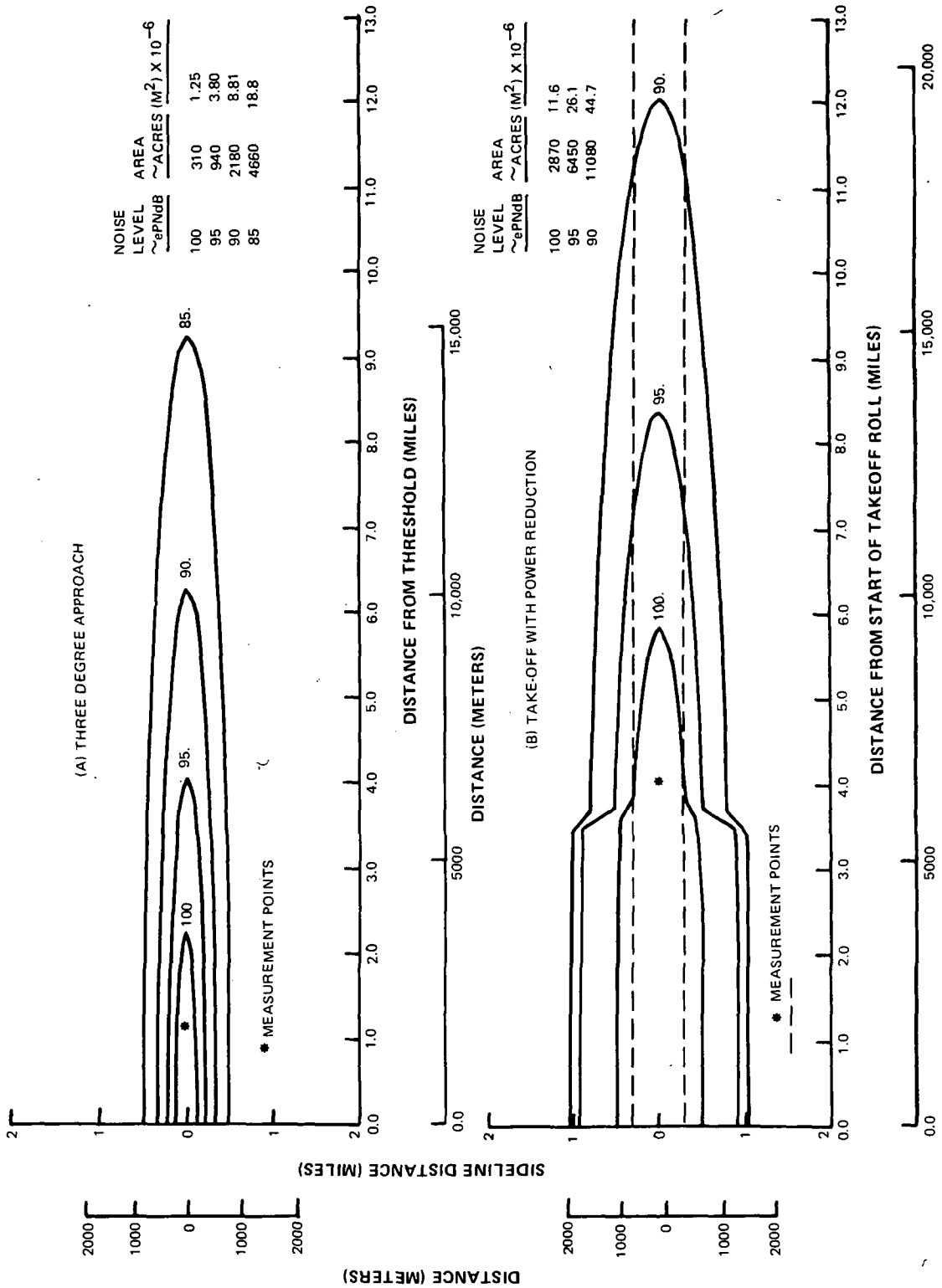

Figure 8 Noise Footprints ~ Aerodynamically Optimum Nacelle

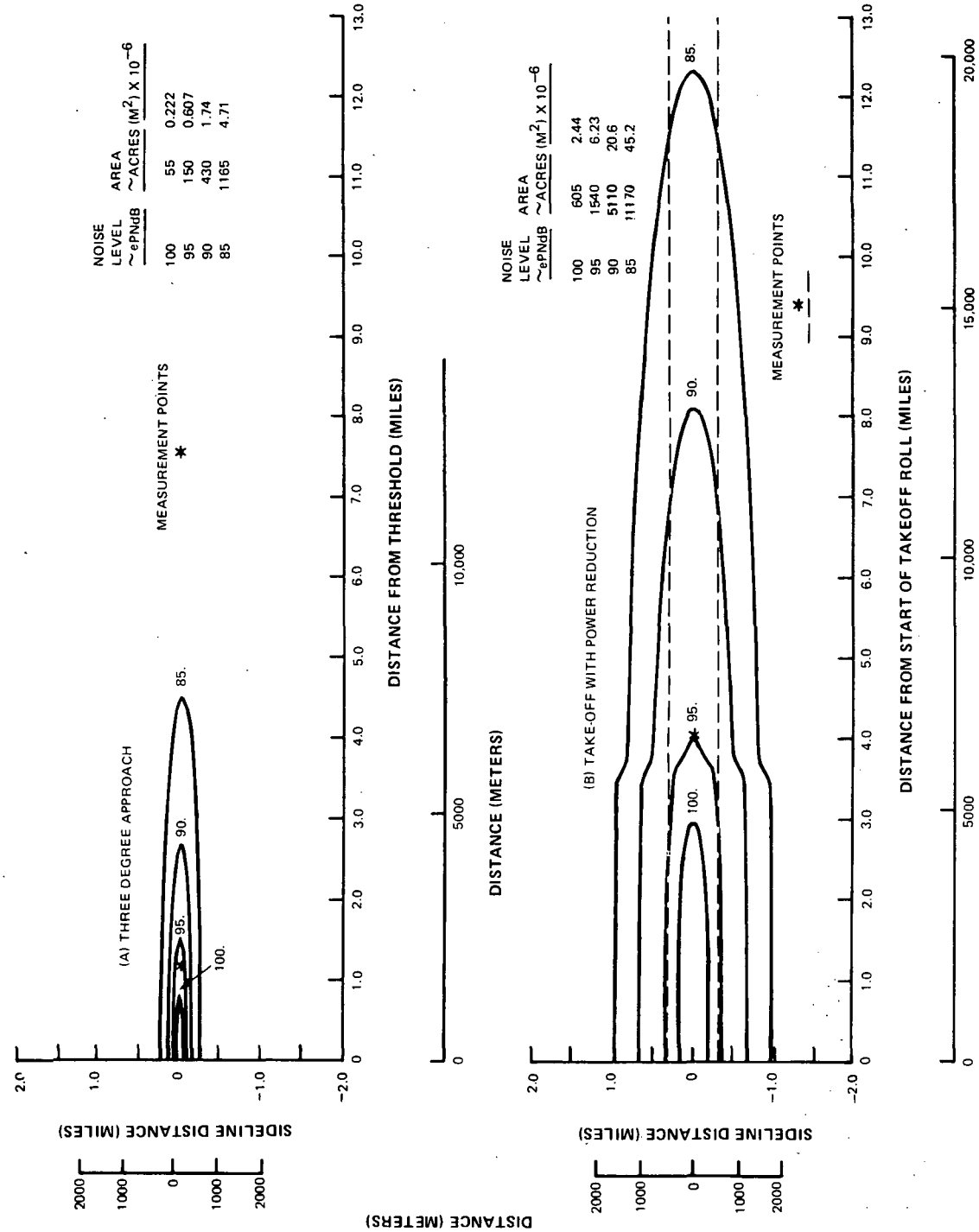

Figure 9 Noise Footprints ~ FAR-9 Nacelle

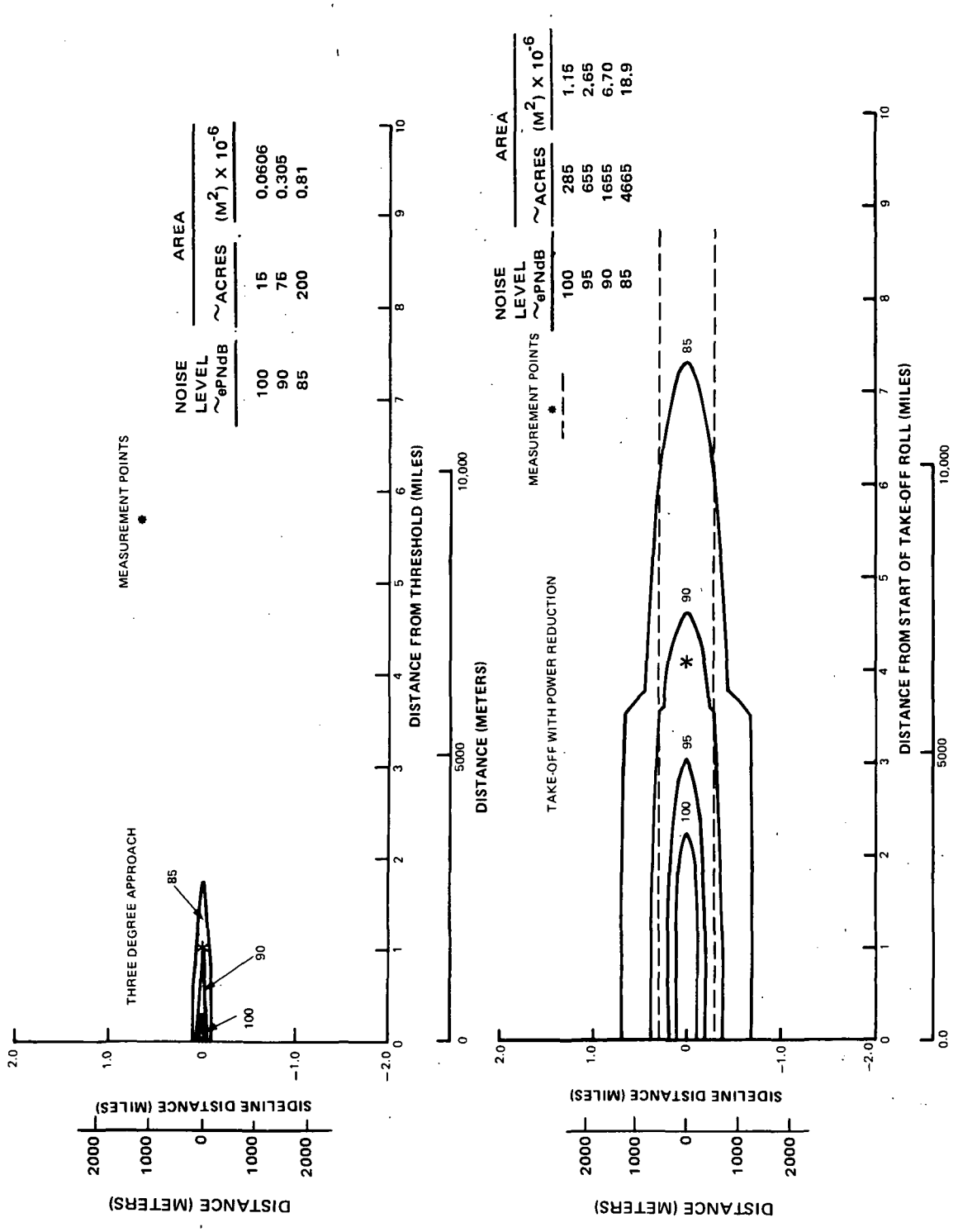

Figure 10 Noise Footprints ~ FAR-15 Nacelle

VARIABLE TURBINE GEOMETRY

Variable high and low pressure turbine geometries were examined to determine the effects of varying these areas on the major engine parameters that affect fan and jet noise. Figure 11 presents a schematic which identifies various engine stations.

Changes in fan noise are directly proportional to changes in fan tip speed ($UT/\sqrt{\theta_{T2}}$) and pressure ratio (FPR), while jet noise changes are directly proportional to changes in jet velocity (VJP-primary, VJD-duct). Table IV lists the changes which occur in these parameters at sideline, cutback and approach for both reductions and increases in turbine areas. For each of these turbine area variations, the STF433 combustor exit temperature (CET) is adjusted to maintain constant engine net thrust (Fn). Changes in total engine inlet corrected airflow (WA_{T2}) are also presented.

TABLE IV
EFFECT OF VARIABLE TURBINE GEOMETRY ON STF433 OPERATION
(Constant Thrust)

Flight Condition	Component	Area Change %	$\Delta(UT/\sqrt{\theta_{T2}})$ %	ΔFPR %	ΔVJP %	Δ VJD %	ΔCET °F (°C)	ΔWA_{T2} %
Sideline	High Turbine (A4)	−10	0	0	−2	0	−60(−33)	0
		+10	0	0	+3	0	+80(44)	0
Sideline	Low Turbine (A41)	−10	0	+1	−2	+1	+140*(78)	0
		+10	0	−1	+3	−1	−70(−39)	0
Cutback	High Turbine	−10	0	0	−2	0	−60(−33)	0
		+10	0	0	+3	0	+70(39)	0
Cutback	Low Turbine	−10	0	+1	−2	+1	+130(72)	0
		+10	0	−1	+3	−1	−80(−44)	0
Approach	High Turbine	−10	0	0	−5	0	−50(−28)	0
		+10	0	0	+1	0	+70(39)	0
Approach	Low Turbine	−10	0	0	−8	+1	+110(61)	0
		+10	0	0	+4	−1	−70(−39)	0

*Exceeds maximum temperature limit

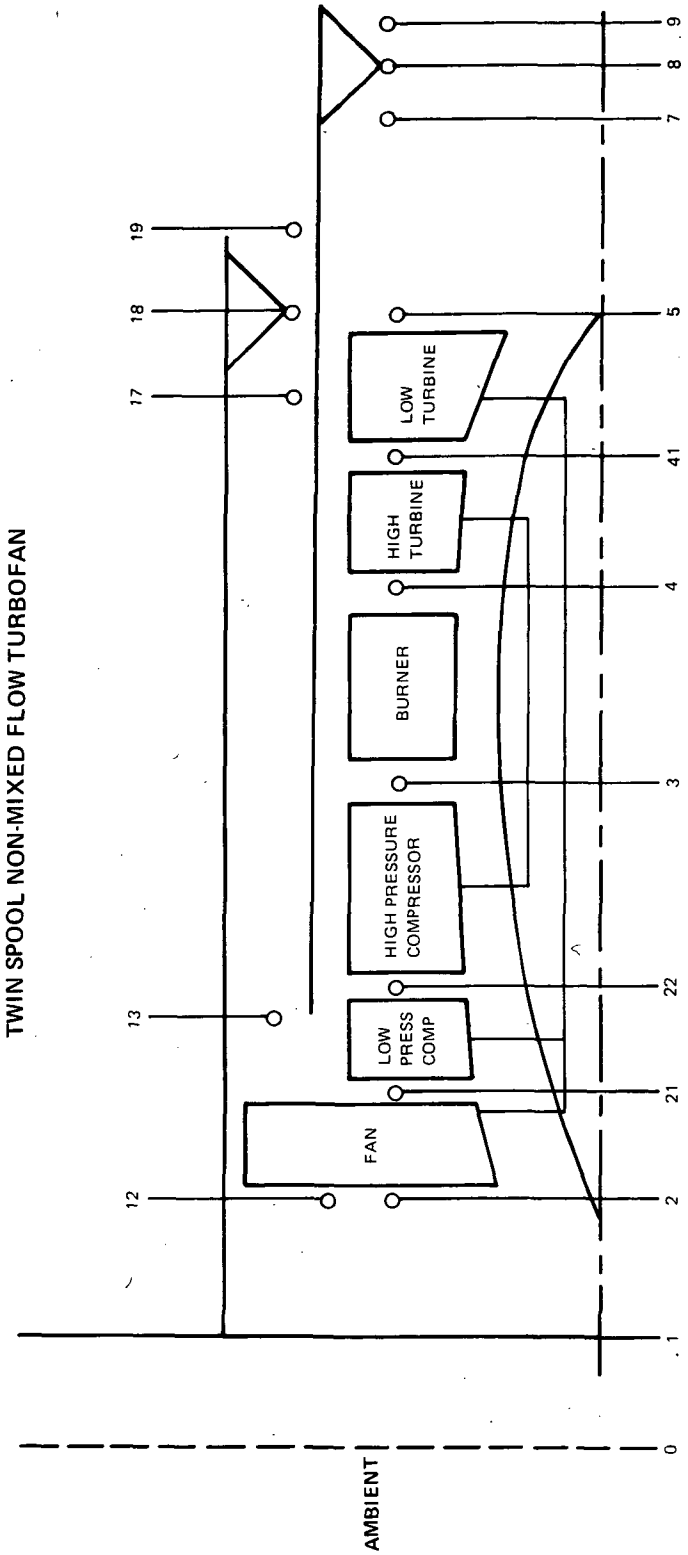

Figure 11 Station Identification Diagram

Table IV shows that variable high and low turbine geometry have a negligible effect on fan operation and fan noise at all three flight conditions. At the sideline and cutback conditions, reductions of 2 percent in primary stream jet velocity can be attained with a 10 percent reduction in high turbine area. This results in a reduction in primary jet noise of about 0.5 ePNdB. At the approach condition, variable turbine geometry provides larger changes in primary jet velocity due to operation at low power settings with an unchoked primary nozzle. However, this reduction in jet velocity is not important, since the jet noise at approach (Figure 1) is more than 30 ePNdB below FAR Part 36 requirements.

VARIABLE NOZZLE GEOMETRY

Variable geometry in the primary and duct nozzles was examined to determine effects on the critical noise parameters. Table V lists the changes which occur in these parameters for both increases and decreases in nozzle areas.

TABLE V

EFFECT OF VARIABLE NOZZLE GEOMETRY ON STF433 OPERATION
(Constant Thrust)

Flight Condition	Component	Area Change %	$\Delta(UT/\sqrt{\theta_{T2}})$ %	ΔFPR %	ΔVJP %	Δ VJD %	ΔCET °F (°C)	ΔWA_{T2} %
Sideline	Primary Nozzle (A8)	−10	−2	−2	+26	−3	+58(32)	−2
		+10	+1	+1	−8	+1	0	+0.5
Sideline	Duct Nozzle (A18)	−10	+1	+5	+7	+6	+85(47)	−6
		+10	+3	−4	+4	−5	+100(56)	+5
Cutback	Primary Nozzle Nozzle	−10	−2	−2	+28	−3	+44(24)	−2
		+10	+1	+1	−8	+1	0	+0.5
Cutback	Duct Nozzle	−10	+2	+4	+7	+7	+25(14)	−6
		+10	+4	−4	+2	−5	+65(36)	+5
Approach	Primary Nozzle	−10	−1	−1	+34	−2	+8(4)	−1
		+10	0	0	−12	0	+2(1)	0
Approach	Duct Nozzle	−10	+2	+2	+5	+7	+25(14)	−6
		+10	+2	−2	+3	−5	+30(17)	+6

Variable primary nozzle (A8) geometry can provide significant reductions in primary stream jet velocity. Opening the primary nozzle area increases the low turbine work output, which results in an increase in fan pressure ratio and reduction in both primary nozzle total pressure and temperature.

Variable duct nozzle (A18) geometry can provide significant reductions in fan pressure ratio and fan duct (VJD) jet velocity, thereby producing reductions in both fan noise and duct jet noise. However, as fan pressure ratio is reduced by increasing the duct nozzle area, the corresponding reduction in fan efficiency requires increases in combustor exit temperature (CET) to maintain constant engine thrust. This increase in combustor temperature also produces increases in primary stream jet velocity (VJP).

VARIABLE FAN GEOMETRY

Improvements in fan efficiency are desired to minimize the increases in combustor exit temperature and primary stream jet velocity which occur as fan pressure ratio is reduced. This can be accomplished by utilizing a variable geometry fan. In addition, variable fan geometry provides airflow increases at constant fan tip speed, thereby reducing fan-generated noise.

Figure 12 shows how the fan efficiency "islands" can be shifted to improve performance as the duct nozzle area is opened, and fan pressure ratio is reduced and airflow is increased.

Table VI shows the effects of variable fan geometry on sideline performance, as fan pressure is reduced 4 percent by opening the duct nozzle area.

TABLE VI

VARIABLE FAN GEOMETRY BENEFITS
(Net Thrust = Constant)

FAN	η_{Fan}	ΔA18 %	ΔA8 %	ΔFPR %	$\Delta(UT/\sqrt{\theta_{T2}})$ %	ΔWA_{T2} %	ΔVJD %	ΔVJP %	ΔCET °F(°C)
Fixed Geometry	0.75	+10	0	-4	+3	+5	-5	+4	+100(56)
Variable Geometry	0.82	+12	0	-4	0	+6	-6	0	+40(22)

Two types of variable fan geometry were examined: (1), variable camber stator inlet and exit guide vanes and (2), variable pitch fan blades.

The main advantage of variable stators is that the mechanical and structural system is less complex than that required to vary the pitch of the rotating blades. However, the variable stator approach would require adding an inlet guide vane assembly with the same extensive

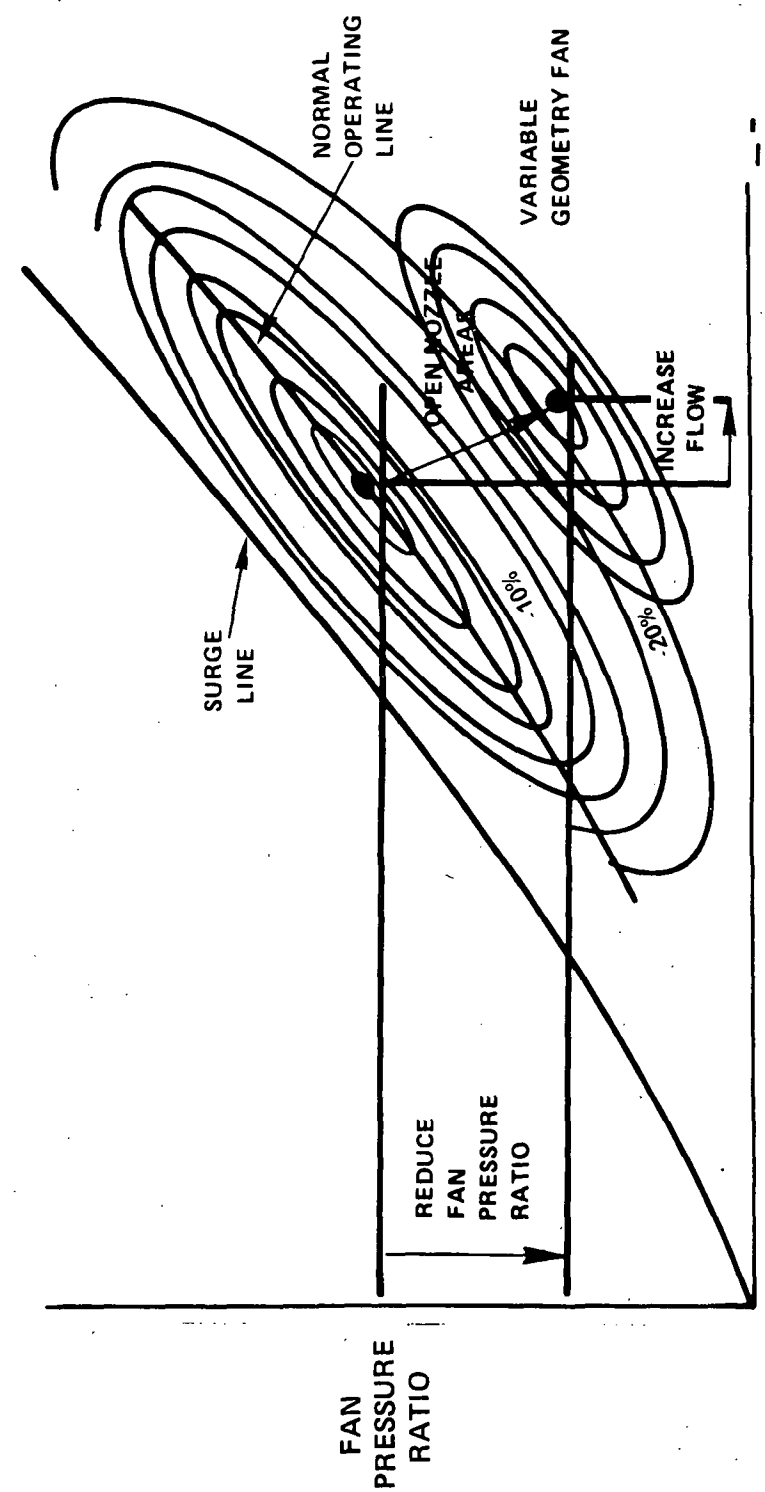

Figure 12 Effect of Variable Fan Geometry on Efficiency

axial spacing as provided between the other rows of fan airfoils. This would cause an increase in overall engine length. Variable pitch fan blades have the potential for higher efficiency gains. In addition, variable blades offer the potential for thrust reversing. For these reasons, the variable pitch fan approach was chosen for preliminary evaluation.

A conceptual drawing of the variable pitch fan arrangement is shown in Figure 13. The basic elements of this system are: the variable pitch actuator; a series of differential gears and bearings to transfer the pitch change signal from static to rotating structure; a pitch lock device to prevent the blades from feathering in the event of an actuation failure; a ring gear to rotate the entire blade assembly in unison; and individual retention bearings to enable each blade to rotate around its radial axis. The effect of this variable pitch fan system on the engine is a 10 to 20 percent improvement in fan efficiency at off-design operation, a 13 percent increase in weight and a 4 percent increase in price.

VARIABLE GEOMETRY ENGINE REQUIREMENTS

Since variable fan and nozzle geometry can produce significant reductions in fan pressure ratio and jet velocities, various combinations of variable fan and nozzle geometries were examined to define the variable geometry required to achieve the goals of reducing sideline and cutback fan and jet noise by 5 ePNdB and approach fan noise by 2.5 ePNdB.

SIDELINE

At the sideline condition, the fixed geometry STF433 described in Table III is operating at an uninstalled net thrust of 24,200 lbs (107,000N) with a fan pressure ratio (FPR) of 1.78, and inlet corrected airflow (WA_{T2}) of 932 lbs/sec. (422Kg/sec), a fan efficiency of 0.88, a combustor exit temperature (CET) which is 100°F (56°C) below the maximum allowable CET, and jet velocities which produce a total jet PNL of 92 PNdB (90 ePNdB).

In order to reduce the treated noise of the STF433 to FAR Part 36 minus 20 ePNdB, the total jet noise must be reduced to a total jet PNL of 87 PNdB (85 ePNdB). To achieve this jet noise level, the sideline fan pressure ratio must be reduced to 1.64. In order to reduce the fan source noise by 5 ePNdB, the fan pressure ratio must be reduced to 1.55.

Figure 14 shows the combustor exit temperatures and fan efficiencies required to maintain constant sideline thrust as fan pressure ratio and inlet corrected airflow are varied. For the STF433 fixed geometry fan, which is shown by the dashed line, a FPR = 1.64 and WA_{T2} = 953 lb/sec (432 Kg/sec) can be achieved without exceeding the maximum CET. However, this results in a total jet noise of 103 PNdB, as shown in Figure 15.

Figure 15 presents the variation in sideline jet noise as airflow is varied for FPR = 1.64 and 1.55. These points represent operation at the maximum allowable combustor temperature. In order to meet the total jet noise goal of 87 PNdB, the airflow must be increased to 1065 lbs/sec (484 Kg/sec) for a fan pressure ratio of 1.64 and 1155 lb/sec (524 Kg/sec) for a fan pressure ratio of 1.55. At these airflows, Figure 14 shows that variable fan geometry must provide efficiencies of 80 (FPR = 1.64) and 86 (FPR = 1.55) percent in order to maintain the CET within its allowable limit. This represents a 20 point efficiency improvement at 1.64 FPR, and a 40-50 point efficiency improvement at the 1.55 FPR.

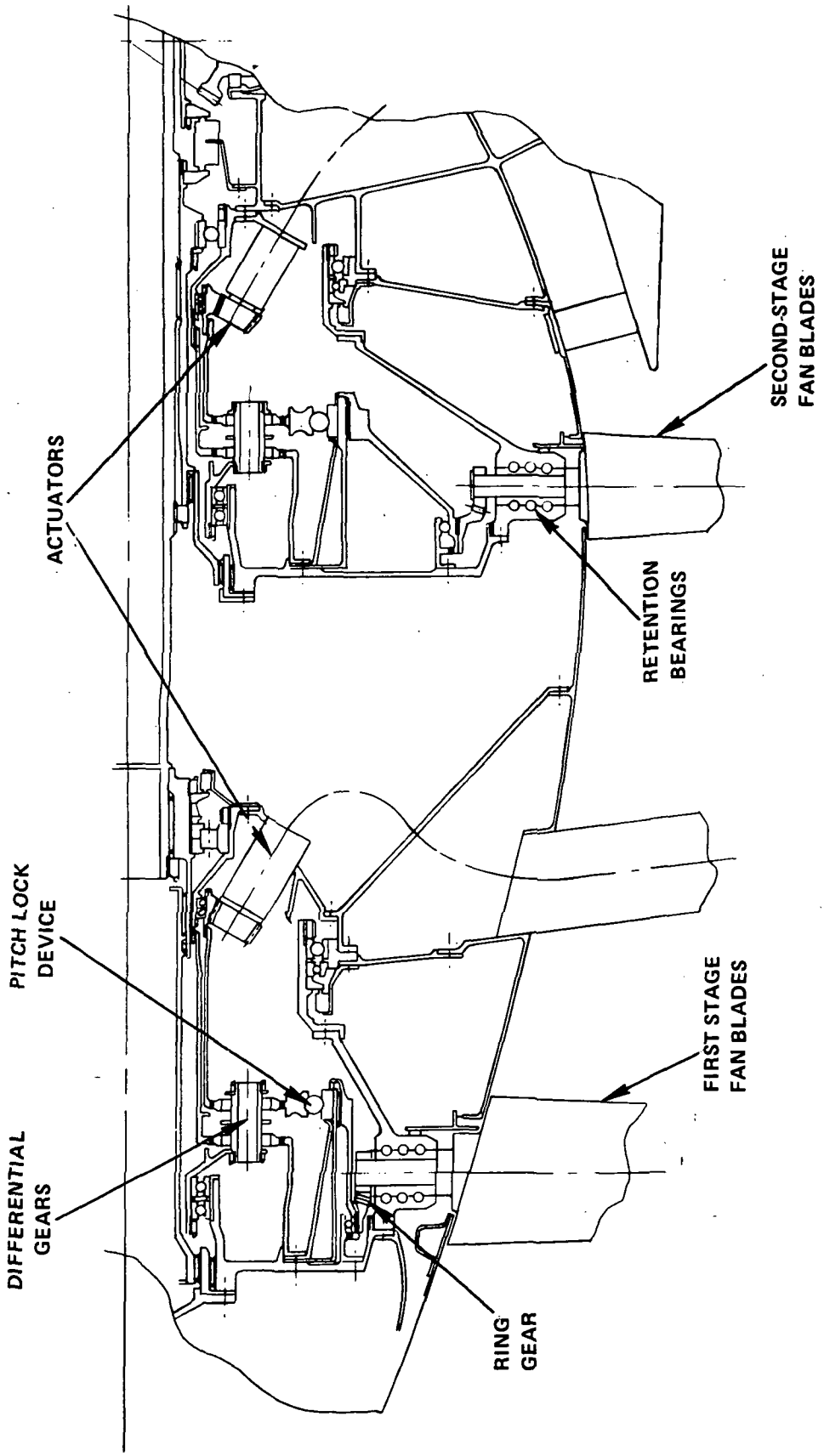

Figure 13 Conceptual Rendering of Variable Pitch Fan

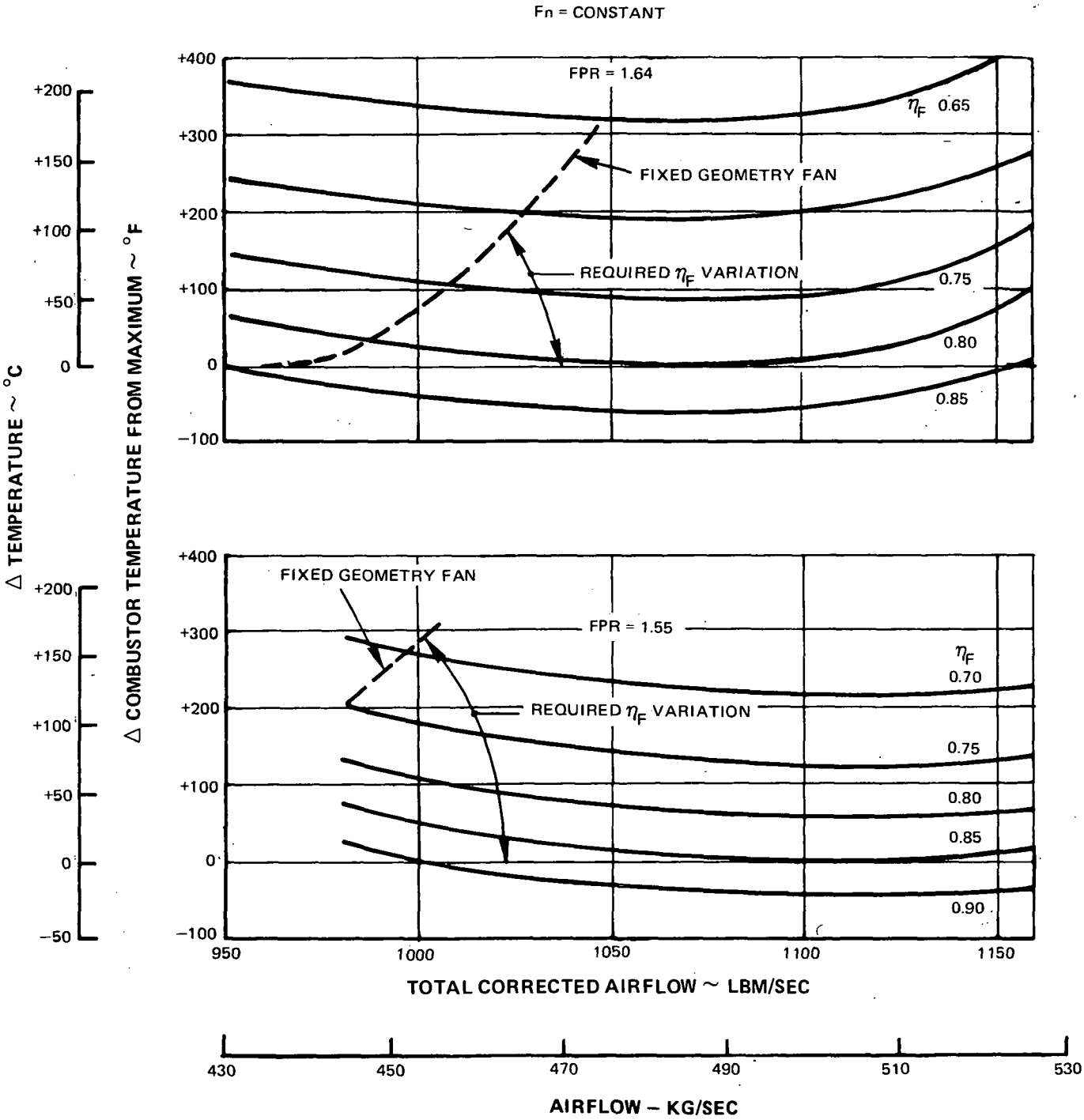

Figure 14 Effect of Fan Efficiency on Sideline Operation

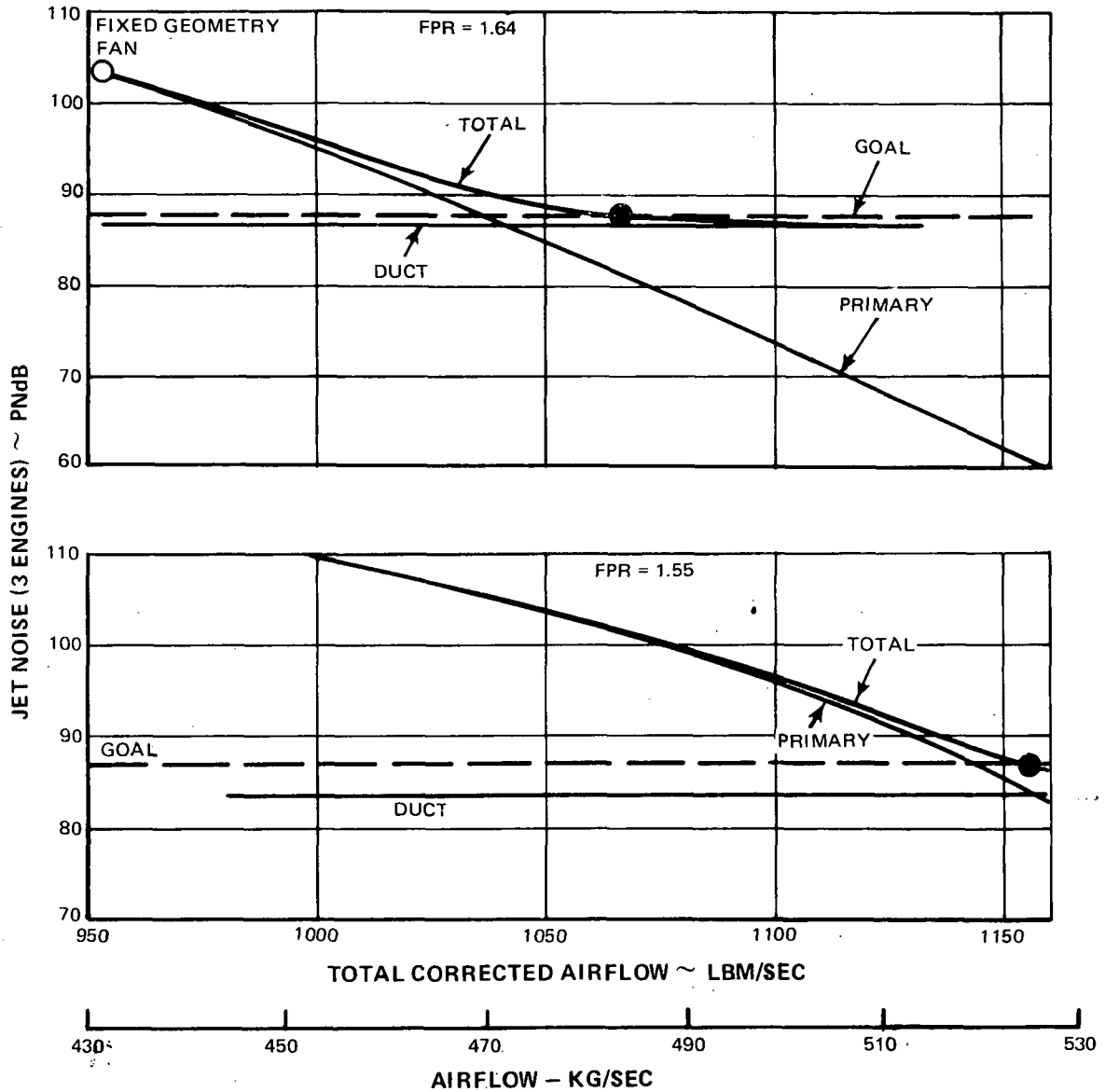

Figure 15 Sideline Jet Noise Trends for Reduced Fan Pressure Ratio Operation

Figure 16 shows the duct and primary nozzle area changes required to achieve these fan pressure ratio and airflow variations.

CUTBACK

At the 3.5 n.mi. (6480 m) (cutback) noise measuring station, the fixed geometry STF433 is operating at a net thrust of 19940 lbs. (88,600 N) with a fan pressure ratio (FPR) of 1.67, an inlet corrected airflow (WA_{T2}) of 880 lbs/sec (400 Kg/sec), a fan efficiency of 0.88, a combustor exit temperature (CET) which is 270°F (150°C) below the maximum allowable CET, and primary and duct jet velocities which produce a total jet PNL of 88 PNdB (86 ePNdB).

In order to achieve a treated fan noise level of FAR minus 20 ePNdB, the cutback total jet noise must be reduced to 84 PNdB (82 ePNdB). To achieve this jet noise level, the fan pressure ratio must be reduced to 1.48. The fan pressure ratio must be reduced to 1.38 to reduce the fan source noise by 5 ePNdB.

Figure 17 shows the combustor exit temperatures and fan efficiencies required to maintain constant cutback thrust as fan pressure ratio and inlet corrected airflow are varied.

Figure 18 presents the cutback jet noise for fan pressure ratios of 1.48 and 1.38 for operation at the maximum allowable combustor temperature. In order to meet the total jet noise goal of 84 PNdB, the airflow must be increased to 1065 lb/sec (483 kg/sec) for a FPR = 1.48 and to ≈ 1200 lb/sec (545 kg/sec) for a FPR = 1.38. At these airflows and fan pressure ratios, Figure 17 shows that variable fan geometry must provide efficiencies of 69 and 78 percent, respectively, for the 1.48 and 1.38 FPR points. Figure 19 shows the duct and primary nozzle area changes required to achieve these fan pressure ratio/airflow variations.

APPROACH

At approach, the fixed geometry STF433 is operating at a net thrust of 8175 lbs (36,400N), (three-degree single segment approach) with a FPR = 1.26, WA_{T2} = 636 lb/sec (288 kg/sec), CET = CET_{Max} minus 965°F (536°C), and a total jet PNL = 86 PNdB (77 ePNdB). Since the combustor temperature is low, variable fan geometry is not required to maintain good fan efficiencies during constant thrust operation.

Figures 20, 21, and 22 show the variations in CET, jet PNL and nozzle areas required to maintain constant approach thrust for FPR = 1.19 and 1.13. In order to achieve a treated noise level of FAR Part 36 minus 20 ePNdB, the total jet noise must be below 93 PNdB (84 ePNdB). Since the treated approach noise of the fixed geometry STF433 (Figure 4) is 17.5 ePNdB below FAR, as shown in Table III, only a 2.5 ePNdB reduction in fan noise is required.

Table VII provides a summary of the sideline and cutback fan pressure ratios, efficiencies, airflows and nozzle areas required to achieve jet and fan noise reductions of 5 ePNdB. Since the approach fan noise reduction is half of the sideline and cutback level,the approach condition was not considered in setting the fan and nozzle variable geometry requirements.

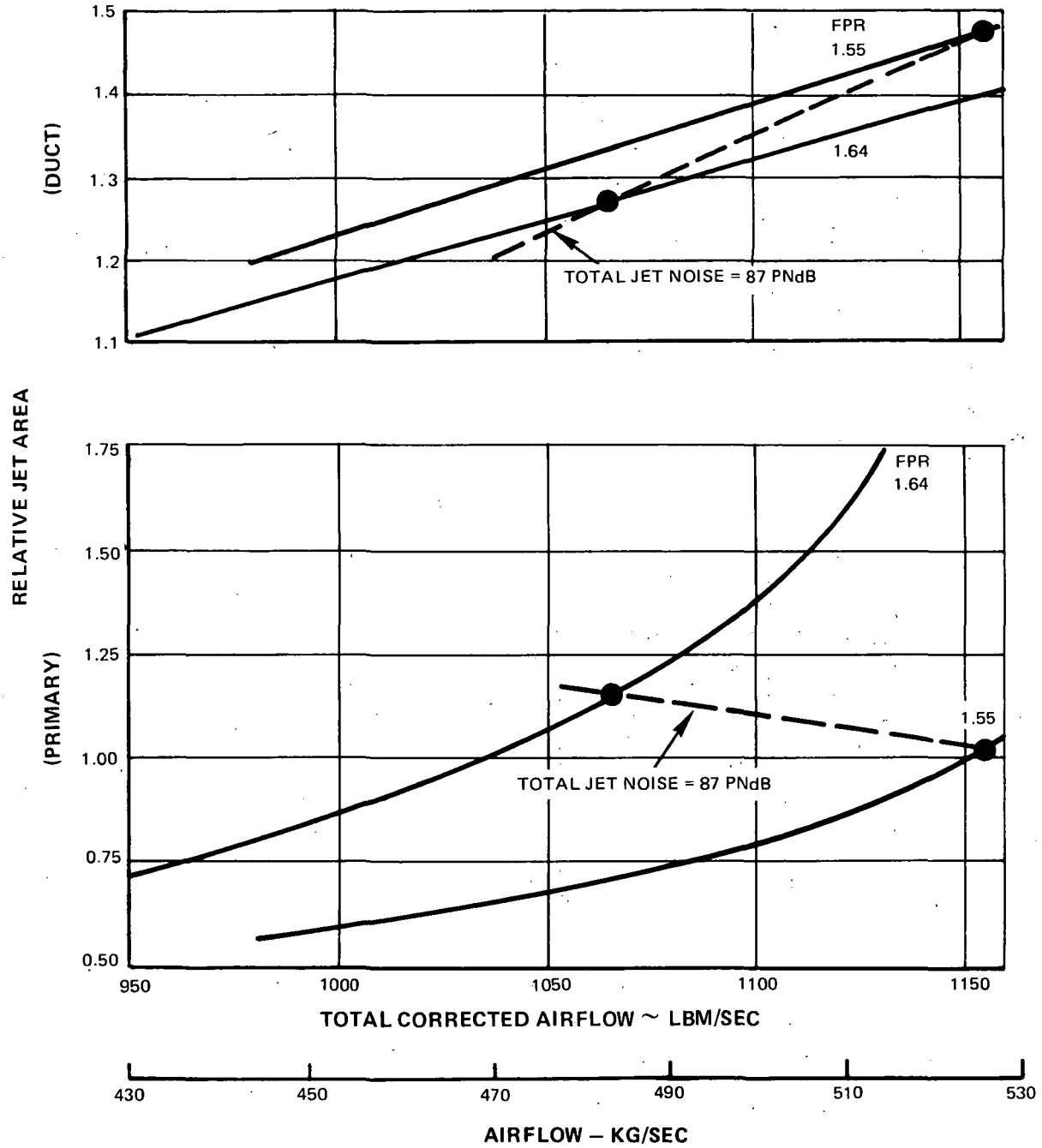

Figure 16 Sideline Nozzle Area Requirements

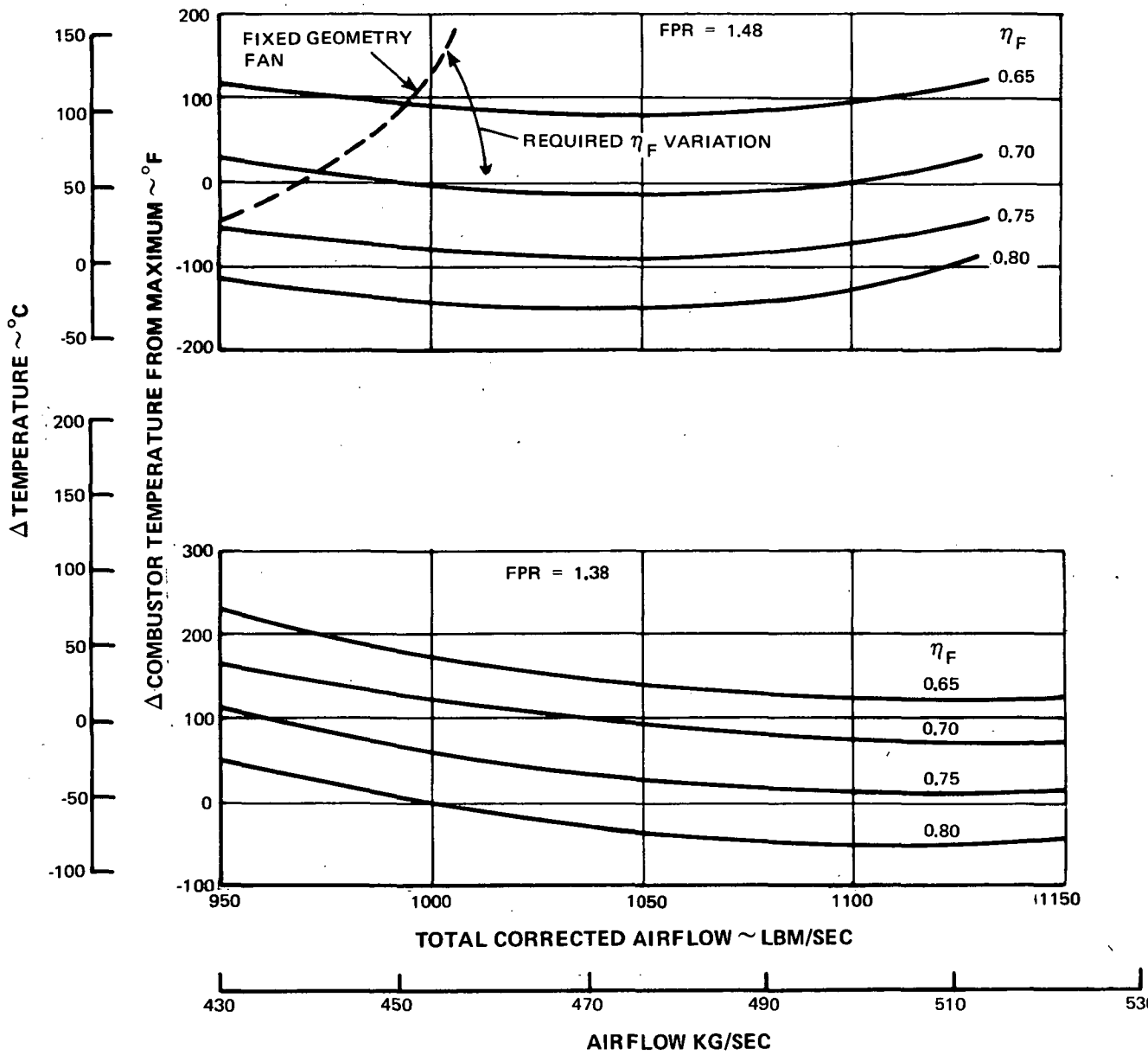

Figure 17 Effect of Fan Efficiency on Cutback Operation

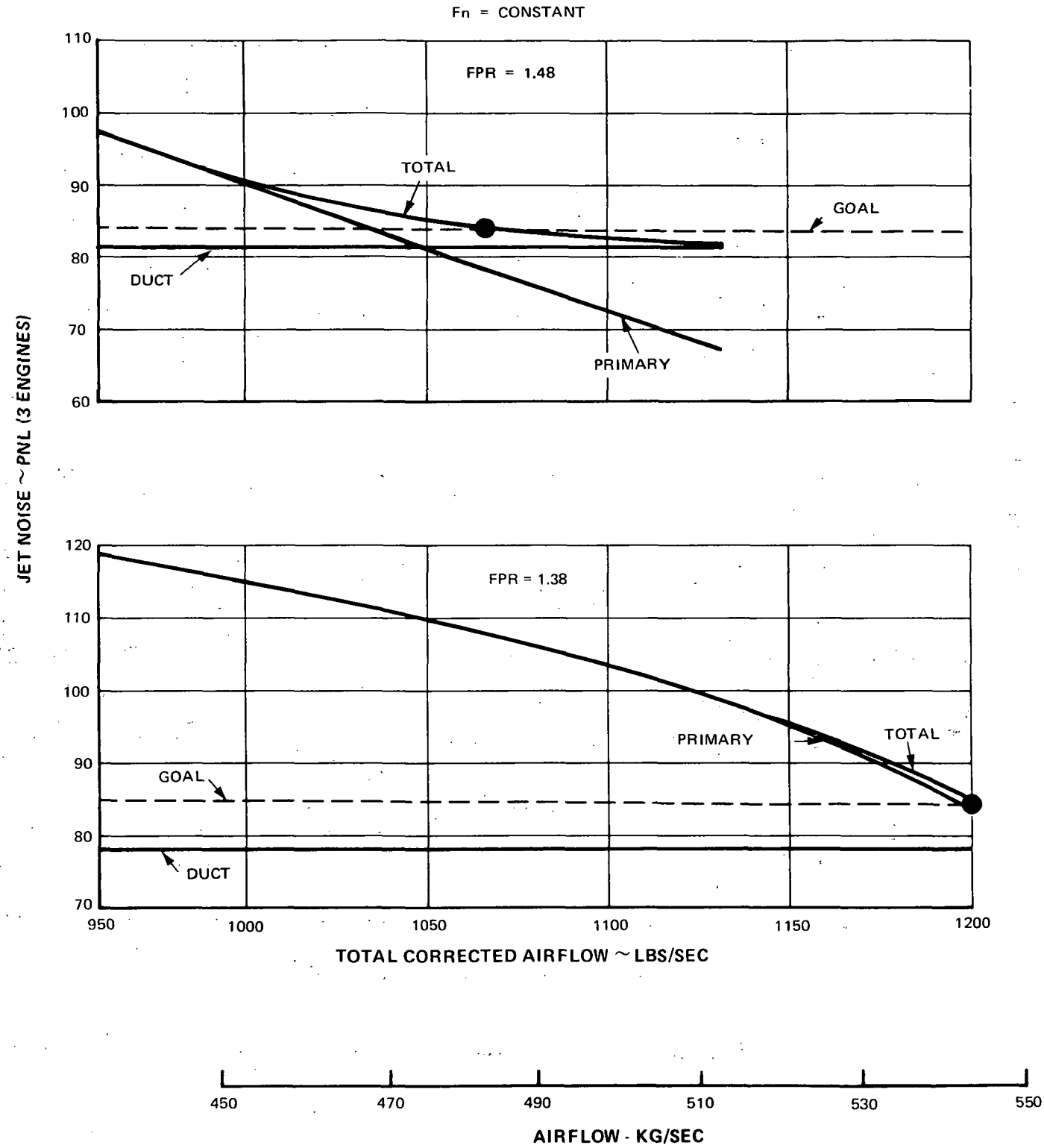

Figure 18 Cutback Jet Noise Trends for Reduced Fan Pressure Ratio Operation

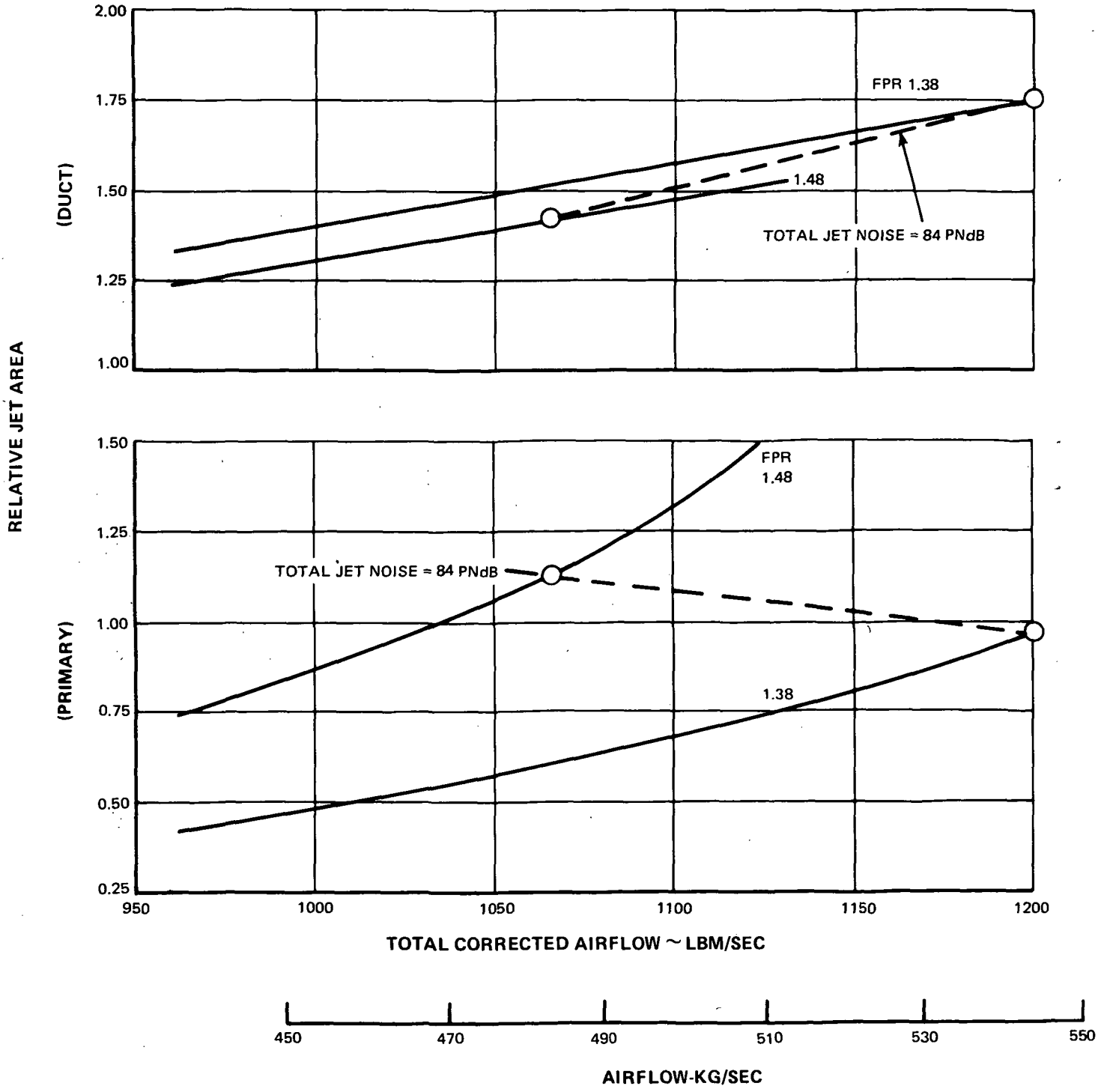

Figure 19 Cutback Nozzle Area Requirements

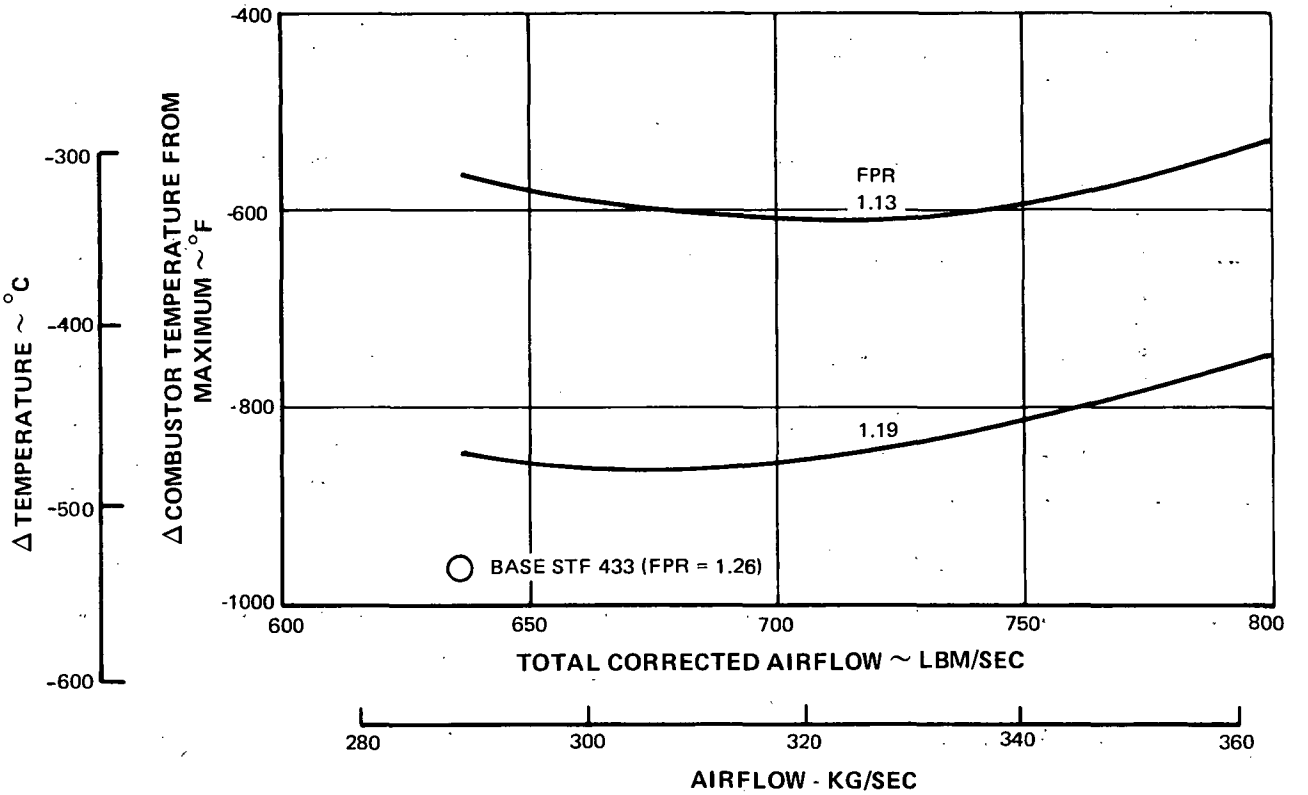

Figure 20 Effect of Fan Efficiency on Approach Operation

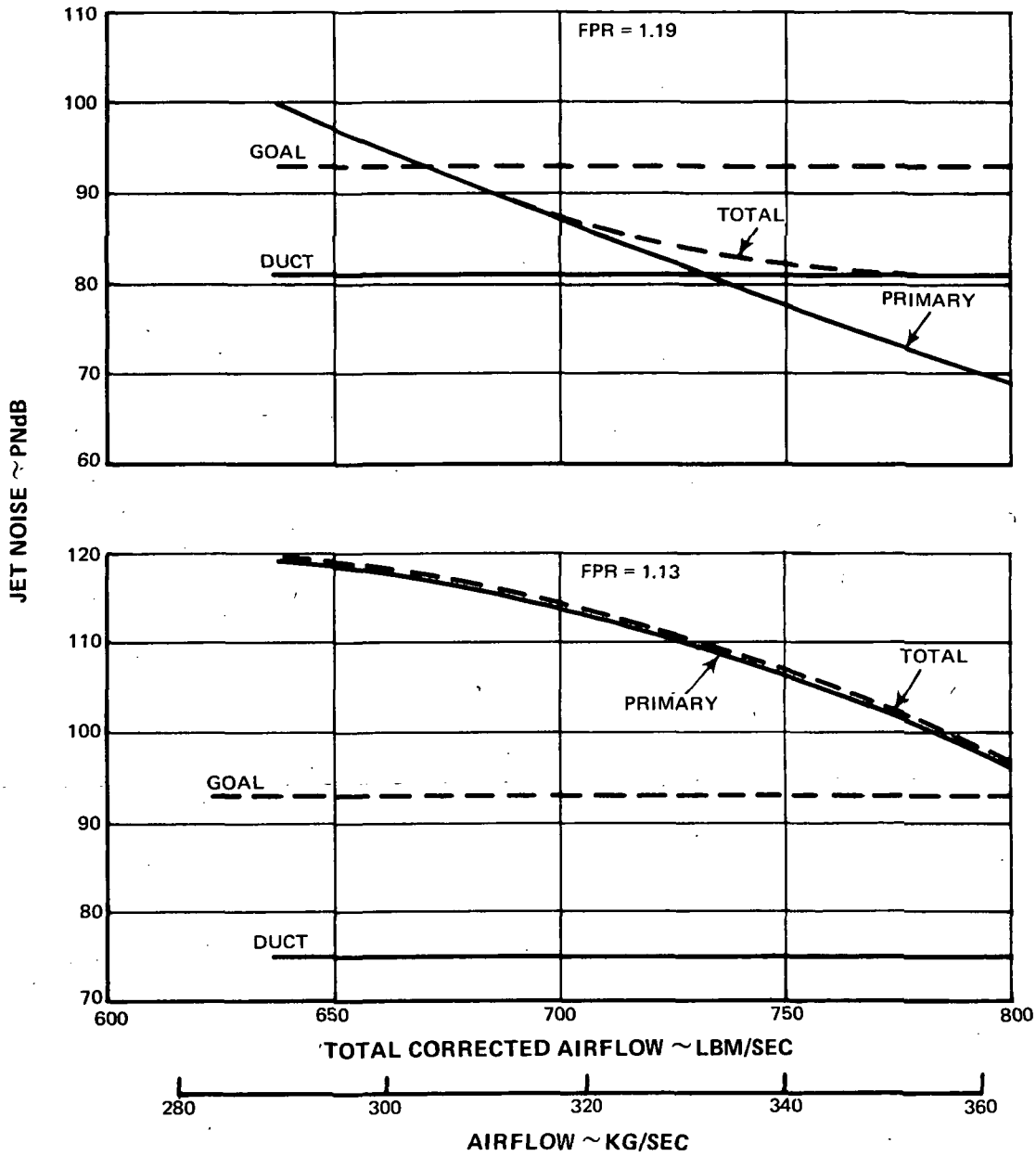

Figure 21 Approach Jet Noise Trends for Reduced Fan Pressure Ratio Operation

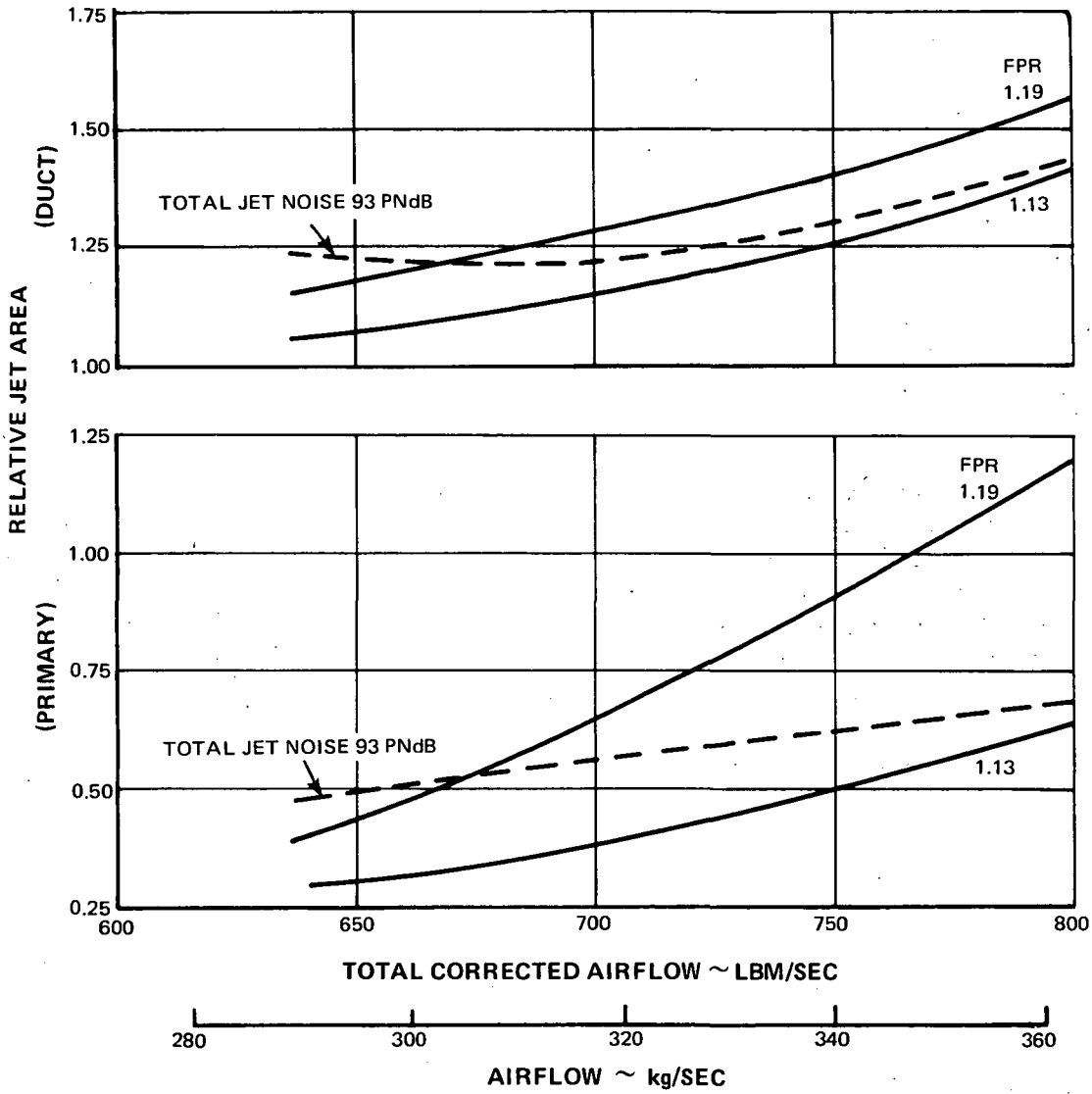

Figure 22 Approach Nozzle Area Requirements

TABLE VII

FAN AND NOZZLE CHANGES TO ACHIEVE NOISE GOALS

	SIDELINE			CUTBACK		
ΔePNdB Fan Noise	0	-3	-5	0	-3.5	-5
ΔePNdB Jet Noise	0	-5	-5	0	-5	-5
Fan Pressure Ratio	1.78	1.64	1.55	1.67	1.48	1.38
Airflow, lb/sec (kg/sec)	930(421)	1065(483)	1155(524)	880(400)	1065(483)	1200(545)
Fan Efficiency	0.88	0.80	0.86	0.88	0.69	0.78
Primary Nozzle Area Change, %	0	+17	+2	0	+13	-3
Duct Nozzle Area Change, %	0	+27	+48	0	+43	+75

A detailed analysis of variable fan geometry performance, which is beyond the scope of this study, is required to determine if these fan pressure ratios, fan efficiencies and airflows can be achieved. It is felt that the fan changes required to achieve the 3-3.5 ePNdB reduction in fan noise are attainable, and that the changes required to achieve the fan noise reduction of 5 ePNdB would require changes in the fan design, such as increased flow area to reduce the velocity of the flow through the fan, in order to improve fan efficiency. Table VIII shows that opening the duct nozzle to achieve the 5 ePNdB fan noise reduction results in choked flow in the fan exit duct. The fan inlet Mach numbers are based on designing the fan at a corrected flow of 1006 lb/sec (454 kg/sec) for an inlet specific flow of 42 lb/sec (19 kg/sec), which corresponds to a fan inlet Mach number of 0.585.

TABLE VIII

STF433 FIXED GEOMETRY FAN OPERATION

	SIDELINE			CUTBACK		
ΔePNdB Fan Noise	0	-3	-5	0	-3.5	-5
Fan Inlet Mach Number	0.52	0.65	0.78	0.48	0.65	0.88
Fan Exit Duct Mach Number	0.45	0.64	Sonic	0.45	0.82	Sonic
Fan (Primary) Exit Mach Number	0.43	0.44	0.42	0.41	0.45	0.41

Table IX shows the changes in fan duct flow (WAD), temperature (TTD), pressure (PTD), corrected airflow (WADC) and Mach Number (Mn) which occur if the fan duct area (A_{DUCT}) is held constant and duct and primary nozzles varied to reduce fan noise by 3-3.5 ePNdB at sideline and cutback.

TABLE IX
STF433 PERFORMANCE COMPARISON

	SIDELINE		CUTBACK	
ΔePNdB Fan Noise	0	-3	0	-3.5
WA_{T2}, lb/sec (kg/sec)	930 (421)	1065(483)	880 (400)	1065(483)
FPR	1.78	1.64	1.67	1.48
BPR	6.8	8.3	7.0	9.0
Duct Nozzle Area Change, %	0	+27	0	+43
WAD, lb/sec (kg/sec)	816(370)	955(433)	752(341)	936(425)
TTD, °R (°K)	652(362)	644(358)	635(353)	630(350)
PTD, psi (kN/m^2)	26.9 (185.5)	24.7 (170.5)	24.4 (168)	21.6 (149)
A_{DUCT}, in^2 (m^2)	2112(1.36)	2112(1.36)	2112(1.36)	2112(1.36)
WA_{DC}, $\frac{lbm\sqrt{°R}\,in^2}{lbf/sec}\left(\frac{kg\sqrt{°K}\,m^2}{sec\ kN}\right)$	777 (38.0)	982 (48.0)	777 (38.0)	1090 (53.3)
Mn	0.45	0.64	0.45	0.82

Increasing the velocity of the fan exhaust flow decreases the effectiveness of the fan duct treatment. At the cutback condition, the duct treatment length/height (L/H) must be increased from 8.5 for a duct Mach number of 0.45 to 25 for a duct Mach number of 0.82 in order to achieve the same amount of fan noise reduction. The increases in treatment and nacelle weights and the loss in cruise performance associated with increasing the treatment (L/H) from 8.5 to 25 result in a much larger penalty than if the nacelle diameter was made larger to provide a 40 percent increase in A_{DUCT} in order to maintain a duct Mach number of 0.45.

VARIABLE GEOMETRY ENGINE SUMMARY

The variable geometry engine selected for evaluation has the same design cycle characteristics as the fixed geometry STF433 and utilizes variable fan and nozzle geometry to achieve a 5 ePNdB reduction in jet noise and a 3 ePNdB reduction in fan noise at sideline and cutback relative to the fixed geometry engine. At the approach condition, a 1.5 ePNdB reduction in fan source noise is achieved by opening the duct nozzle 40%. Table X provides a summary of the nozzle area changes and untreated noise levels at the sideline, cutback and approach conditions.

TABLE X

FIXED (F.G.) VERSUS VARIABLE (V.G.) GEOMETRY STF433

	Sideline		Cutback		Approach	
	F.G.	V.G.	F.G.	V.G.	F.G.	V.G.
Relative Primary Area	1.0	1.17	1.0	1.10	1.0	1.0
Relative Duct Area	1.0	1.27	1.0	1.43	1.0	1.40
Inlet Airflow, lb/sec (kg/sec)	930(421)	1065(483)	880(400)	1065(483)	635(288)	760(344)
Fan Pressure Ratio	1.78	1.64	1.67	1.48	1.26	1.19
Bypass Ratio	6.8	8.3	7.0	9.0	8.6	10.0
Δ Jet ePNL α FAR	-16	-21	-17	-22	-29	-36
Δ TOTAL ePNL α FAR	+1	-2	+3.5	0	-2	-3.5

The addition of the variable pitch fan and variable primary and duct nozzles result in an increase of 15 percent in engine weight and 23 percent in engine cost.

Additional treatment must be added in order to achieve the FAR minus 20 ePNdB noise goal, since the fan source noise was only reduced by 3 ePNdB through the use of variable geometry. Figure 23 shows the untreated and treated noise levels for the fixed and variable geometry engines. In order to achieve the increased noise reduction, the inlet (L/H) was increased from 7.0 to 9.0 and the aft duct (L/H) from 8.5 to 12.6. These requirements resulted in an optimum nacelle configuration, shown in Figure 24, which includes inlet and duct wall treatment, 2 inlet rings and 3 duct splitters. The addition of this extra treatment resulted in increases of 47 and 57 percent in treatment weight and cost, respectively. The increases in inlet and fan duct treatment produce larger inlet and duct pressure losses, which result in an increase in cruise fuel consumption of 1.2 percent.

The increase in fan duct area to maintain low duct Mach numbers at sideline and cutback resulted in a 14 percent increase in nacelle diameter which, combined with the requirement for added treatment, resulted in a 22 percent increase in nacelle length. This larger nacelle is 50 percent heavier and costs 70 percent more than the FAR-15 nacelle for the fixed-geometry engine. The 14 percent increase in maximum nacelle diameter does offer one advantage over the nacelle of the fixed-geometry engine (Figure 6). Since the inlet throat area requirements are the same for both nacelles, the "fatter" inlet lip may eliminate the use of blow-in-doors or variable inlet geometry to satisfy the airflow requirements of the engine at take-off. Figure 25 presents a comparison of the FAR-20 ePNdB nacelle with the untreated aerodynamically optimum nacelle.

Table XI presents a summary of the engine performance and noise, nacelle weight and dimensions for the fixed and variable geometry engines.

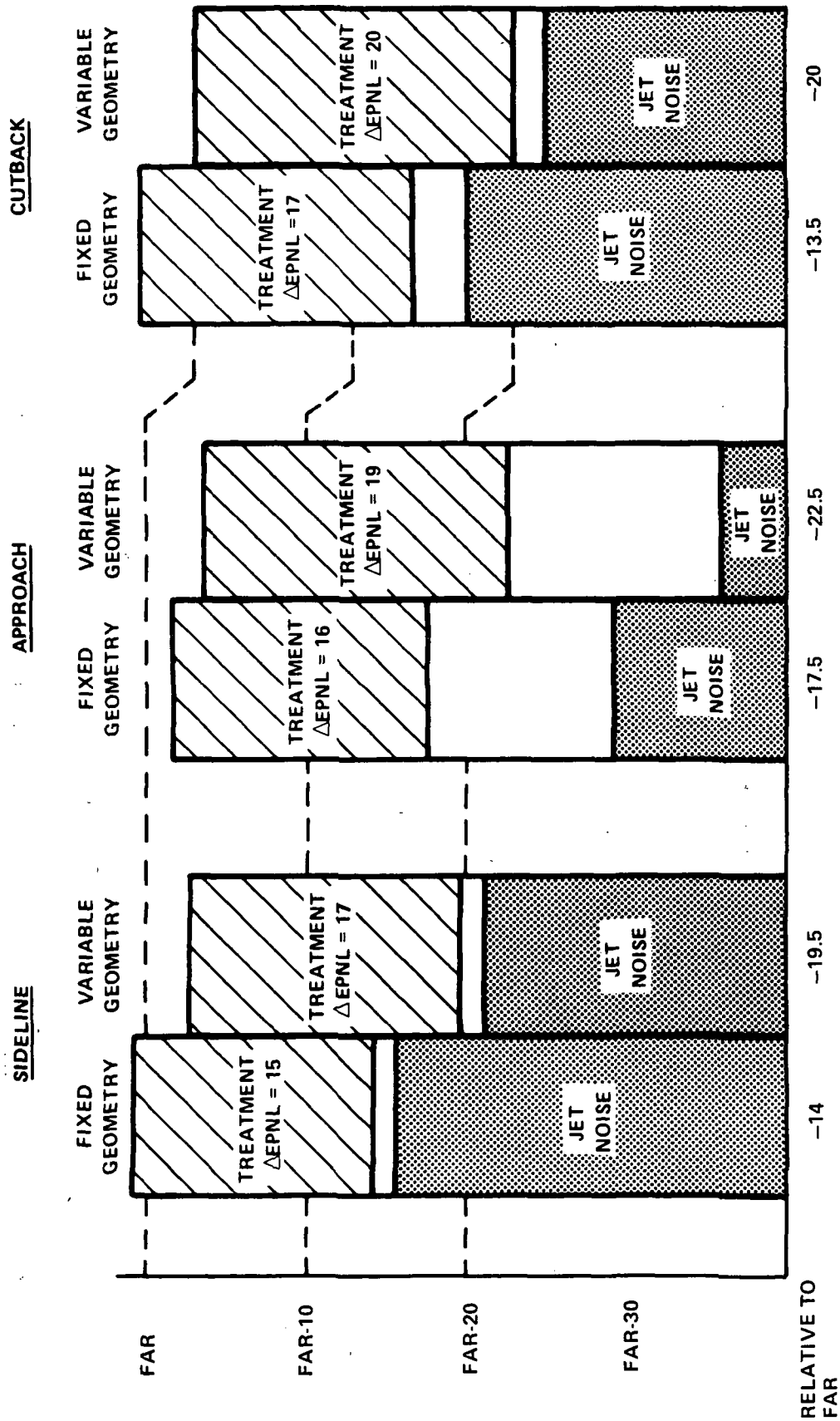

Figure 23 Fixed and Variable Geometry Engine Noise Comparison

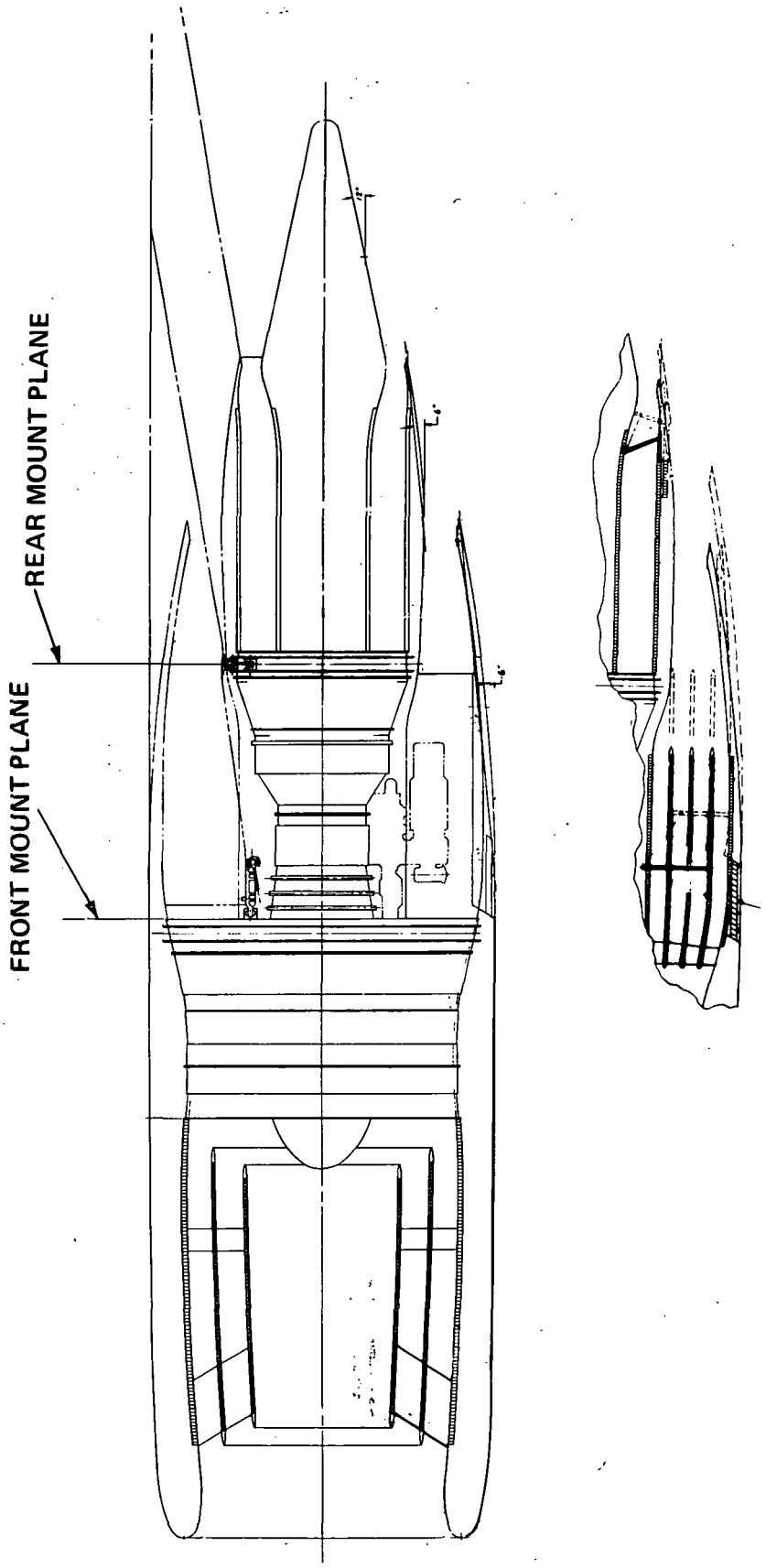

Figure 24 Treated Nacelle (FAR-20) for Variable Geometry Engine

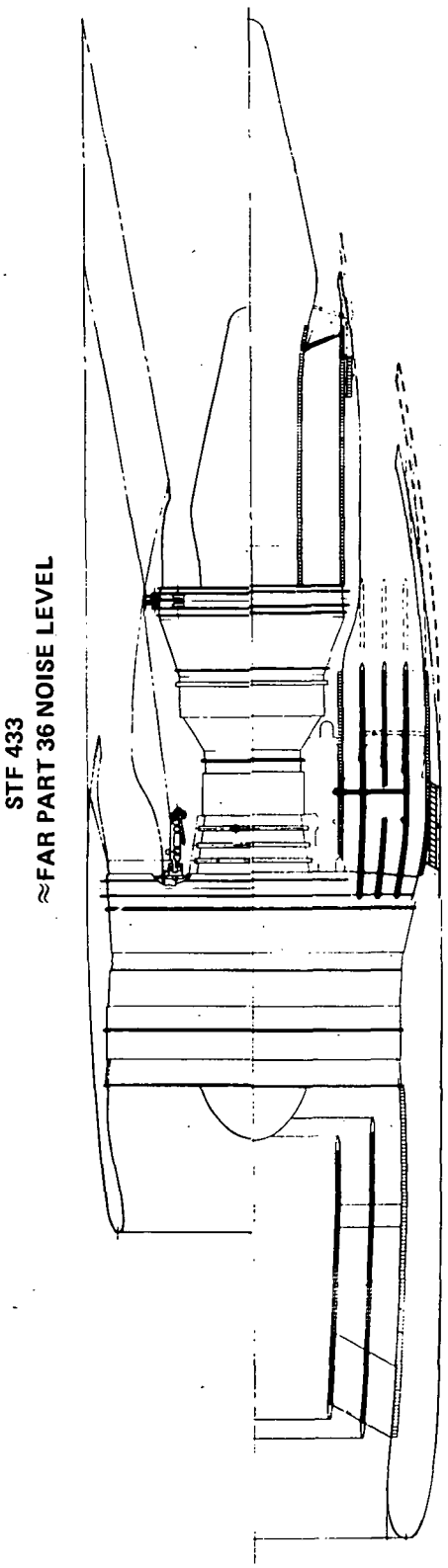

Figure 25 Comparison of FAR and FAR-20 Nacelles

TABLE XI

FAR-15 VERSUS FAR-20 STF433 SUMMARY

Engine	Fixed Geometry STF433	Variable Geometry STF433
Wall Treatment	Yes	Yes
Inlet Rings	2	2
Aft Duct Splitter	1	3
Sideline Noise α FAR	-14.0	-20
Cutback Noise α FAR	-13.5	-20.5
Approach Noise α FAR	-17.5	-22.5
Uninstalled SLTO Thrust, lbs(N)	31790.(141400)	35440.(157600)
Bare Eng. Weight, lbs (kg)	5430.(2460)	6850.(3110)
Nacelle Weight, lbs (kg)	1226(556)	2288.(1038)
Treatment Weight, lbs (kg)	915 (415)	1531 (694)
Max. Nacelle Diameter, in (m)	83.1 (2.11)	100.1(2.543)
Max. Nacelle Length, in (m)	315 (8.01)	406(1.03)

NOISE FOOTPRINTS

A comparison of the noise footprint areas for the fully treated, fixed and variable geometry STF433 for a three degree approach and a take-off with power reduction at the 3.5 n. mi. (6480 M) noise reference point is presented in Table XII, and in Figures 26 and 27. Single segment approach footprint areas are also presented for the fixed geometry engine for glide slope angles of 4.5 and 6.0 degrees. Increasing the glide slope angle 4.5° reduces the noise level of the fixed geometry engine to that of the variable geometry engine. Figures 28 and 29 show how far the take-off and 3° approach noise contours extend in directions perpendicular (sideline) and parallel to the flight path.

Figures 30 and 31 show how the fully treated fixed and variable geometry engine noise footprints compare with those of the current DC-10 and L-1011 trijets which meet FAR-12 to FAR-14 ePNdB at sideline, FAR-3 to FAR-7 ePNdB at the 3.5 n. mi. (6480 M) station, and FAR +1 to FAR-4 ePNdB at approach. At 90 ePNdB, which corresponds to a noise level of FAR-16 ePNdB for the study engines, the approach footprints of the fixed and variable geometry engines are negligible. During take-off, the footprints areas of the fixed and variable geometry engines are 25 and 10 percent, respectively, of the current trijet levels. The small area affected by these study engines and the small delta in area which exists between these engines indicates that future noise regulations should consider both absolute noise level and the area covered by the desired noise level.

TABLE XII

STF433 NOISE FOOTPRINT SUMMARY
Constant Noise Contour Areas, acres (m^2)

Cycle	Condition	GSA Degrees	100 ePNdB	95 ePNdB	90 ePNdB	85 ePNdB
Fixed Geometry	Approach	3	10(40500.)	30(121000.)	75(304000.)	200(809000.)
		4.5	0	10(40500.)	20(80900.)	60(243000.)
		6	0	0	0	10(40500.)
Variable Geometry	Approach	3	2.5(10100.)	7(28300)	20(80900.)	60(243000.)
Fixed Geometry	Take-Off		290(1170000.)	660(2670000.)	1660 (6,720,000.)	- -
Variable Geometry	Take-Off		150(607000.)	290(1170000.)	640(2590000.)	1570(6350000.)

STF456 (GEARED FAN) TURBOFAN

The previous section describes the propulsion system required to meet FAR Part 36 minus 20 ePNdB with variable component geometry. This section describes a propulsion system which achieves the FAR -20 ePNdB noise goal with fixed component geometry. In order to reach this noise goal, reductions of 5-6 ePNdB in both fan and jet source noise area are required, relative to the fixed-geometry STF433. The STF456 cycle which evolved from these noise criteria is a 10 bypass ratio (BPR) fan-high engine with a low tip speed, 1.67 fan pressure ratio (FPR) two-stage fan and a ten-stage 15.3 pressure ratio high compressor. The combustor exit temperature is the same as the STF433. Addition of a main reduction gearbox between the fan and the low pressure turbines enables designing each component for its optimum speed, thereby combining the low tip speed fan with a high speed (high efficiency) low pressure turbine.

Details of the cycle characteristics of the STF456 relative to the fixed geometry STF433 are presented in Table XIII. The uninstalled cruise thrust specific fuel consumption (TSFC) of the STF456 is 6.8 percent lower than that of the STF433. About 5 percent of this difference is due to the high bypass ratio of the STF456, and the remainder from the STF456's higher fan and low pressure turbine efficiencies. Due to its lower fan pressure ratio, the STF 456 has a 27 percent lower specific thrust than the STF433.

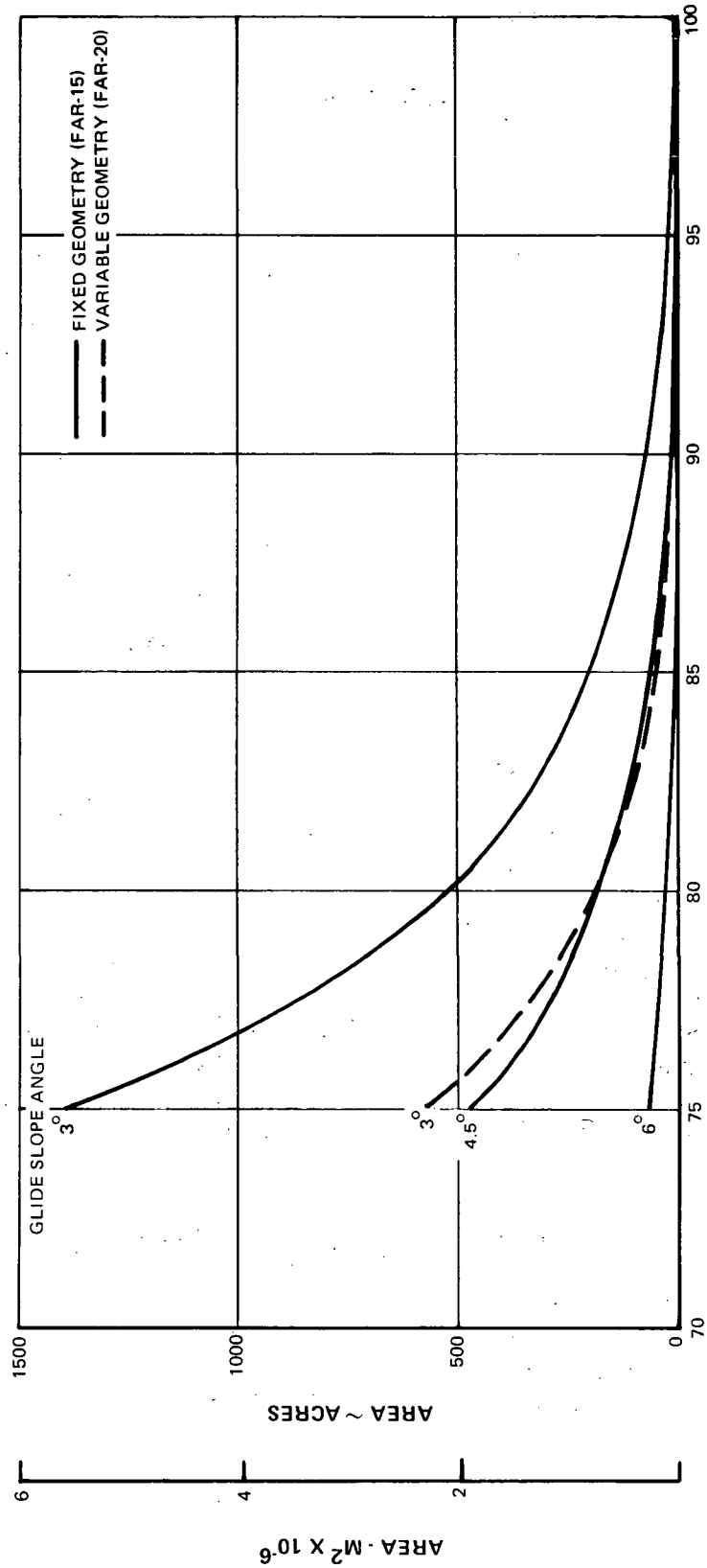

Figure 26 Approach Footprint Areas for Fixed and Variable Geometry Engines

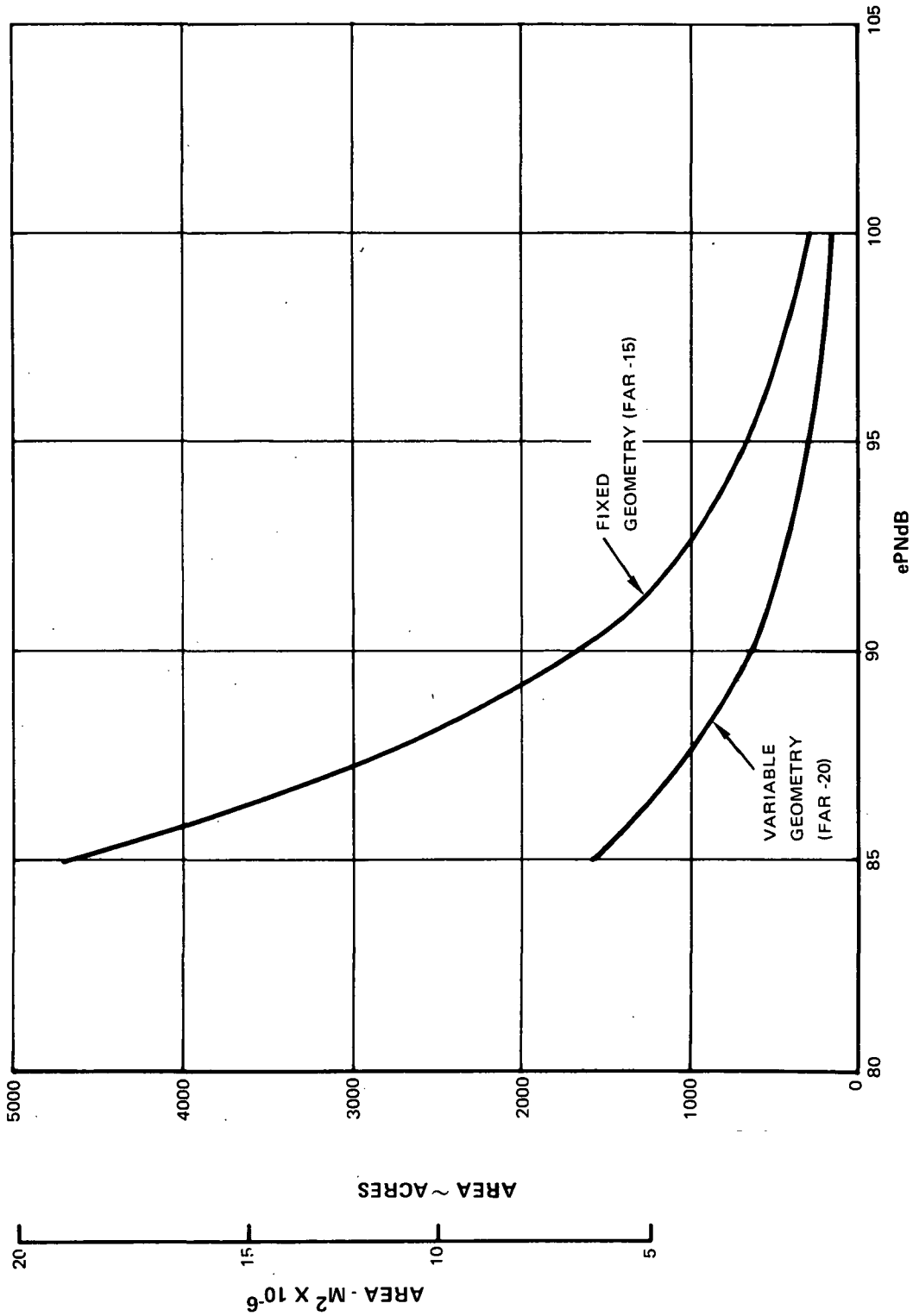

Figure 27 Take-off Footprint Areas for Fixed and Variable Geometry Engines

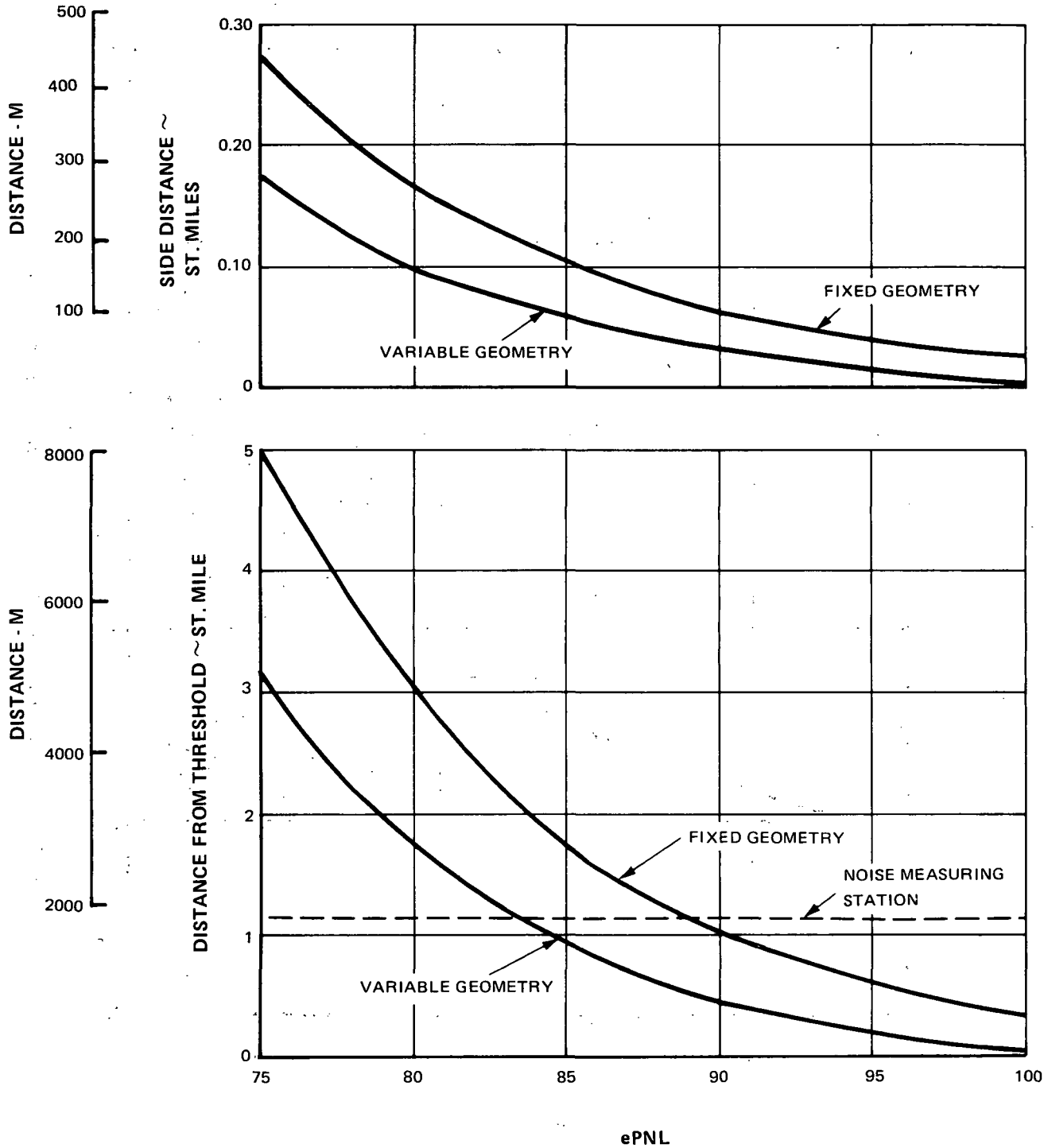

Figure 28 Approach Footprint Extension

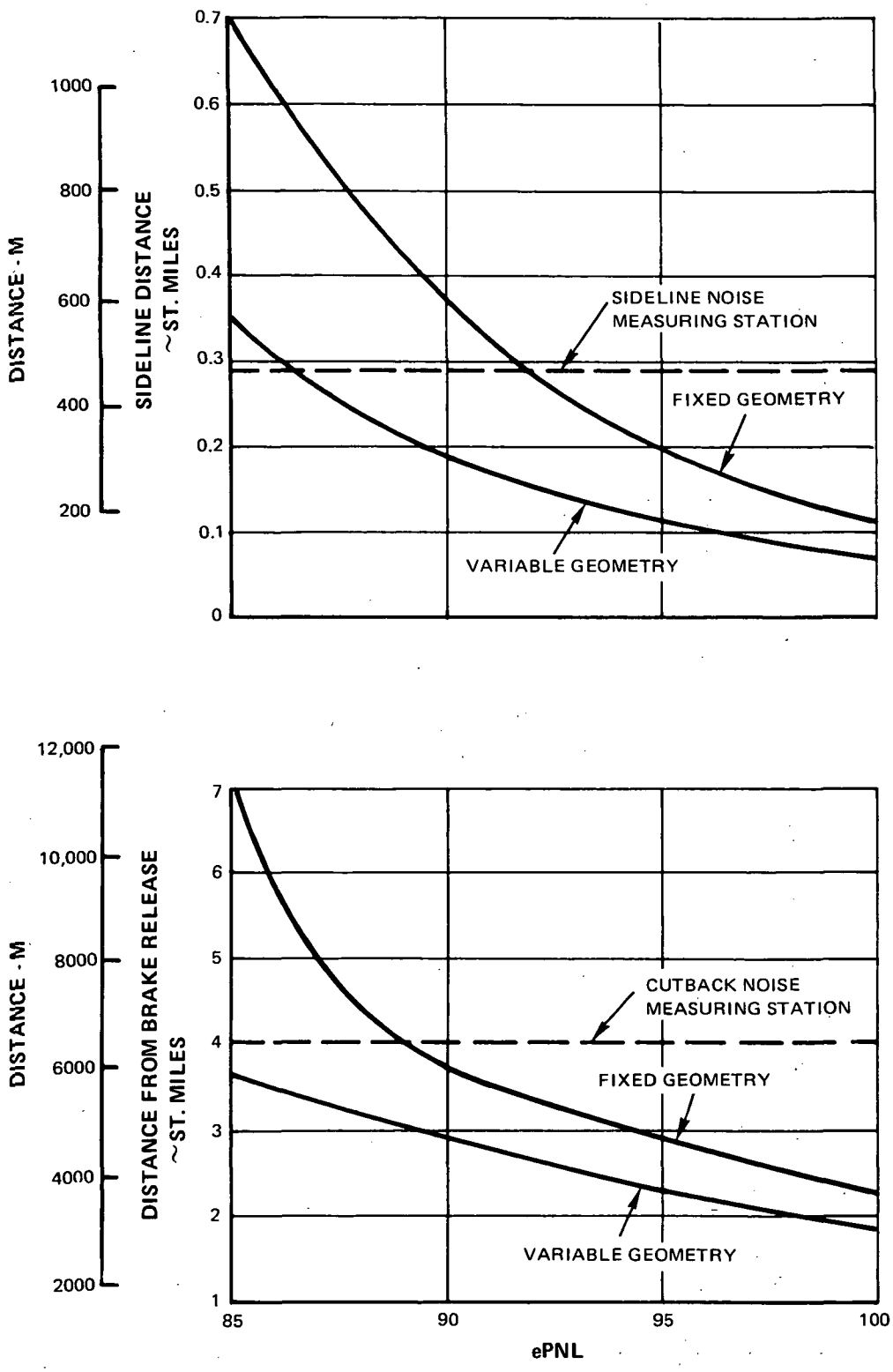

Figure 29 Take-off Footprint Extension

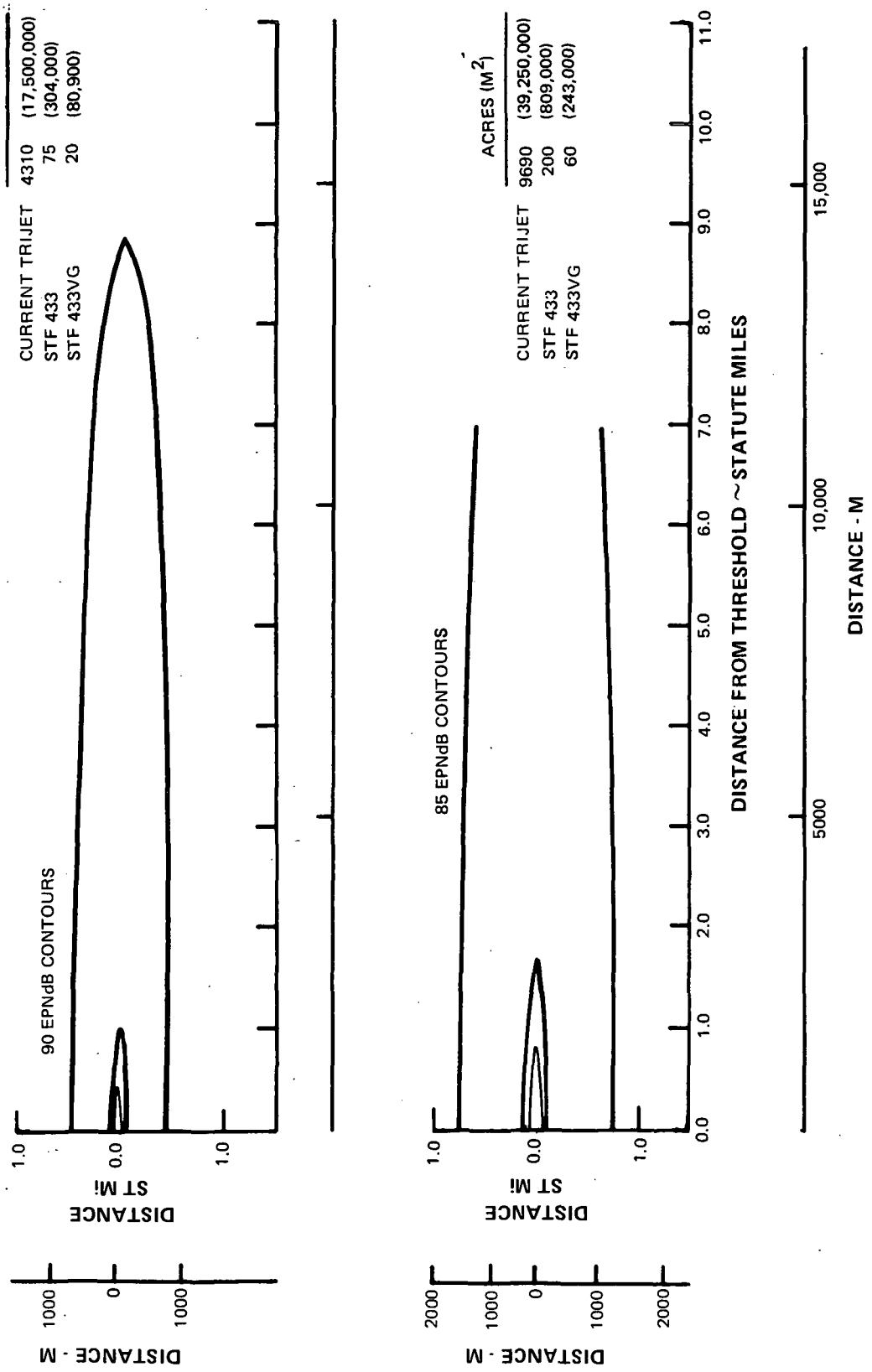

Figure 30 Comparison of Three-Degree Approach Footprints With Those of Current Trijets

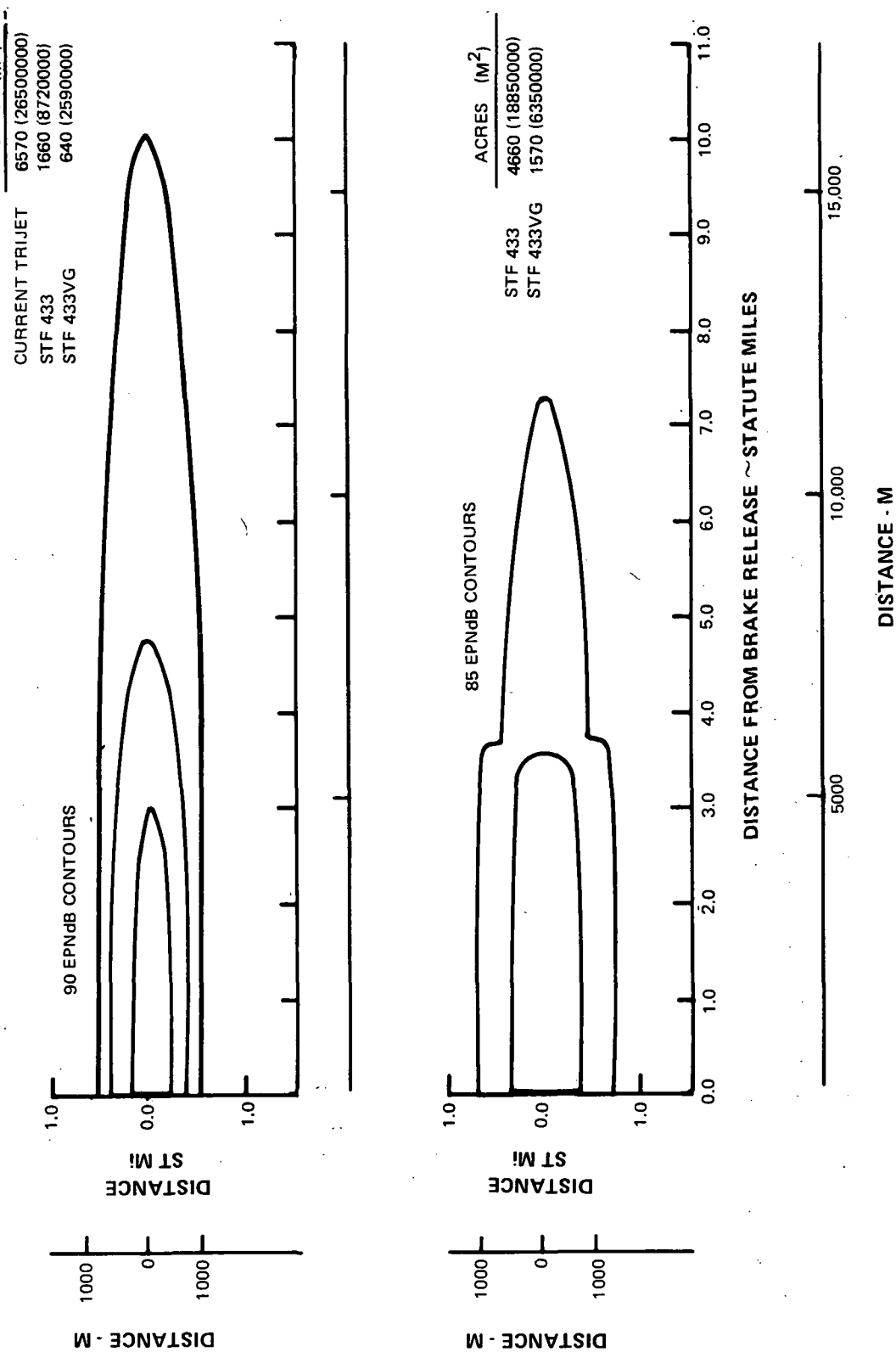

Figure 31 Comparison of Take-off Footprints With Those of Current Trijets

TABLE XIII

STF456 - STF433 CRUISE CYCLE COMPARISON

	STF433	STF456
Number of Fan Stages	2	2
Fan Pressure Ratio	1.97	1.67
Fan Tip Speed, ft/sec (m/sec)	1230 (375)	1030 (314)
Fan Efficiency Change	0	+0.006
Bypass Ratio	6.5	9.9
Number of HPC Stages	9	10
High Compressor Pressure Ratio	13.0	15.3
Overall Pressure Ratio	25.6	25.6
Low Pressure Turbine Stages	4	3
Low Turbine Efficiency Change, %	0	+4.0
Loss in LPT Efficiency For Gear, %	0	-1.5
Gear Ratio	---	2.3
Relative TSFC, %	0	-6.8
Relative Specific Thrust, %	0	-27

A conceptual drawing of a geared, two stage fan showing the gearbox located behind the fan is presented in Figure 32. With this reduction gearbox, the low pressure turbine operates at a rotational speed approximately twice that of the fan. This speed difference allows the turbine to operate at a high efficiency (lower load factor), and with one less stage, without compromising the low tip speed feature of the low noise fan. The gearbox consists of two concentric gears, the sun gear splined to the low spool shaft and the ring gear splined to the two stage fan. Five pinions supported by a stationary carriage transmit the torque from the sun gear to the ring gear. The nominal horsepower for this gearbox is 30,000 hp. Its lubrication and cooling system is integral with the engine oil system. An oil-to-air heat exchanger located in the fan exit case supplements the heat removal capacity of the normal oil-to-fuel heat exchanger.

The gearbox and low pressure turbine are new components defined specifically for this geared engine. The other engine components were derived directly from the components of the STF433 engine.

The untreated noise of the STF456 is compared with that of the fixed and variable geometry STF433 at the sideline and approach conditions in Table XIV. Since the STF433 sideline and cutback noise levels, Figure 23, are nearly equal, cutback noise levels were not calculated for the STF456. The ratio of take-off/cruise thrust for the STF456 is the same as that for the STF433.

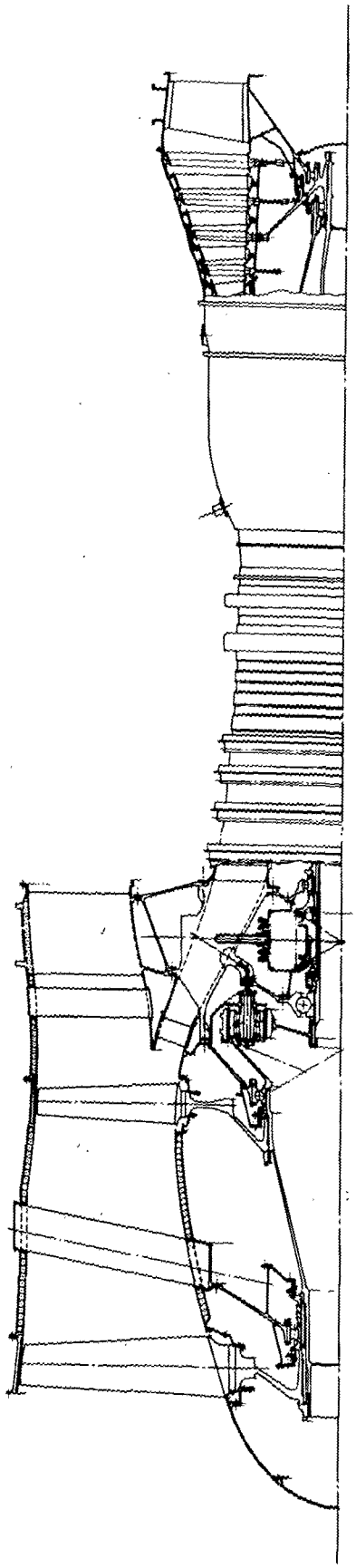

Figure 32 Conceptual Drawing of Geared Two-Stage Fan

TABLE XIV

STF456-STF433 NOISE COMPARISON

	Sideline			Approach		
	STF433 F.G.	STF433 V.G.	STF456	STF433 F.G.	STF433 V.G.	STF456
FPR	1.78	1.64	1.49	1.26	1.19	1.17
BPR	6.8	8.3	10.6	8.6	10.0	13.1
$U_{Tip}/\sqrt{\theta_{T2}}$ ft/sec (m/sec)	1115 (340)	1115(340)	920 (280)	742 (226)	810 (247)	621 (189)
VJP, ft/sec (m/sec)	990 (302)	800 (244)	775 (234)	325 (99)	390 (119)	245 (75)
VJD, ft/sec (m/sec)	800 (244)	720 (219)	610 (186)	420 (128)	340 (103)	322 (98)
3-Engine Noise α FAR, ΔePNdB						
Jet Noise	-16	-21	-25	-29	-36	-38
Untreated Total Noise	+1	-2	-5	-2	-3.5	-7

The STF456's high bypass ratio, low fan pressure ratio cycle yields source noise reductions of 9 ePNdB in jet noise and 5-6 ePNdB in total noise relative to the fixed geometry STF433.

The STF456 installed in a treated (FAR -20) nacelle is shown in Figure 33. Due to the STF456's 6 ePNdB reduction in source noise, the treatment requirements to achieve FAR minus 20 ePNdB are nearly the same as that of the fixed geometry (FAR -15) STF433. The treatment arrangement consists of extensive inlet and duct wall treatment, two inlet rings and two aft duct splitters. This treatment configuration minimizes nacelle weight and internal performance losses to achieve the desired treatment(L/H).

A comparison of the noise footprint areas for the fixed geometry STF433 and the STF456 for a three-degree approach and a take-off with power reduction at the 3.5 n. mi. (6.47 km) noise reference is presented in Figures 34 and 35.

The treated engine noise, nacelle weight and dimensions of the STF456 relative to the fixed and variable geometry STF433 are summarized in Table XV.

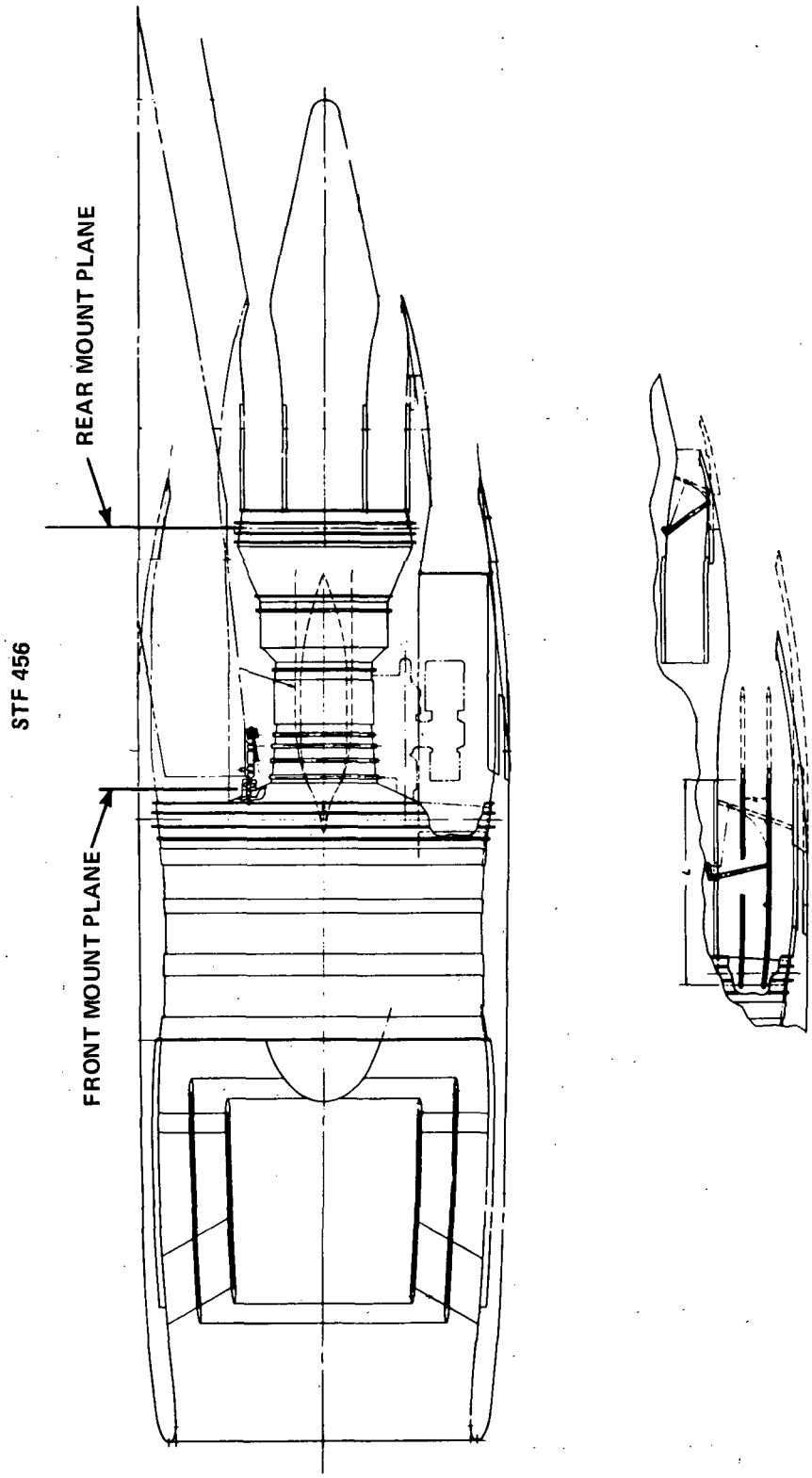

Figure 33 Treated Nacelle (FAR-20) for the STF456 Geared Fan Engine

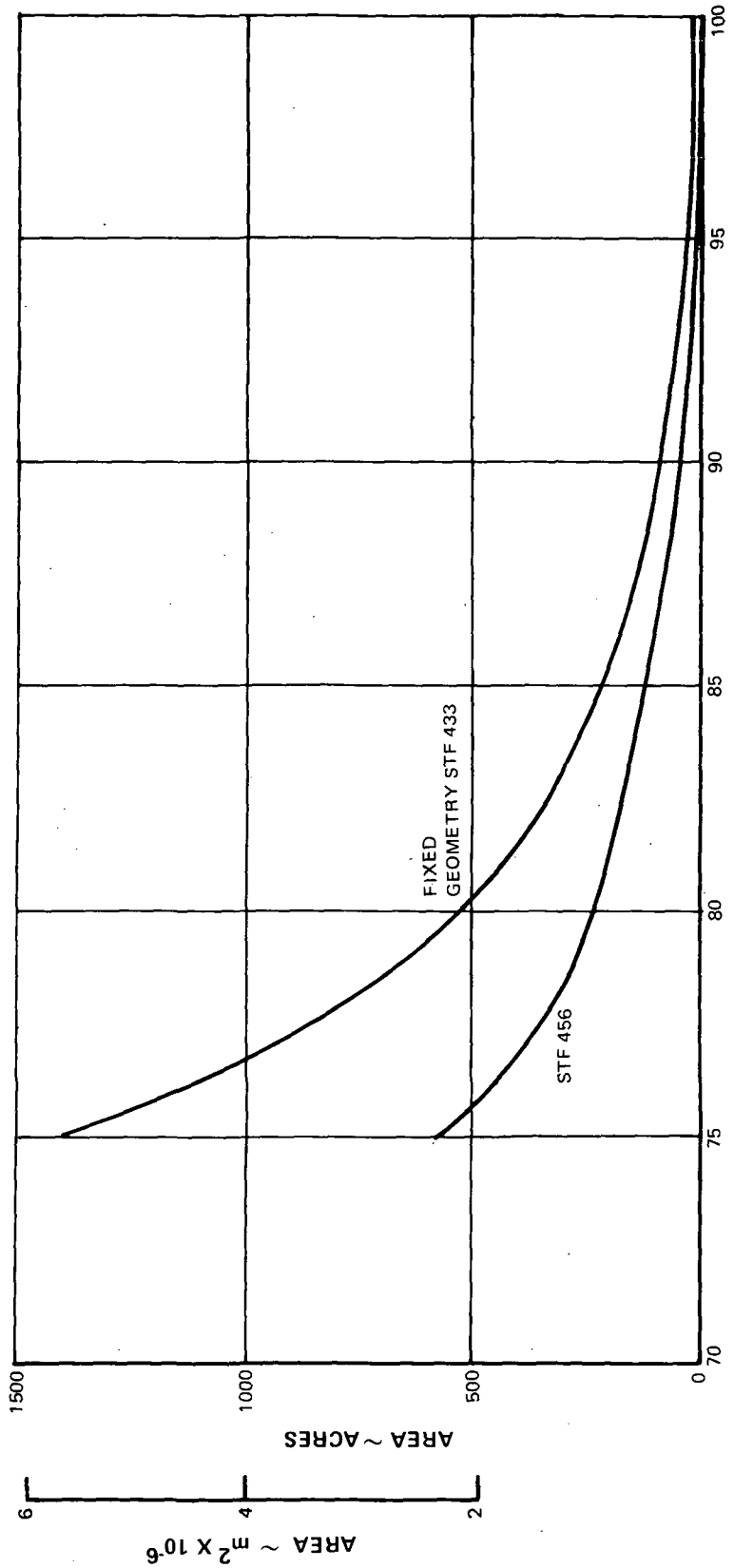

Figure 34 Three-Degree Approach Footprint Areas

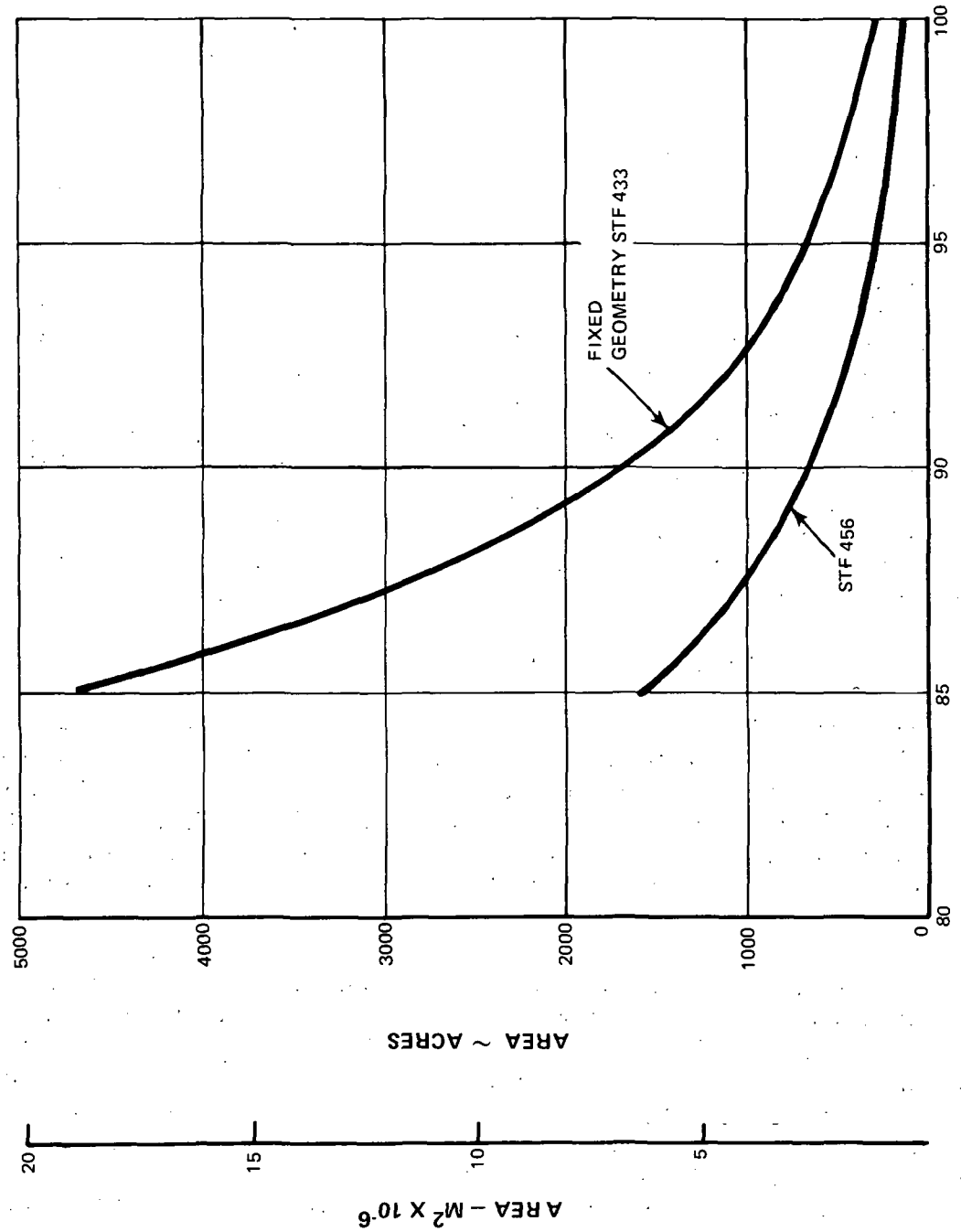

Figure 35 Take-off Footprint Areas with Cutback at 3.5 n. mi. FAR Noise Reference Point

TABLE XV

STF456 INSTALLATION SUMMARY

	FIXED GEOMETRY STF433	VARIABLE GEOMETRY STF433	STF456
Noise Goal α FAR, ΔePNdB	-15	-20	-20
Wall Treatment	Yes	Yes	Yes
Inlet Rings	2	2	2
Inlet L/H	7.0	9.5	6.0
Aft Duct Splitters	1	3	2
Aft Duct L/H	8.5	12.5	9.0
Sideline Noise α FAR, ΔePNdB	-14.0	-20.0	-20.0
Cutback Noise α FAR, ΔePNdB	-13.5	-20.5	---
Approach Noise α FAR, ΔePNdB	-17.5	-22.5	-20.5
Uninstalled SLTO Thrust, lbf (N)	31790(141400.)	35440(157600)	35650(158600.)
Bare Eng. Weight, lbm (kg)	5430(2460)	6850(3110)	7190(3260)
Nacelle Weight, lbm (kg)	1225(556)	2290(1040)	1690(766)
Treatment Weight, lbm (kg)	915(415)	1530(695)	1165(530)
Max. Nacelle Dia., in (m)	83.1(2.11)	100.1(2.54)	98.8(2.51)
Max. Nacelle Length, in (m)	315(8.01)	406(10.3)	361(9.17)

STF457 (DIRECT DRIVE) TURBOFAN

The impact on performance and noise of substituting a single stage, high tip speed, direct drive fan for the STF456's two-stage geared fan was investigated. This cycle, designated STF457, has the same design cycle characteristics as the STF456. The cycle characteristics of the STF457 are compared with the STF456 and the STF433 in Table XVI. The TSFC and specific thrust of the STF457 suffer relative to the STF456 due to the lower efficiencies of the high tip speed single-stage fan and the low velocity ratio, four-stage low pressure turbine.

For the same design pressure ratio (1.67), the single-stage fan operates at a tip speed that is almost 50 percent higher than the two-stage fan. This speed increase imposes a 2.1 percent fan efficiency penalty. Even though the fan for this STF457 engine has a higher tip speed, the size of the fan for this 10 BPR cycle relative to the gas generator size leads to a low rotational speed for the low spool. This necessitates either a reduction gearbox between the fan and low pressure turbine or an advanced, highly-loaded, low speed, four-stage low pressure turbine, similar to the STF433 design. A direct-drive arrangement with the advanced turbine was selected for this evaluation. The resulting turbine definition was a four-stage design with the same load factor and efficiency as the STF433 low pressure turbine.

The untreated noise of the STF457 compared with that of the STF456 at the sideline and approach conditions is presented in Table XVII.

TABLE XVI

STF457 DIRECT DRIVE, SINGLE STAGE FAN
Cycle Comparison at Cruise

	STF433	STF456	STF457
Fan Stages	2	2	1
Fan Pressure Ratio	1.97	1.67	1.67
Fan Tip Speed, ft/sec (m/sec)	1230(375)	1030(314)	1500(457)
Fan Efficiency Change, %	0	+0.6	-1.5
Bypass Ratio	6.5	9.9	9.9
High Compressor Pressure Ratio	13.0	15.3	15.3
Overall Pressure Ratio	25.6	25.6	25.6
Low Pressure Turbine Stages	4	3	4
Low Turbine Velocity Ratio	0.33	0.42	0.33
Low Turbine Efficiency Change, %	0	+4.0	0
Δ-Gear Efficiency, %	0	-1.5	0
Gear Ratio	-	2.3	-
Relative Uninstalled TSFC, %	0	-6.8	-3.2
Relative Specific Thrust, %	0	-27	-33

TABLE XVII

STF457-STF456 NOISE COMPARISON

	Sideline		Approach	
	STF456	STF457	STF456	STF457
FPR	1.49	1.47	1.17	1.17
BPR	10.6	10.6	13.1	12.9
$U_{TIP}/\sqrt{\theta_{T2}}$, ft/sec (m/sec)	920(280)	1315(401)	621(189)	890(271)
OPR	20.7	20.6	10.1	10.1
VJP, ft/sec (m/sec)	775(236)	655(200)	245(75)	192(53)
VJD, ft/sec (m/sec)	610(186)	595(181)	322(98)	316(96)
3 Engine Noise, ePNL α FAR				
Jet ΔePNdB	-25	-27	-38	-38
Untreated Total Δ ePNdB	-5	-3	-7	+3

At sideline, the single-stage fan is 2 ePNdB noisier than the two-stage fan. At approach the STF457 is 10 ePNdB noisier than the STF456. Figure 36 shows the total noise comparison between fixed geometry single-and two-stage fans as a function of tip speed. Noise values for sideline and approach are shown.

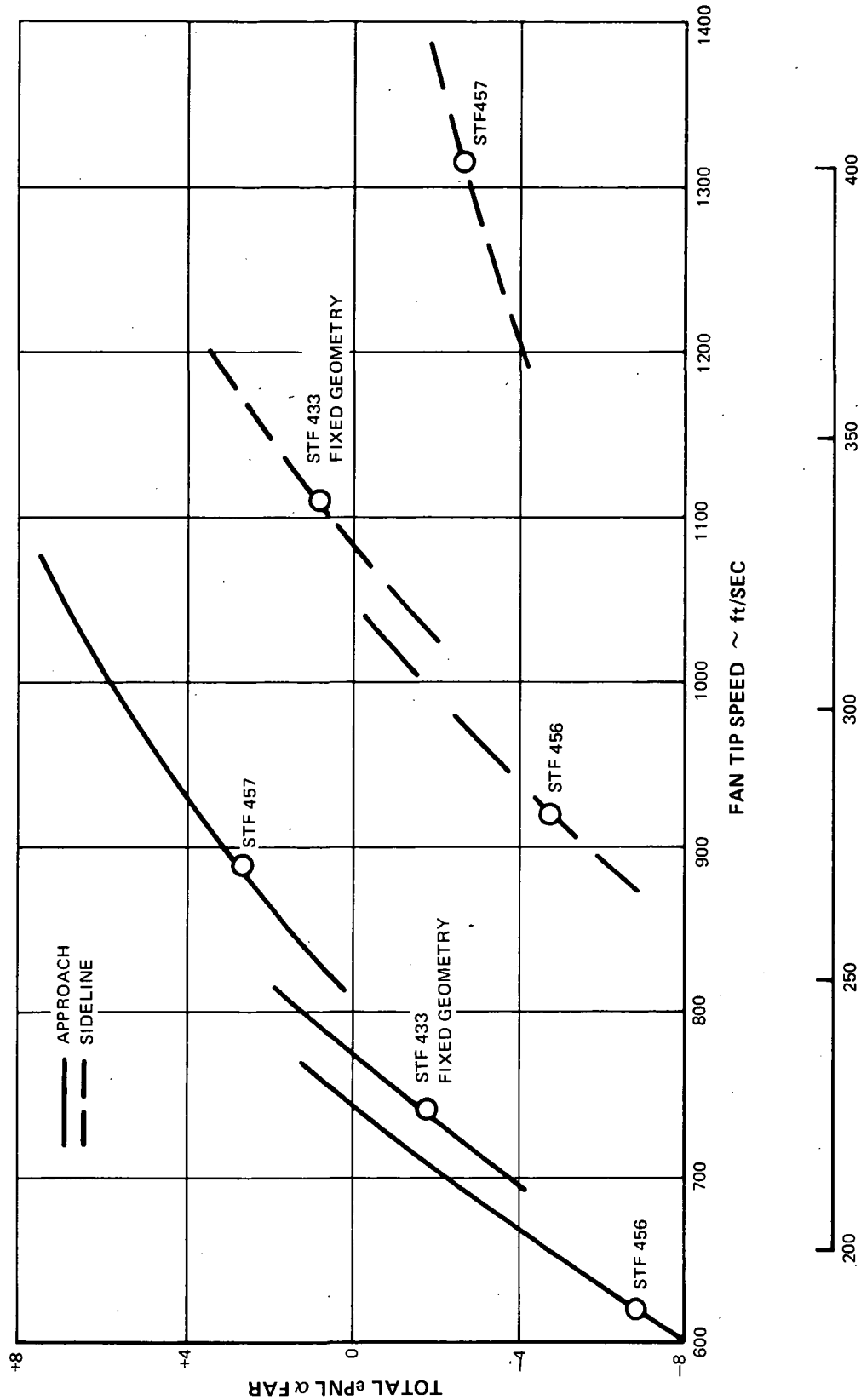

Figure 36 Sideline/Approach Untreated Total Noise Comparison

The STF457 was installed in the STF456's treated nacelle. Since the STF457 had a single stage fan and did not have a gearbox, the overall length was considerably less than that for the two-stage, geared STF456. This allowed for more room in the nacelle for more acoustic treatment. The inlet treatment L/H was increased from 6.0 to 7.1 and fan duct L/H was increased from 9.0 to 11.5. The treated engine noise, nacelle weight and dimensions of the STF457 relative to the STF456 and the fixed geometry STF433 are summarized in Table XVIII. Since the STF433 cutback and sideline noise are nearly equal, no cutback noise estimates were calculated for the STF457.

TABLE XVIII

STF456 INSTALLATION SUMMARY

	Fixed Geometry STF433	STF456	STF457
Wall Treatment	Yes	Yes	Yes
Inlet Rings	2	2	2
Aft Duct Splitter	1	2	2
Sideline Noise α FAR, ΔePNdB	-14.0	-20.0	-16.5
Cutback Noise α FAR, ΔePNdB	-13.5	---	---
Approach Noise α FAR, ΔePNdB	-17.5	-20.5	-16.0
Uninstalled SLTO Thrust, lbf (N)	31790(141400.)	35650(158600)	37340(166100)
Bare Eng. Weight, lbm (kg)	5430(2460)	7190(3260)	6030(2740)
Nacelle Weight, lbm (kg)	1225(556)	1690(766)	1775(805)
Treatment Weight, lbm (kg)	915(415)	1165(528)	1450(657)
Max. Nacelle Dia., in (m)	83.1(2.11)	98.8(2.51)	101.1(2.57)
Max. Nacelle Length, in (m)	315(8.01)	361(9.17)	369(3.37)

The treated STF457 achieves FAR -16 ePNdB noise levels. More acoustic treatment (increasing L/H) would not significantly reduce the noise from the present levels, but engine performance losses and treatment weight would be increased. In order to achieve the FAR -20 ePNdB noise goal by reducing the fan source noise an additional 4 ePNdB, a single-stage fan cycle with a design fan pressure ratio of 1.55-1.6 and a bypass ratio of 11 to 12 would be required. This higher bypass ratio - lower fan pressure ratio cycle will result in increased nacelle diameter, length and weight and acoustic treatment weight.

FORE/AFT FAN CONCEPT

The STF433 engine flowpath was modified by placing the second fan stage over the low pressure turbine in order to obtain maximum spacing between the two fan stages. This aft-fan arrangement can be obtained without affecting the cycle by adding a supercharging stage to the high compressor to offset the displacement of the second fan. In this scheme, shown schematically in Figure 37, the fan duct between the first and second fans would contain acoustic wall treatment such that both the aft noise of the forward fan and the inlet noise of the aft fan would be attenuated. In effect, the fan source noise would be that of a single-stage, low tip speed, low pressure ratio fan.

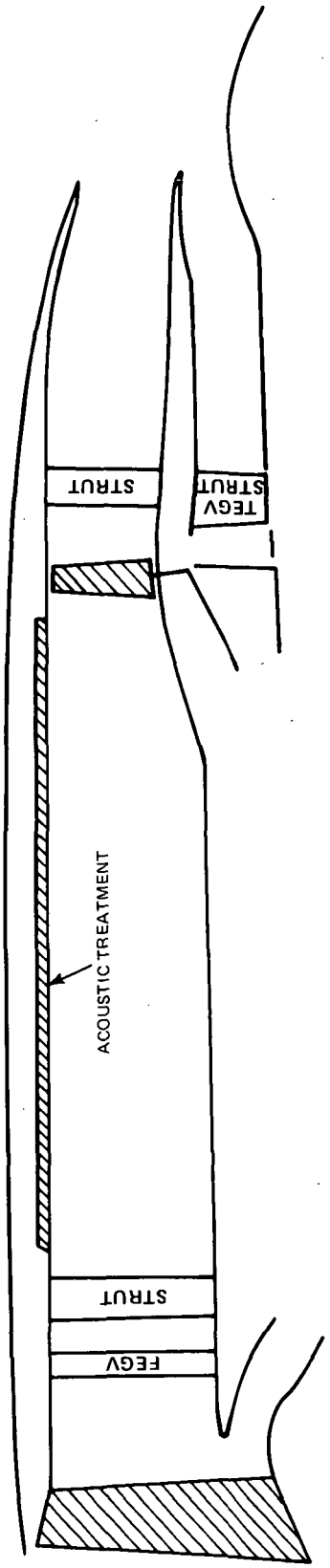

Figure 37 Schematic of a Fore/Aft Fan Concept

The untreated noise of the fore/aft fan concept is compared with that of the fixed geometry STF433 in Table XIX. Fan source noise is reduced by 0 to 4 ePNdB at the noise measuring conditions relative to the fixed geometry STF433.

TABLE XIX

NOISE SUMMARY OF THE FORE/AFT FAN CONCEPT

	Sideline		Cutback		Approach	
	STF433	Fore/Aft Fan	STF433	Fore/Aft Fan	STF433	Fore/Aft Fan
FPR	1.78	1.35/1.31	1.67	1.31/1.27	1.26	1.13/1.11
BPR	6.8	6.8	7.0	7.0	8.6	8.6
$U_{Tip}/\sqrt{\theta_{T2}}$ ft/sec (m/sec)	1115 (340)	1115/1050 (340/320)	1050 (320)	1050/990 (320/302)	742 (226)	742/697 (226/212)
OPR	21.6	21.6	19.2	19.2	10.1	10.1
3 Engine Noise, ePNL α FAR						
Jet, ΔePNdB	-16	-16	-17	-17	-29	-29
Untreated Total, ΔePNdB	+1	-4	+3	-1	-2	-2

The fore/aft fan requires a smaller amount of acoustic treatment to reach the jet noise floor at sideline. The treated noise of the fore/aft fan is compared with that of the fixed geometry STF433 in Table XX.

TABLE XX

FORE/AFT FAN TREATED NOISE SUMMARY

	Fixed Geometry STF433	Fore/Aft Fan
Wall Treatment	Yes	Yes
Inlet Rings	2	2
Inlet (L/H)	7.0	4.0
Inter-Fan Duct Wall Treatment	---	Yes
Aft Duct Splitters	1	1
Aft (L/H)	8.4	6.0
Sideline Noise α FAR, ΔePNdB	-14	-14
Cutback Noise α FAR, ΔePNdB	-14	-13
Approach Noise α FAR, ΔePNdB	-18	-16

A conceptual drawing of an aft fan is shown in Figure 38. In this concept, the third stage of the low pressure turbine is redesigned to serve as a structural member between the turbine assembly and the aft-fan rotor. This enables driving both the fore and aft fans with one, four-stage turbine assembly. The drawing indicates all support for the aft-fan rotor would be provided by the turbine rotor and its static structure. Although this arrangement is considered feasible, there are numerous problems attending this design including; thrust balancing the fan, the effect of maneuvering loads from the fan rotor on turbine tip clearance, cooling the fan disc, and preventing leakage of hot gas from the turbine into the surrounding compartments. Because of these complications to the engine and the penalties they would manifest on engine weight and reliability, and also considering the limited noise benefit for this fore/aft fan arrangement, no further evaluation was conducted for this concept.

VARIABLE GEOMETRY STF433: ALTERNATE POD DESIGNS

Three alternate pod designs for the variable geometry STF433 were evaluated to assess their impact on noise, acoustic treatment penalties, and aircraft TOGW and economics. The three alternate pod designs which were evaluated are:

- External Accessories
- Choked Inlet
- Co-planar Nozzle/Umbrella Reverser

External Accessories

The installation drawing of the variable geometry STF433 (Figure 24), shows the accessory package located in the fan duct stream. Moving the accessory package to a position below the fan case, as shown in Figure 39, makes them more accessable and removes flow blockage caused by these accessories when they are located in the duct. This allows more room for acoustic treatment in the duct, which reduces the treatment length and results in an overall nacelle length reduction of 23 in. (.584 m) for a fixed engine size. Removing the flow blockage in the duct also allows the nacelle symmetrical diameter to be reduced by 3 in (.076m). However, a local external fairing, extending 7 in (0.178 m) below the symmetrical diameter, must be placed over the external accessory package. The reductions in nacelle length and diameter produce a 12 percent reduction in nacelle weight.

A detailed comparison of the two nacelles for engines sized to accomplish the design mission is presented in Table XXI.

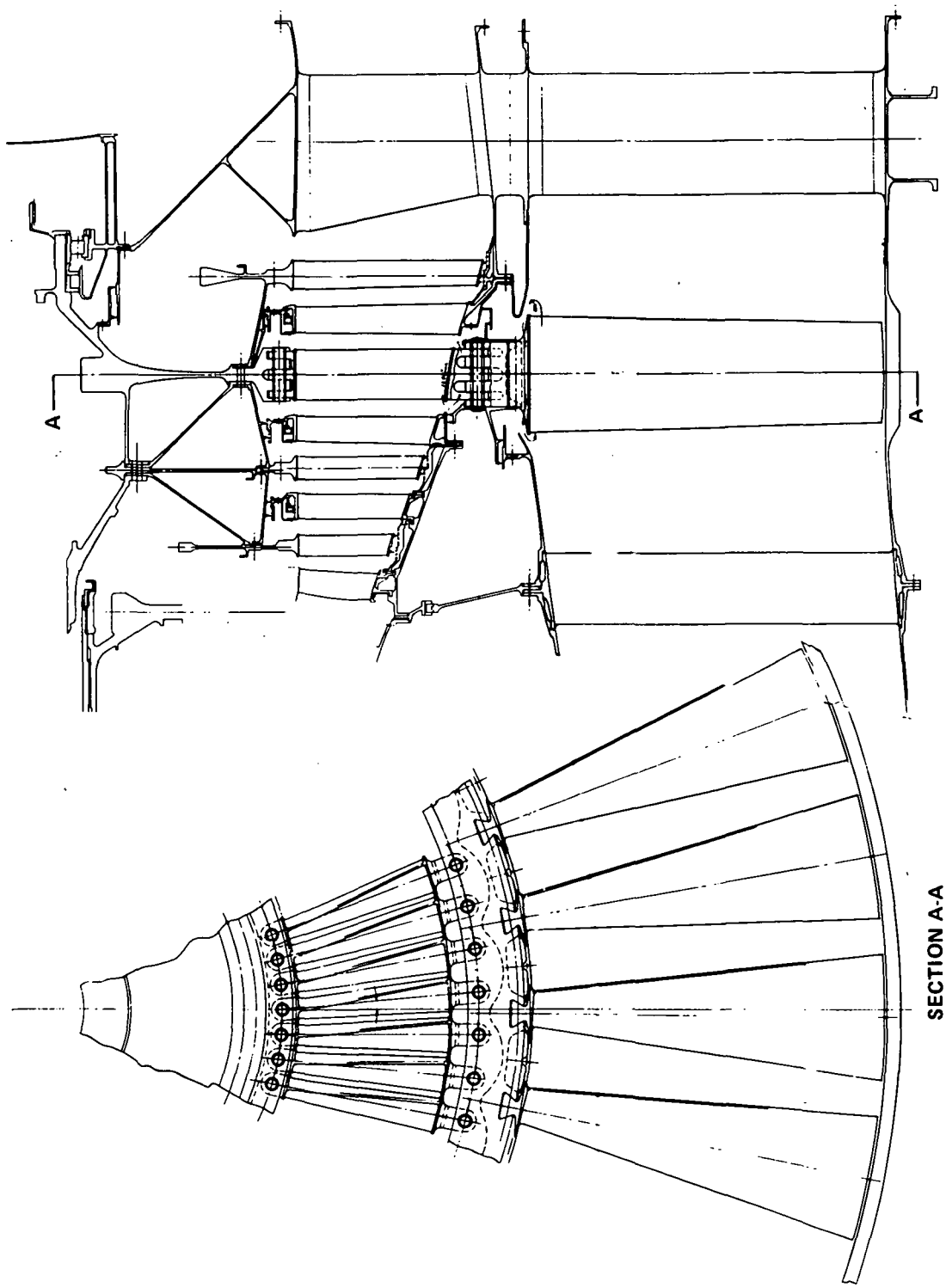

Figure 38 Conceptual Drawing of Aft Fan

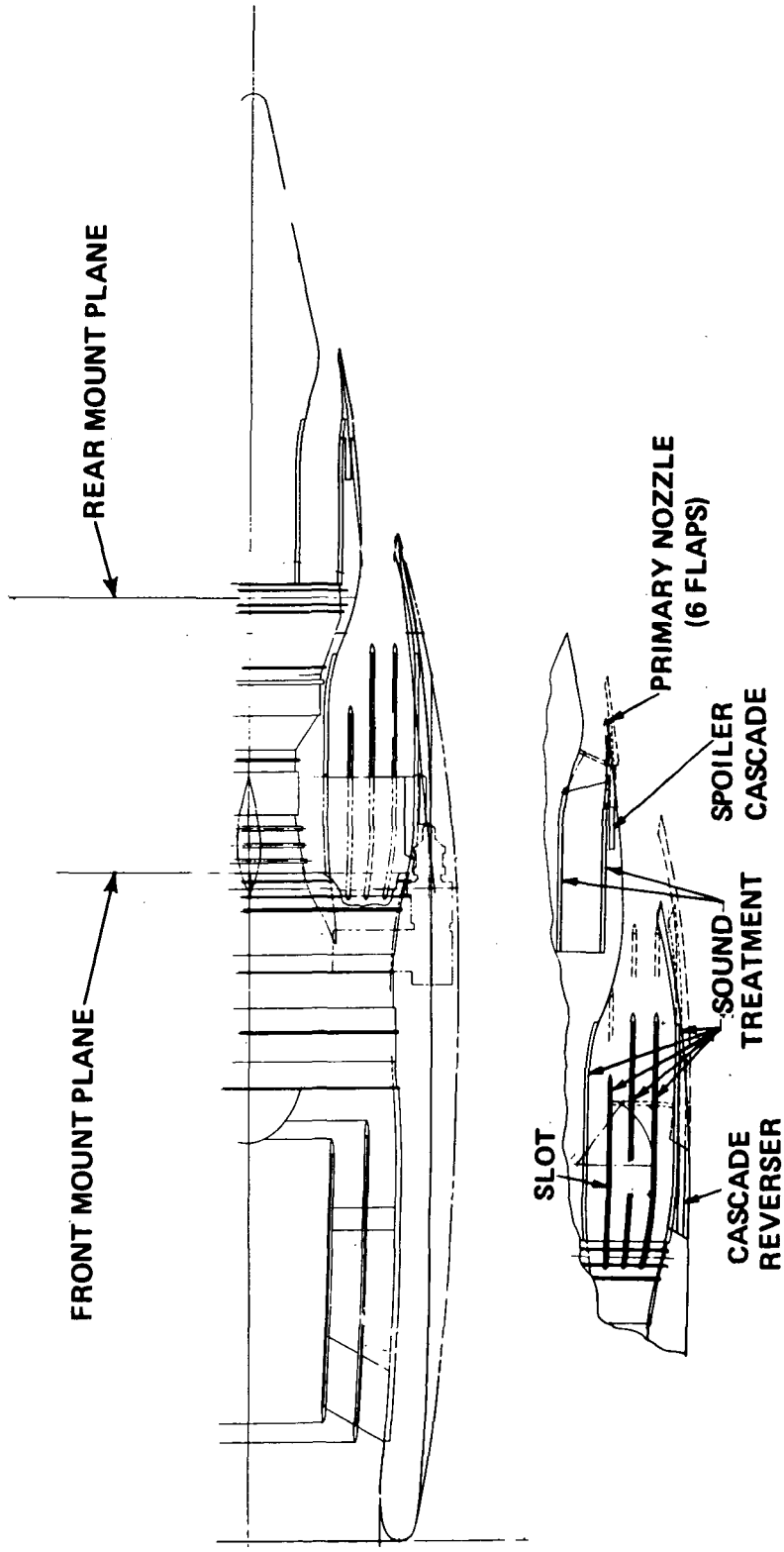

Figure 39 Treated (FAR-20) Nacelle With External Accessories

TABLE XXI

INTERNAL - EXTERNAL ACCESSORIES POD SUMMARY

	Variable Geometry STF433	
	Internal Accessories	External Accessories
Wall Treatment	Yes	Yes
Inlet Rings	2	2
Aft Duct Splitter	3	3
Sideline Noise α FAR, ΔePNdB	-20.0	-20.0
Cutback Noise α FAR, ΔePNdB	-20.5	-20.5
Approach Noise α FAR, ΔePNdB	-22.5	-22.5
Uninstalled SLTO Thrust, lbf, (N)	35440(157600)	35270(156900)
Bare Engine Weight, lbm (kg)	6850(3110)	6810(3090)
Nacelle Weight, lbm (kg)	2290(1040)	2015(915.)
Treatment Weight, lbm (kg)	1530(695)	1520(690)
Max. Nacelle Dia., inches (m)	100.1(2.54)	96.6(2.45)
Max. Nacelle Length, inches (m)	406(10.3)	381(9.68)

Since the external accessories arrangement was superior in vehicle performance, and also improved engine maintainability, it was used in conjunction with the following alternate pod designs.

Choked Inlet

Fan noise can be kept from propagating from the engine inlet if the airflow at the inlet throat were choked, thereby eliminating the need for inlet acoustic treatment. Such a variable geometry inlet would be very efficient at cruise, eliminating the high performance losses of extensive acoustic treatment.

The inlet throat area requirements to choke the inlet flow to the variable geometry STF433 are detailed in Table XXII. The variable geometry STF433 is well suited to use a choked inlet, since the inlet throat area variation is reduced by using the variable duct and primary nozzles and variable pitch fan to increase engine flow handling capabilities.

TABLE XXII

INLET THROAT AREA REQUIREMENTS FOR VARIABLE GEOMETRY STF433

Operating Condition	Engine Corrected Flow, lb/sec (kg/sec)	Inlet Area In^2	(M^2)	%Δ	Throat Mn
Cruise	1006 (456)	3100	(2.0)	Base	0.76
Sideline, Cutback	1065 (483)	3090	(1.99)	-0.3	1.0
Approach	800 (362)	2340	(1.51)	-25	1.0

A mechanical concept for a choked inlet is shown in Figure 40. Choking the inlet for low noise operation is provided by translating an axisymmetric plug to control the inlet throat area. This figure shows the three basic operating positions: fully retracted for normal cruise operation, translated slightly forward (with nozzle areas opened) for take-off, and fully forward for approach. The control and actuation system for the translating plug is located within the assembly. The entire unit is supported by struts which are, in turn, supported by extensions from the fan case. It should be noted that this conceptual definition is preliminary and other choked inlet configurations must be evaluated before an optimum design can be selected. One area in particular that requires study is the degree of choking required at the throat and the effectiveness of acoustic wall treatment in conjunction with a "soft" choke condition. Another is the capability for emergency translation to the fully-open position in the event of a missed approach.

The variable geometry STF433 installed in a nacelle utilizing a variable geometry inlet is shown in Figure 41. The extensive inlet treatment shown in Figure 39 was removed. Inlet pressure loss at cruise was reduced from 0.025 to 0.005, increasing specific thrust by 3.9 percent and reducing TSFC by 2.2 percent.

The choked inlet pod is compared with the FAR -20 ePNdB pod which utilizes inlet wall treatment and 2 rings in Table XXIII. Choked inlet tests conducted during the Fall of 1967 using a JT8D engine, produced a reduction in fan inlet noise of 20 PNdB. However, fan aft noise increased by 2 PNdB. No complete explanation can be made for this phenomenon. It may be that the choked inlet causes flow disturbances which interact with the fan blades, causing an increase in fan source noise. Since the fan source noise of the STF433 is aft-dominant, a 2 PNdB increase in aft noise increases the total noise by 1-2 ePNdB. Table XXIII also shows that a significant pod (treatment plus nacelle) weight reduction is obtained with the choked inlet.

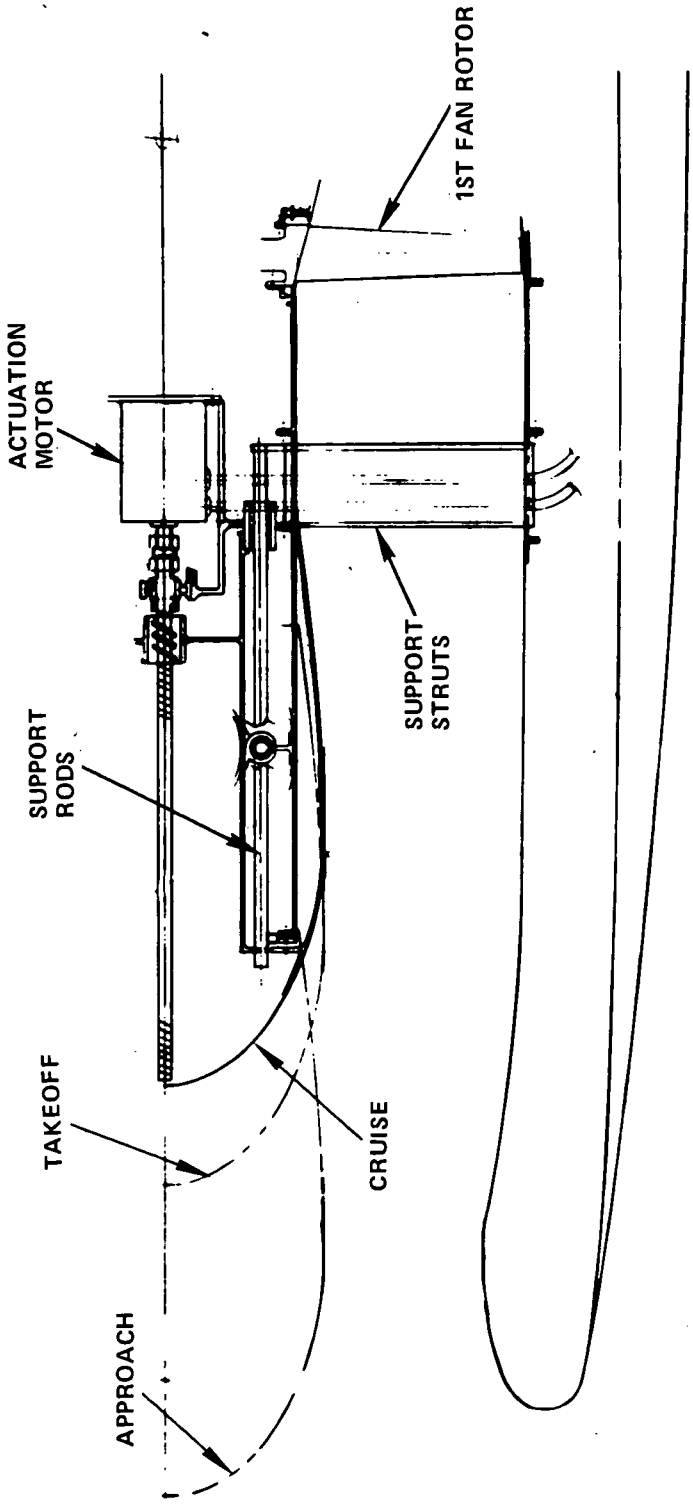

Figure 40 Mechanical Concept for Choked Inlet

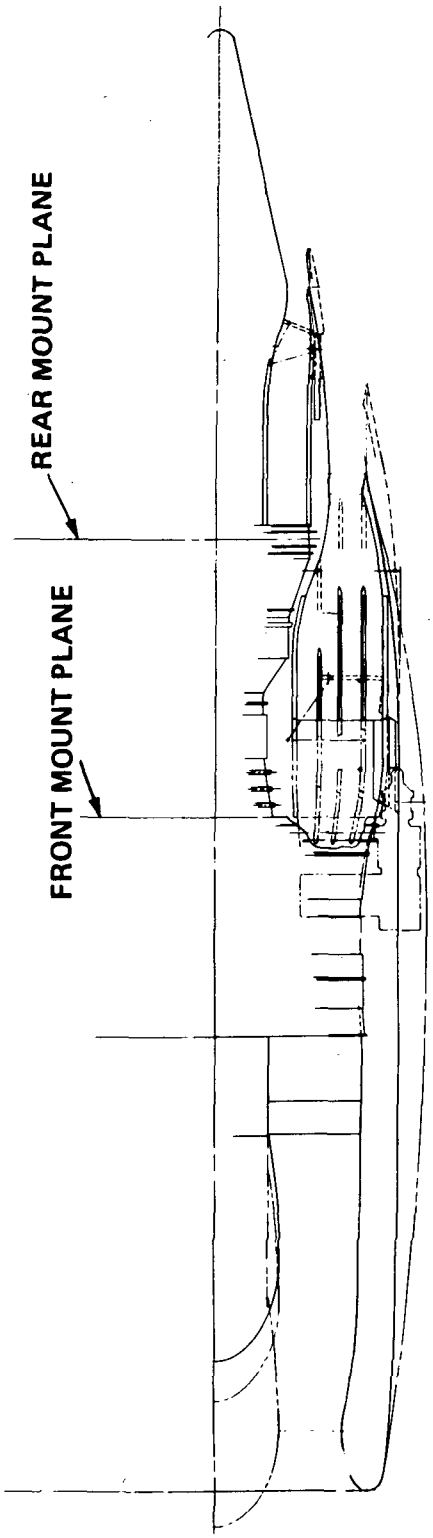

Figure 41 Choked Inlet Nacelle

TABLE XXIII

CHOKED INLET POD SUMMARY

	Variable Geometry STF433 (External Accessories)	
	Treated Inlet	Choked Inlet
Wall Treatment	Yes	Duct Only
Inlet Rings	2	No
Aft Duct Splitter	3	3
Sideline Noise α FAR, ΔePNdB	-20.0	-18.0
Cutback Noise α FAR, ΔePNdB	-20.5	-18.5
Approach Noise α FAR, ΔePNdB	-22.5	-21.5
Uninstalled SLTO Thrust, lbf (N)	35270(156900.)	32160. (143100.)
Bare Engine Weight, lbm (kg)	6809. (3090.)	6115. (2770.)
Nacelle Weight, lbm (kg)	2014. (915.)	2337. (1060.)
Treatment Weight, lbm (kg)	1523 (690)	749 (340)
Max. Nacelle Diameter, inches, (m)	96.6 (2.45)	92.2 (2.34)
Max Nacelle Length, Inches, (m)	381.1 (9.68)	380.7 (9.67)

Co-planar Nozzle/Umbrella Reverser

A co-planar nozzle/umbrella reverser was evaluated as an alternate to the separate nozzle/cascade reverser design. Two improvements were anticipated for this design. First, the increase in duct length for the co-planar nozzle configuration was expected to lead to a reduction in number of acoustic splitters in the fan duct. If the number of splitters could be reduced from three to one or two, and the reverser positioned somewhere other than in the fan duct, then these splitters could be designed to retract to the inner and/or outer surfaces of the fan duct. This would reduce duct losses during climb and cruise operation. The second associated benefit was to define a thrust reverser configuration with improved operational and maintainability characteristics relative to those being used in the new wide-body transports.

The first improvement did not materialize, mainly because reducing the number of duct splitters from three while maintaining the 0.45 duct Mach number for the high treatment effectiveness presented a severe penalty in nacelle contour. As shown in Figure 42, if acceleration within the fan nozzle does not begin before the inner wall diameter is increased around the turbine exit case, the diameter of the outer duct wall must be increased to meet the 0.45 Mach number area requirements. For the L/H duct treatment necessary to meet the FAR -20 goal, three splitters are required to avoid this diameter penalty. Retracting three concentric splitters is a difficult problem and no acceptable concept to accomplish this has yet been defined.

Promise of obtaining the second improvement was accomplished with the reverser design shown in Figure 42. The aerodynamic configuration for this umbrella reverser is based on wind tunnel tests conducted at P&WA^{TM}. When deployed, the umbrella which consists of a series of hinged segments, reverses both the primary and fan streams. Its kinematic design, in combination with the variable primary and duct nozzles, prevents back pressuring the primary stream in the transition stage. The "V" fence with trips provides a targeting capability so that direct impingement of reversed air on the fuselage and runway can be avoided. A failsafe locking device prevents premature or inadvertent deployment of the reverser. The entire reverser, when stowed, is contained within the afterbody which has been lengthened to accommodate the umbrella segments. As shown, the reverser assembly is supported off the turbine exit case. In this location, it has the potential for improved maintainability.

The potential benefits of this reverser relative to a conventional cascade reverser are summarized in Table XXIV. The potential problems for this reverser are also listed. This preliminary definition indicates that the umbrella reverser has sufficient merit to justify a more detailed design evaluation.

TABLE XXIV

CO-PLANAR NOZZLE WITH UMBRELLA REVERSER

Potential benefits over cascade reverser:

- One assembly in place of two
- Improved maintainability
- Eliminates need to block duct in region of acoustic splitters
- Duct acoustic splitters could be retracted

Potential problems:

- Common reverser can cause fan/engine exhaust interactions
- Reverser assembly hung off turbine exhaust case
- Failsafe characteristics
- Questionable targetability

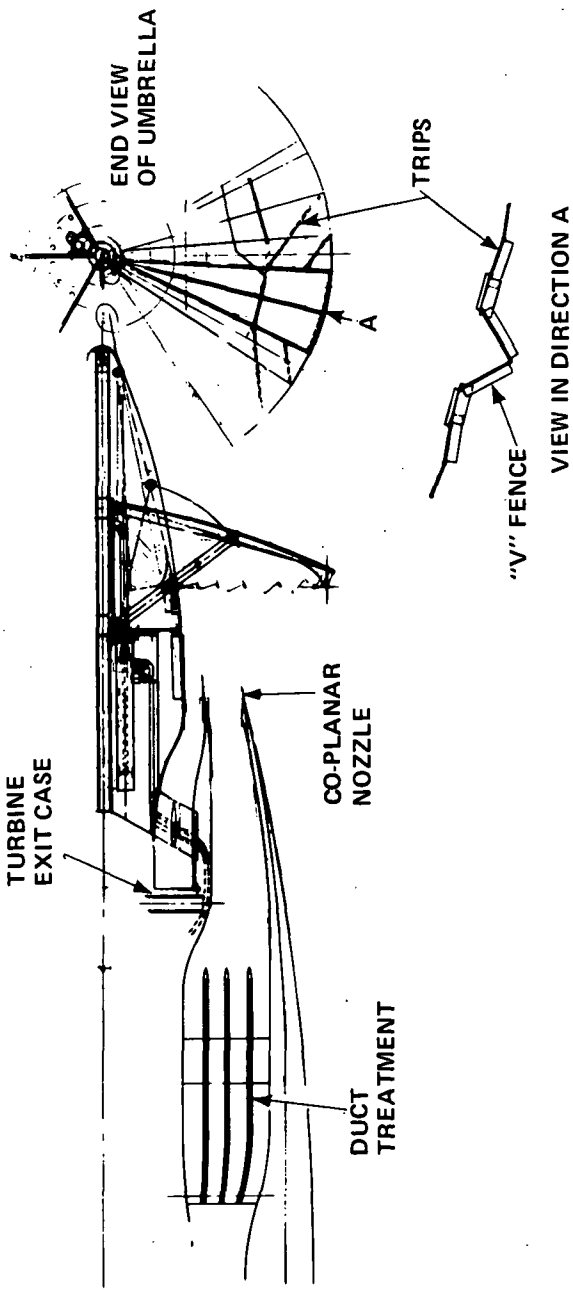

Figure 42 Conceptual Drawing of a Co-planar Nozzle and Umbrella Reverser

The nacelle configuration for the co-planar nozzle/umbrella reverser design is shown in Figure 43. There is no change in nacelle diameter but the overall length is increased approximately 16 inches because of the longer afterbody.

The installation characteristics for this design are summarized in Table XXV. As shown in this table, the noise characteristics are unchanged. There is, however, a possible noise improvement in the reverse mode that may be obtained with this concept. With the umbrella reverser, all fan exit noise is exposed to the duct treatment during reversing, thereby reducing fan-generated noise. In contrast, the cascade reverser is located forward of the fan duct acoustic treatment, which allows fan noise to circumvent the duct treatment. Tests of these reverser concepts are required to determine if noise improvements can be attained with this umbrella reverser concept.

TABLE XXV

CO-PLANAR NOZZLE/UMBRELLA REVERSER SUMMARY

	Variable Geometry STF433 (External Accessories)	
	Cascade Reverser	Co-planar Nozzle/ Umbrella Reverser
Wall Treatment	Yes	Yes
Inlet Rings	2	2
Aft Duct Splitter	3	3
Sideline Noise α FAR, ΔePNdB	-20.0	-20.0
Cutback Noise α FAR, ΔePNdB	-20.5	-20.5
Approach Noise α FAR, ΔePNdB	-22.5	-22.5
Uninstalled SLTO Thrust, lbf (N)	35270. (156900.)	35180. (156500.)
Bare Engine Weight, lbm (kg)	6810 (3090.)	6790 (3080.)
Nacelle Weight, lbm (kg)	2010 (915.)	2220 (1010.)
Treatment Weight, lbm (kg)	1520 (690.)	1450 (657.)
Max. Nacelle Diameter, inches (m)	96.6 (2.45)	96.5 (2.45)
Max. Nacelle Length, inches (m)	381 (9.68)	397 (10.10)

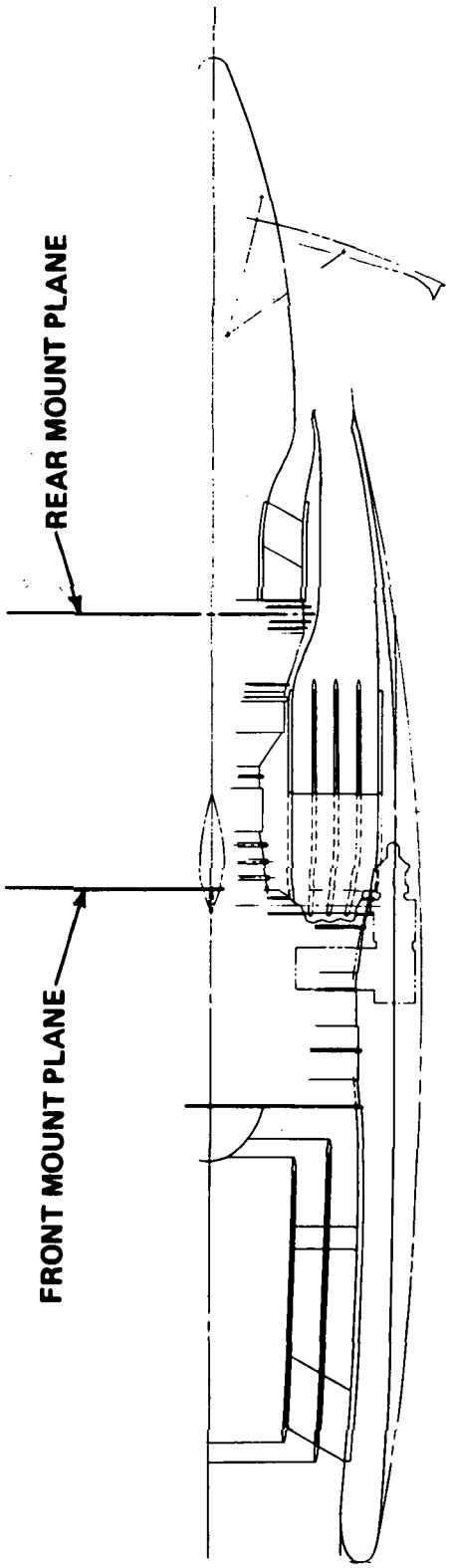

Figure 43 Treated (FAR-20) Nacelle With Umbrella Reverser - STF 433 Variable Geometry Engine

SYSTEMS EVALUATION

Aircraft performance and economic evaluations of the engines studied during this task were conducted in order to determine the system penalties associated with the attainment of low noise. The aircraft model used for these studies was designed for Mach 0.9 cruise and had a design range of 3000 N. Mi. (5550 km). Table XXVI presents a summary of the general aircraft characteristics and the advancements in aircraft structural and aerodynamic technologies and acoustic treatment and jet noise technologies used in this study.

TABLE XXVI

AIRCRAFT CHARACTERISTICS FOR SYSTEMS EVALUATION

Number of Passengers	200
Design Cruise Mach Number	0.90
Design Range, N.Mi. (km)	3000 (5550)
Cruise Altitude, Ft. (m)	36000 (11000)
Take-off Field Length, Ft. (m) (1000 ft Elevation 90 F)	8300 (2530)
Approach Speed @ Max. Landing Wt., Kts. (m/sec)	145 (74.5)
Approach Speed @ End Mission Wt., Kts. (m/sec)	135 (69.4)
Max. T. O. Wing Loading, lbf/ft^2 (N/m^2)	135 (6410)
Wing Sweep at Quarter Chord, Deg.	36.5
Wing Aspect Ratio	7.6
Cruise Lift/Drag ratio	13.9

Structures Technology

Ten-percent reduced structural weight relative to current technology

Aerodynamics Technology

Supercritical airfoil technology

1985 Acoustic Treatment Technology

Thirty-five percent increase in peak attenuation and 100 percent improvement in band width relative to current technology (reference 1).

1985 Jet Noise Technology

Reduced jet noise levels at jet velocities below 1000 ft/sec (305 m/sec) (reference 1).

A summary of the engines evaluated is presented in Table XXVII.

TABLE XXVII

ENGINE EVALUATION SUMMARY

Case	Engine	Description	Noise Level, ePNdB
1	STF433	Optimum aerodynamic untreated nacelle	FAR36
2	STF433	Wall treated nacelle	FAR36-9
3	STF433	Wall treatment + 2 inlet rings + 1 exhaust duct splitter	FAR36-15
4	Variable Geometry STF433 VG	Wall treatment + 2 inlet rings + 3 exhaust duct splitters	FAR36-20
5	STF433 VG	External Accessories	FAR36-20
6	STF433 VG	Choked Inlet	FAR36-20
7	STF433 VG	Umbrella Reverser	FAR36-20
8	STF456	Geared Two-Stage Fan BPR=10	FAR36-20
9	STF457	Single-Stage Fan BPR= 10	FAR36-16

A comparison of buried (center) engine weight, podded engine weight, pod drag and installed cruise thrust and fuel consumption at 36000 ft (11000m), 0.9 Mn for these propulsion systems is presented in Table XXVIII. The values in Table XXVIII reflect the engine sizes required for the resulting aircraft. These engines weights include the bare engine, thrust reversers, nacelle structure, engine accessories, strut, mount and acoustic treatment. The buried engine weight includes the center duct weight.

The results of the aircraft performance and economics evaluation are shown graphically in Figures 44, 45 and 46. These results are presented in terms of the changes in design gross weight (TOGW), direct operating cost (DOC) and Δ percent return-on-investment (ROI) resulting from the noise reduction relative to FAR36. Table XXIX lists the specific values of TOGW, DOC and ROI calculated for each case.

TABLE XXVIII

INSTALLED WEIGHT AND PERFORMANCE SUMMARY

Case	Buried Engine Weight ~ lbm/ Eng. (kg/Eng.)	Podded Engine Weight ~ lbm/Pod (kg/Pod)	Pod Drag ~ lbf/Pod (N/Pod)	Cruise TSFC ~ lbm/hr/lbf (g/sec/N)	Cruise Thrust ~ lbf (N)
1	8278 (3760)	7916 (3500)	494 (2195)	0.6778 (.0194)	6750 (30100)
2	8918 (4050)	9002 (4080)	589 (2620)	0.6820 (.0193)	6930 (30800)
3	10276 (4660)	10335 (4700)	632 (2810)	0.6985 (.0198)	7215 (31800)
4	12789 (5800)	13737 (6230)	1002 (4460)	0.7070 (.020)	7890 (35100)
5	12720 (5770)	13401 (6080)	988(4390)	0.7070 (.020)	7854 (34950)
6	11081 (5030)	12088 (5480)	918 (4080)	0.6913 (.0196)	7530 (33500)
7	12643 (5740)	13530 (6150)	950 (4220)	0.7092 (.02005)	7810 (34800)
8	13737 (6230)	13504 (6120)	799 (3550)	0.6547 (.0185)	7230 (32200)
9	13124 (5960)	12856 (5830)	832 (3770)	0.6894 (.0195)	7400 (32900)

TABLE XXIX

TOGW, DOC AND ROI SUMMARY

Case	1	2	3	4	5	6	7	8	9
TOGW ~ lbm	284100	292200	304300	332400	330700	317300	330600	316900	323200
TOGW ~ (kg)	128870	132500	138000	150770	150000	143900	150000	143700	146600
DOC ~ $/Block-hr	862.6	881.2	910.0	982.1	978.4	951.2	981.5	942.1	951.2
ROI, %	39.99	38.84	37.12	33.11	33.31	34.42	33.09	34.91	34.98
% Δ TOGW	Base	2.8	7.1	17.0	16.4	11.7	16.4	11.5	13.7
% Δ DOC	Base	2.2	5.5	13.9	13.4	10.3	13.9	9.2	10.3
% Δ ROI	Base	-1.15	-2.87	-6.88	-6.68	-5.57	-6.9	-5.08	-5.01

The STF433 with the optimum aerodynamic untreated nacelle meets FAR36 and is used as the base for comparing TOGW, DOC and ROI of the various engines and acoustic treatment schemes studied. The STF433, using wall treatment only, achieves FAR36-9 ePNdB with penalties of +2 percent TOGW, +2 percent DOC and -1 percent Δ ROI. These penalties result principally form the increased nacelle weight and drag over the optimum nacelle.

FAR 36 - 15 ePNdB is achieved with the STF433 using wall treatment, two inlet rings and one fan duct splitter. This noise level is achieved with penalties of +7 percent TOGW, +6 percent DOC and -3 percent Δ ROI. This configuration incurs the same nacelle weight and drag penalties as the FAR36-9 ePNdB nacelle, but the extensive addition of acoustic treatment results in significant thrust and TSFC penalties. The reduction in uncycled thrust and the increase in fuel consumption, account for approximately 60 percent of the TOGW increment and 50 percent of the economic penalty. The remainder of the economic penalty is due to the increased weight and cost of acoustic treatment.

The FAR -20 ePNdB noise level is obtained with the variable geometry STF433. The penalties for the STF433 V.G. with accessories located in the fan duct (case 4) are +17 percent TOGW, +14 percent DOC and -7 percent Δ ROI. With respect to the uncycled characteristic of Case 1, the variable geometry STF433 experiences TOGW penalties of +1.5 percent due to engine weight, and +3.4 percent due to nacelle weight, +4.4 percent due to nacelle drag, +3 percent due to increased fuel consumption, +2.4 due to thrust and +2.4 percent due to acoustic weight. ROI penalties are: -1.1 percent due to nacelle weight, -.8 due to nacelle drag, -.9 percent due to TSFC, -1.1 percent due to thrust loss, -1.6 percent due to acoustic weight (and associated cost), -1.0 percent due to engine weight and price and .5 percent due to reverser price.

The penalties for the STF433 V.G. with externally located accessories (case 5) and +16.5 percent TOGW, +13.5 percent DOC, and -6.5 percent Δ ROI. The use of externally mounted accessories reduces the penalties in TOGW due to nacelle weight to +2.8 percent and the penalty due to nacelle drag to +4.4 percent. The Δ ROI penalty is reduced by approximately 0.2 percent by the reduced penalty in nacelle weight and cost.

These penalties are reduced by the use of a choked inlet which eliminates the inlet rings and inlet wall treatment with an attendant reduction of 2 percent in cruise fuel consumption. The system penalties for the choked inlet are +12 percent TOGW, +10 percent DOC and -5.5 percent Δ ROI. It is thus seen that the use of the choked inlet results in a significant reduction in system penalties for the FAR 36-20 ePNdB noise level.

The least economic penalty for the FAR 36 - 20 ePNdB noise goal is obtained with the BPR = 10, fixed geometry, two-stage geared fan, STF456 engine. From Figures 44, 45 and 46, it can be seen that the system penalties for the STF456 are +12 percent TOGW, +9 percent DOC and -5 percent Δ ROI. While this engine does enjoy a fuel consumption advantage, this advantage is offset by the increased engine weight and the increased nacelle weight and drag. Economically the fuel consumption advantage is offset by the thrust loss (uncycled) with the resultant ROI penalty due primarily to engine weight, acoustics weight (and associated cost) and engine price.

Figures 44, 45, and 46 show that the single-stage 10 BPR STF 457, which meets a FAR 36-16 ePNdB noise level, has penalties of +13 percent TOGW, +10 percent DOC and a -5 percent Δ ROI. The TOGW and economic penalties for the single-stage STF457 are due primarily to acoustic weight, pod drag and an uncycled thrust loss. The economic penalty is in spite of the uncycled engine price advantage of the single stage configuration. At the same noise level, a corresponding two-stage fan engine would have a +8 percent TOGW, +7 percent DOC and -3.5 percent Δ ROI.

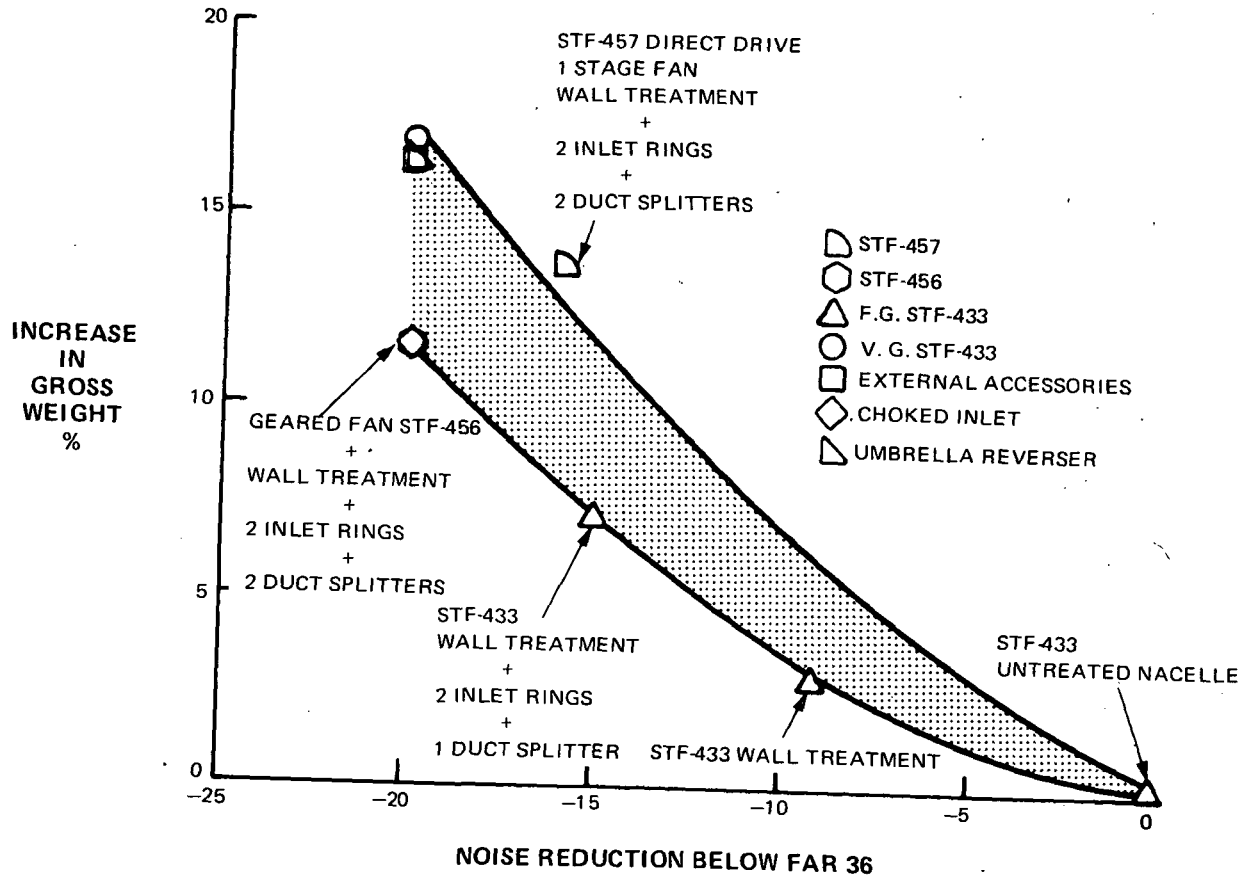

Figure 44 *Effect of Noise Level On Gross Weight ATT Mach 0.90 Configuration*

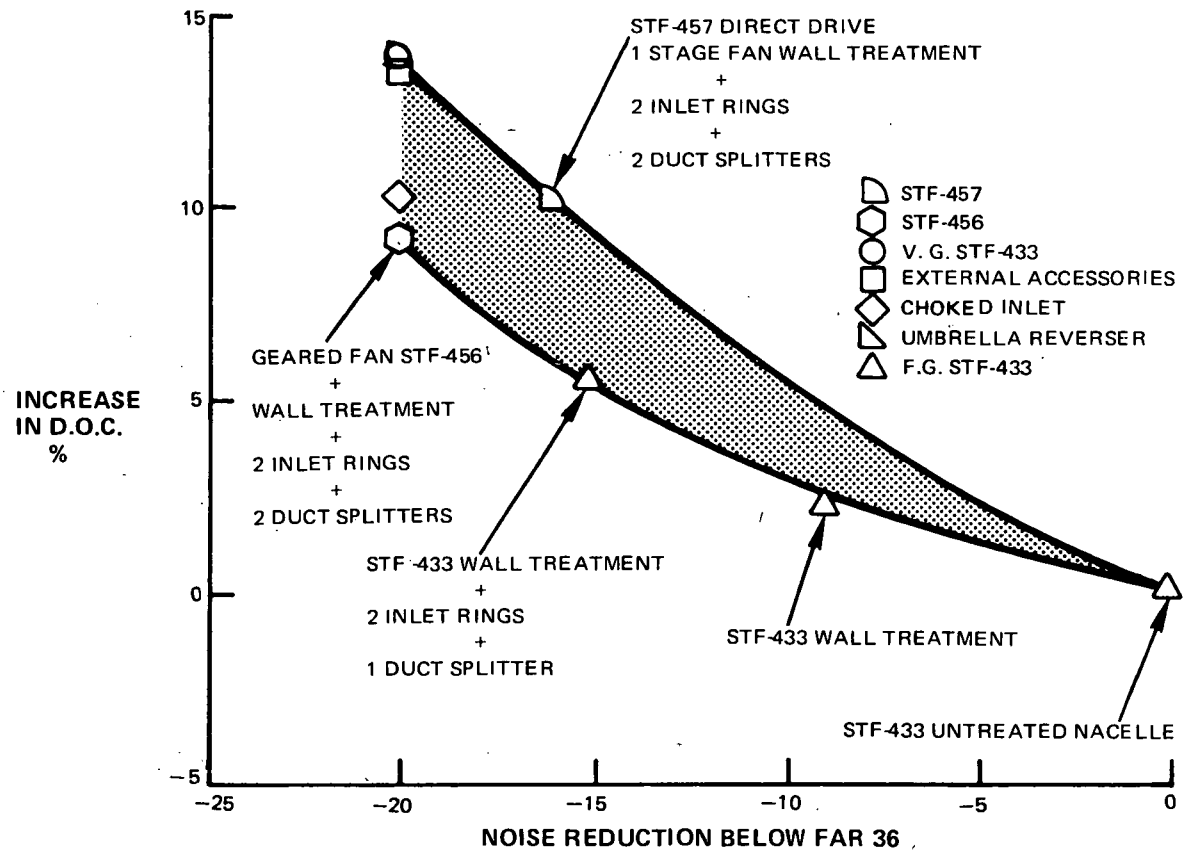

Figure 45 Effect of Noise Level On Direct Operating Cost - ATT Mach 0.90 Configuration

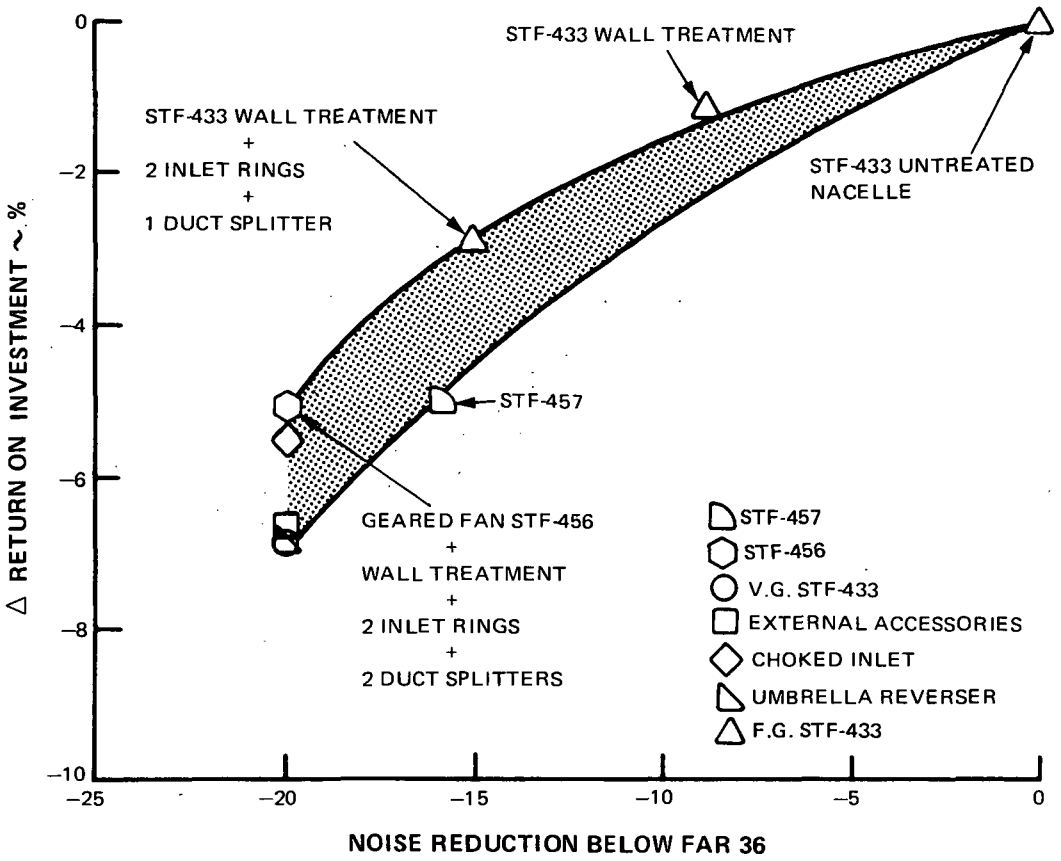

Figure 46 Effect of Noise Level On Investment (ROI) - ATT Mach 0.90 Configuration

A comparison of the penalties for the fixed geometry STF456 and the variable geometry STF433 shows that the TOGW, DOC and ROI penalties are less for the fixed geometry STF456 than for the variable geometry STF433. The advantage of the STF433 in base engine weight, price and drag are offset by the superior fuel consumption and less complex (expensive) pod of the STF456. A mission summary comparison of the STF433,the variable geometry STF433 and the STF456 is presented in Table XXX.

TABLE XXX

SUMMARY OF AIRCRAFT AND MISSION CHARACTERISTICS
Design Range = 3000 N. Mi.

Case	3	4	8
Engine	STF 433	STF433 Variable Geometry	STF 456
Noise Level, ePNdB	FAR-15	FAR-20	FAR-20
Takeoff Gross Weight lbm (kg)	304300 (138000)	332400 (151000)	316900 (144000)
Operating Weight Empty lbm (kg)	164200 (74500)	179500 (81400)	177000 (80300)
Lift/Drag	14.0	13.6	13.8
Mission Fuel Summary			
Takeoff Fuel ~ lbm (kg)	1015 (460)	1125 (510)	875 (395)
Climb Fuel ~ lbm (kg)	10240 (4650)	12055 (5470)	14095 (6390)
Cruise Fuel ~ lbm (kg)	69925 (31700)	78525 (35600)	66195 (30000)
Reserves ~ lbm (kg)	18195 (8240)	20435 (9260)	18060 (8190)

CONCLUSIONS

Analytical studies were conducted to investigate concepts other than fixed geometry twin spool turbofans for future CTOL subsonic commercial transports. Propulsion systems with noise levels ranging from FAR Part 36 to 20 ePNdB lower than FAR Part 36 were examined, and aircraft gross weight, direct operating cost and return on investment calculated for a 200 passenger, 3000 nautical mile aircraft.

Two propulsion systems, one with a fixed geometry, 10.0 bypass ratio, low tip speed, geared two-stage fan (STF456) and another with a variable geometry, 6.5 bypass ratio, low tip speed, direct-drive two-stage fan (STF433VG) were designed to meet FAR – 20 ePNdB noise levels with extensive acoustic treatment. The geared fan system, which reduces the fan and jet noise to the required level by proper selection of cycle characteristics, produces a return on investment (ROI) which is 2 percent higher than that of the system which uses variable fan and nozzle geometry to effectively increase the bypass ratio in order to meet the jet noise requirement. Relative to a system which just meets FAR Part 36, the geared fan system achieves FAR minus 20 ePNdB at the expense of a 5 percent reduction in ROI.

Noise footprint contours were calculated for all propulsion systems. Comparisons of these footprint areas and the economic penalties required to achieve low noise levels are presented in Figures 47 and 48 for a 3° approach and take-off, respectively. Reducing the engine-generated noise to FAR –8 ePNdB, which is the current estimated airframe generated noise floor, produces significant reductions in footprint area with a Δ ROI penalty of 1 percent. Adding inlet rings and duct splitters to further reduce noise provides diminishing area reductions with high economic penalties.

If it is necessary to achieve large noise reductions in the inlet, the use of a choked inlet, to replace the inlet wall treatment and acoustic rings, can provide the required noise reductions with significant benefits in subsonic cruise performance and aircraft economics. For example, improvements of 2 percent in cruise specific fuel consumption and 1 percent in ROI were achieved for the STF433VG when a choked inlet was substituted for inlet wall treatment and acoustic rings.

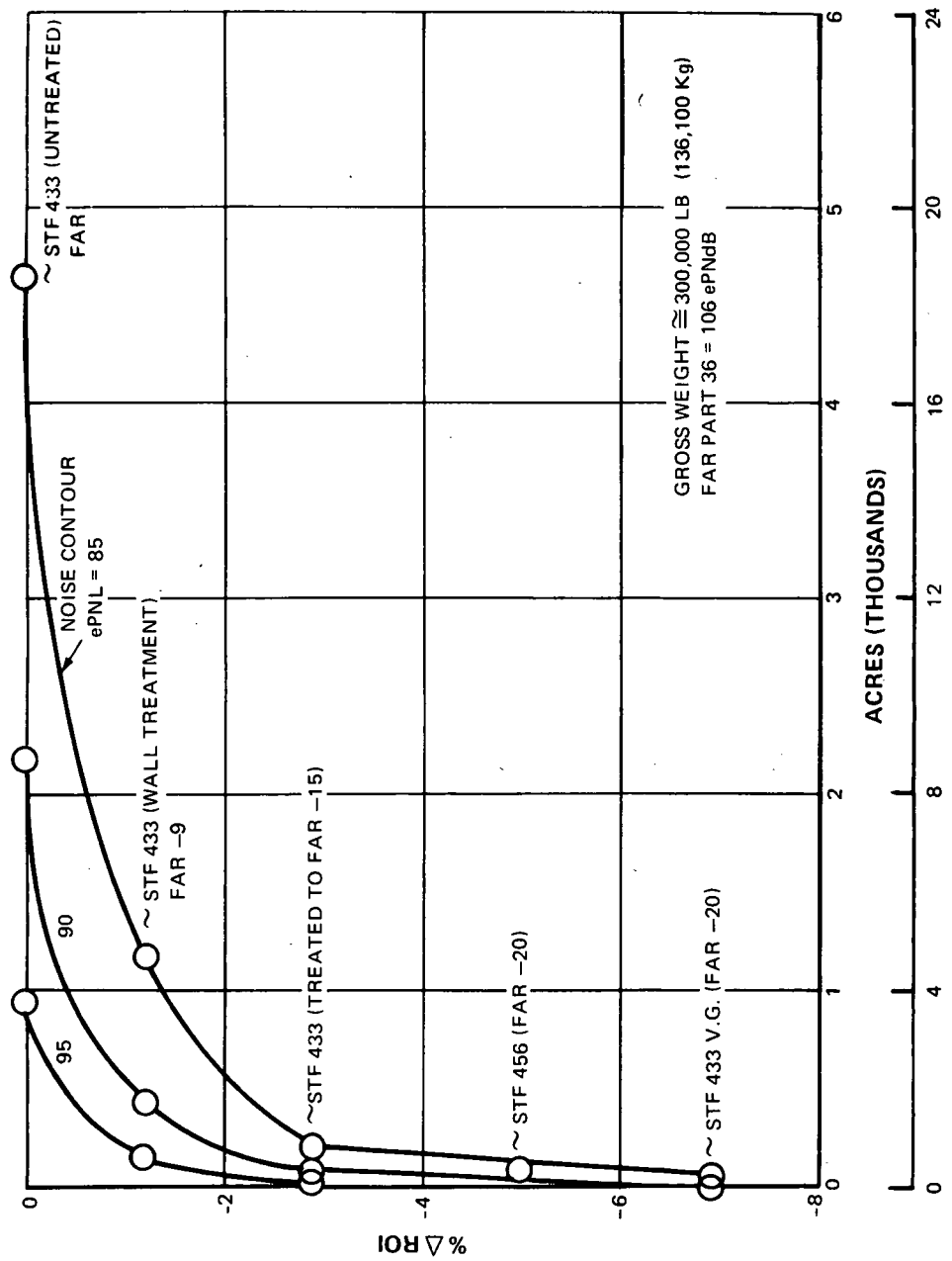

Figure 47 Percent Δ ROI Versus Noise Contour Area for a Three-Degree Approach

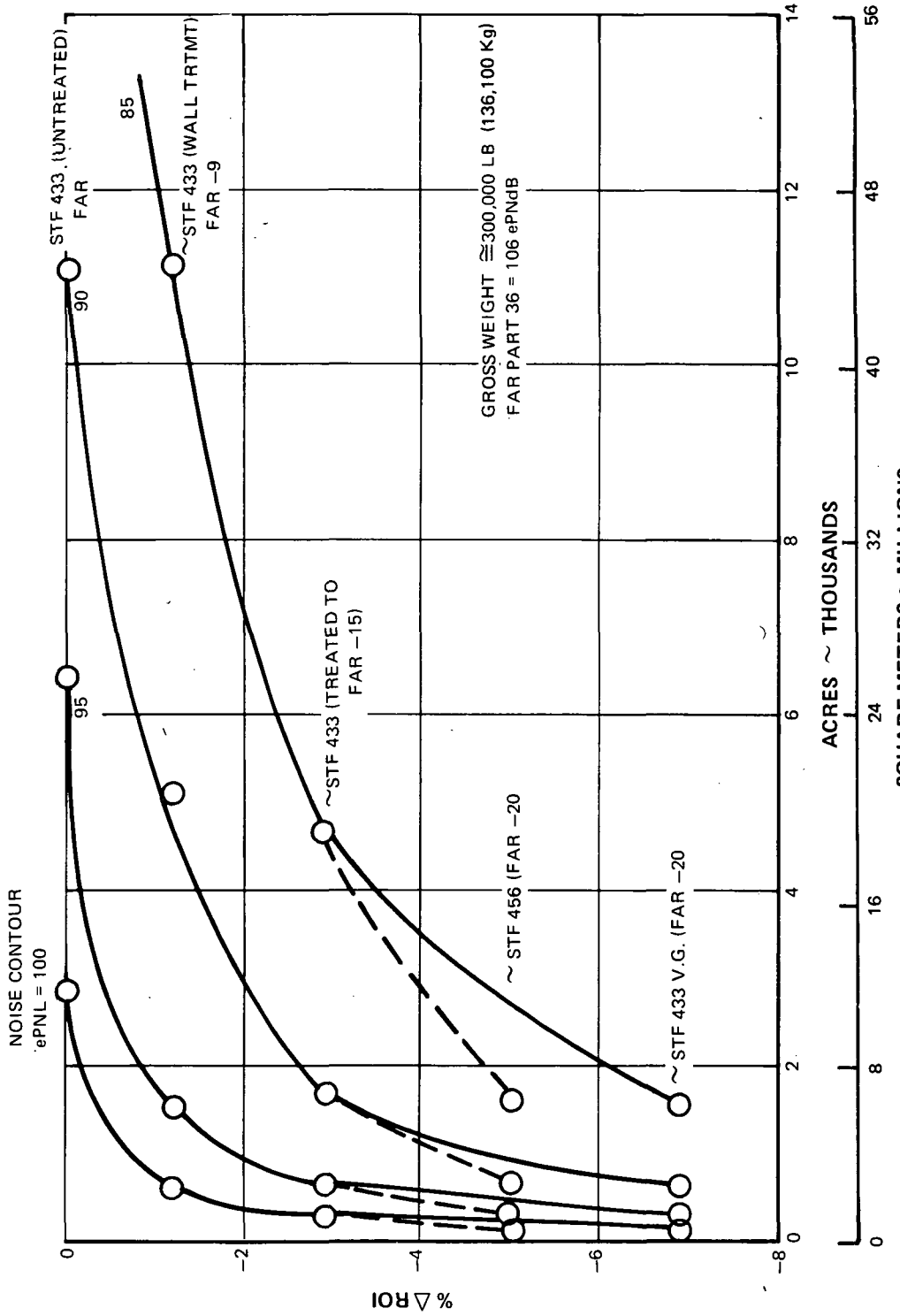

Figure 48 Percent Δ ROI Versus Noise Contour Area At Take-Off With Cutback

RECOMMENDATIONS

Selection of propulsion systems for future economical transports requires careful consideration of the aricraft mission, noise regulations and aircraft economics in order to define a system which will be acceptable to the airport community and airlines.

Aircraft cruise speeds between Mach 0.90 and 0.98 and noise goals of FAR Part 36 minus 10, 15 and 20 have been examined during the present and reference 1 studies. Figure 49 shows the effect of cruise speed and noise on the cycle characteristics selected to meet these noise goals with minimum penalty to the aircraft gross weight and economics. If design cruise speed is decreased, the optimum bypass ratio tends to increase. The propulsion systems selected to achieve these noise goals incorporate advanced technology components and materials and utilize low tip speed, two-stage fans with advanced acoustic treatment. As bypass ratio is increased, the optimum cycle fan pressure ratio decreases, thereby permitting lower fan tip speeds. Since the fan pressure ratios required for these cycles are in the range attainable with single- and two-stage fans, acoustic and performance testing of both high tip speed single-stage fans and low tip speed two-stage fans should be performed over the range of fan pressure ratios between 1.6 and 2.1 to determine the differences between forward and aft propagated noise characteristics.

Future noise regulations and fan designs may also require major advances in low pressure turbine technology. For the 1.95 fan pressure ratio required for a FAR minus 15 ePNdB system, a two-stage fan has a higher efficiency than a single-stage fan. However, if direct drive systems are used, the high speed turbine used with the single-stage fan will be more efficient than the low speed turbine required by the two-stage fan. Development of a high efficiency low speed turbine is recommended. A high work – low speed turbine may also be required to drive a single-stage, 1.7 pressure ratio fan, if noise goals of FAR minus 20 ePNdB are required. If a two-stage, 1.7 pressure ratio fan is selected, development of a gearbox may be necessary.

Acoustic and economic studies of a Mach 0.9 commercial aircraft indicate that a noise goal of FAR minus 10 ePNdB will provide significant noise footprint area reductions with small economic penalties. Future noise regulations should consider noise footprints in conjunction with absolute noise levels to establish the point of diminishing return.

Noise abatement procedures have also been proposed. Uniform procedures need to be established in order that their contribution to noise reduction can be fully evaluated. Noise abatement procedures may affect both cycle selection and treatment requirements for future aircraft.

Studies should be conducted to determine the impact of thrust reverser operation on community noise. If it is a problem, studies to develop reverser concepts which will reduce this noise should be conducted.

Propulsion systems designed for FAR −10 to −20 noise targets may require extensive inlet and fan duct acoustic treatment. Further experimental and analytical studies of variable geometry choked inlets and static acoustic treatment rings are recommended to determine the

performance, weight, cost, complexity, maintainability and reliability of these noise reduction systems. Acoustic tests should be performed to evaluate the impact of the choked inlet support struts on noise emanating from the exit of the fan. Design of a choked inlet for low power approach operation should also consider the use of a variable fan duct nozzle to increase the inlet airflow. This will both reduce the amount of inlet area variation required, and reduce fan-generated noise by reducing fan pressure ratio at the expense of the added cost, weight and complexity of the variable nozzle.

Design of advanced propulsion systems for future low noise transports must center around integration of the engine with the nacelle and airframe. The various disciplines that require study are: integration of acoustic treatment with nacelle structure; methods of reducing the performance penalties of acoustic treatment such as retractable acoustic rings; techniques to improve maintainability/reliability characteristics despite the complications of extensive acoustic treatment; new concepts for integrating thrust reversers with acoustic treatment and variable nozzles; and optimizing the nacelle design for the contrasting requirements of low noise and good cruise performance. To start with, these areas require exploratory study to discover, evaluate and screen advanced concepts. The next step would be to conduct more detailed design studies in the areas that show the most potential. Table XXXI lists the areas that are recommended for future study.

TABLE XXXI

RECOMMENDATIONS

- INTEGRATED ENGINE/NACELLE DESIGN STUDY
  - ACOUSTIC TREATMENT AND RELATED PROBLEMS
    - FOREIGN OBJECT DAMAGE
    - ANTI-ICING
    - PERFORMANCE LOSSES
    - INTEGRAL STRUCTURE
    - REVERSERS INTEGRAL WITH TREATMENT
    - RETRACTABLE RINGS AND SPLITTERS
    - ENGINE ACCESS WITH EXTENSIVE TREATMENT
  - MAINTAINABILITY/RELIABILITY IMPROVEMENTS
  - VARIABLE NOZZLE/REVERSER COMBINATIONS
  - INLET DESIGN; TAKE-OFF NOISE AND PERFORMANCE VS CRUISE PERFORMANCE

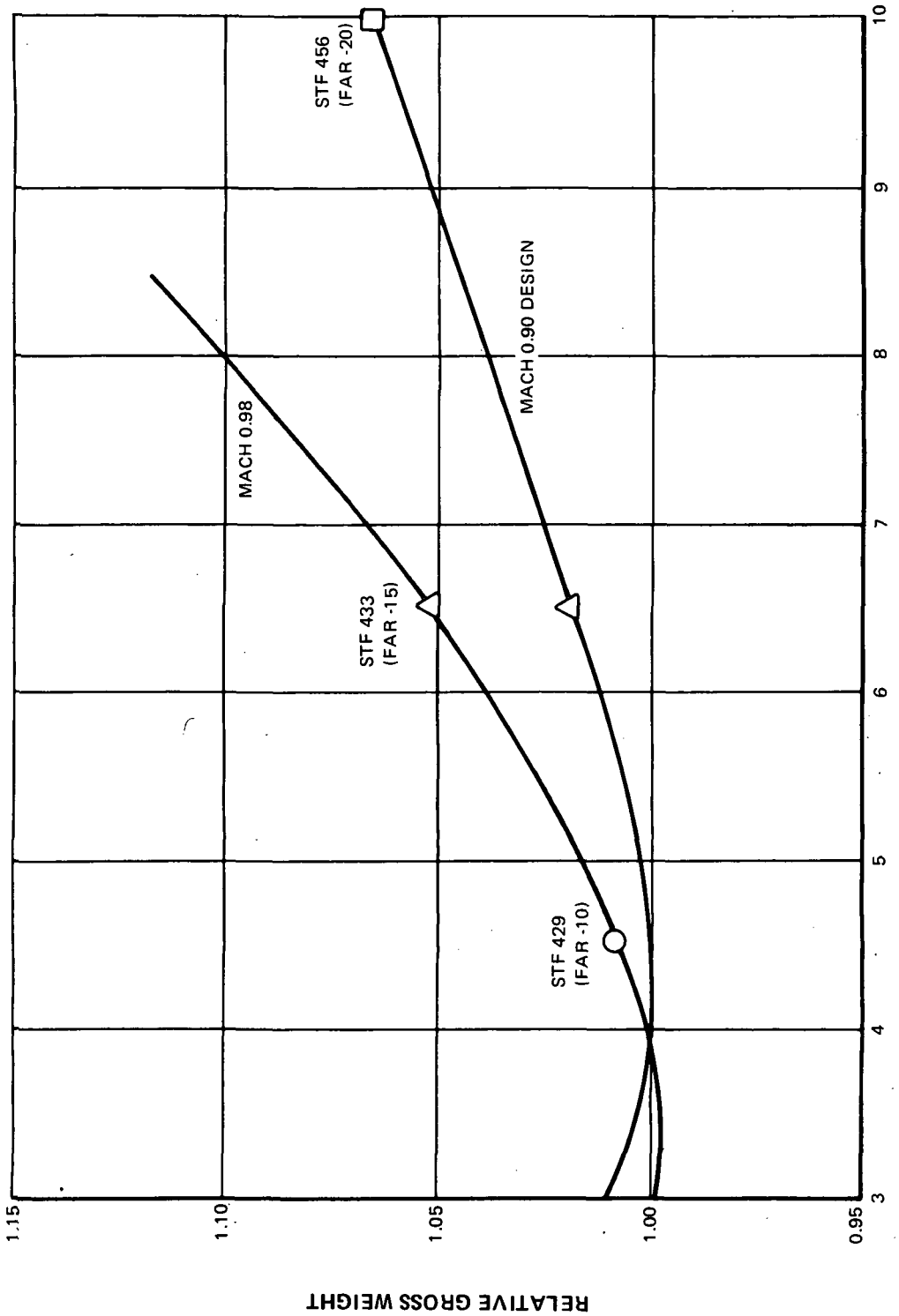

Figure 49 Impact of Cruise Speed On Bypass Ratio Selection

LIST OF SYMBOLS

A	Area, ft^2, (m^2)
A18	Fan Duct Exhaust Nozzle Throat Area, ft^2, (m^2)
A8	Primary Exhaust Nozzle Throat Area, ft^2 (m^2)
A_{DUCT}	Fan Duct Area, in^2, (m^2)
BPR	Bypass Ratio
CET	Combustor Exit Temperature, °F, (°K)
DOC	Direct Operating Cost, ¢/seat-mi; Direct airplane costs including flying operation, direct maintenance (with burden) and flight equipment depreciation as defined in the Civil Aeronautics Board (CAB) Uniform System of Accounts and Reports
ePNL	Effective Perceived Noise Level, ePNdB
FAR	Federal Aviation Regulations
FPR	Fan Pressure Ratio
Fn	Total Net Thrust, lbf, (N)
L/H	Ratio of Acoustic Treatment Length to Passage Height
MND	Fan Duct Stream Mach Number
OPR	Overall Fan-Compressor Pressure Ratio
PNL	Perceived Noise Level, PNdB
PTD	Fan Duct Total Pressure (P_{t13}), psia, (N/m^2)
ROI	Return On Investment, %, After-tax annual return on total investment in flight equipment plus related spares, based on a discounted cash flow analysis.
SLTO	Sea Level Take-Off
STF	Study Turbofan
TOGW	Aircraft Take-Off Gross Weight, lbm, (kg)

TSFC	Thrust Specific Fuel Consumption, lbm/hr-lbf, (g/sec - N)
TTD	Fan Duct Total Temperature (T_{T13}), °F, (°K)
$UT/\sqrt{\theta_{T2}}$	Corrected Fan Tip Speed, ft/sec, (m/sec)
VJD	Fan Duct Nozzle Relative Exhaust Velocity, ft/sec, (m/sec)
VJP	Primary Stream Nozzle Relative Exhaust Velocity, ft/sec, (m/sec)
WAD	Fan Duct Stream Flow Rate (W13) lbm/sec, (kg/sec)
WADC	Fan Duct Stream Corrected Airflow $W13\sqrt{T_{T13}}/P_{T13}$, $\frac{\text{lbm}\sqrt{°R}\,\text{in}^2}{\text{lbf - sec}}$ $\left(\frac{\text{kg}\sqrt{°K}\,\text{m}^2}{\text{kN - sec}}\right)$
WA_{T2}	Total Corrected Fan Inlet Airflow $W2\sqrt{\theta_{T2}}/\delta_{T2}$, lbm/sec, (kg/sec)
η	Efficiency
δ_{TX}	Relative Total Pressure at a given engine station (PTX/14.7 psia), (PTX/101200 N/m^2)
θ_{TX}	Relative Total Temperature at a given engine station (TTX/518.7°R), (TTX/288°K)

REFERENCES

1. Brines, Gerald L.; "Studies for Determining the Optimum Propulsion System Characteristics for use in a Long Range Transport Aircraft"; NASA CR-120950 (Contractors Reference No. PWA-4449); Pratt & Whitney Aircraft Division of United Aircraft Corporation, July, 1972

DISTRIBUTION LIST

	Copies
National Aeronautics and Space Administration **Washington, DC 20546**	
Code R, Mr. Roy P. Jackson	1
Code RD-M, Mr. Edwin C. Kilgore	1
Code RD-P, Mr. George W. Cherry	1
Code RD-T, Dr. Seymour C. Himmel	1
Code AAD-2, Dr. J. Ian Dodds	1
Code RG, Mr. Gerald G. Kayten	2
Code RH, Mr. Albert J. Evans	1
Code RA, Mr. William S. Aiken	1
Code RL, Mr. Harry W. Johnson	2
Code RW, Mr. George C. Deutsch	1
Code RE, Mr. Frank J. Sullivan	1
Code RX, Mr. Richard J. Wisniewski	1
National Aeronautics and Space Administration **Ames Research Center** **Moffett Field, CA 94035**	
Code D, Dr. Hans M. Mark	1
Code FAV, Mr. Rodney O. Bailey	1
National Aeronautics and Space Administration **Lewis Research Center** **21000 Brookpark Road** **Cleveland, OH 44135**	
Mr. B. T. Lundin, Director, MS: 3-2	1
Dr. B. Lubarsky, MS: 3-3	1
Mr. M. A. Beheim, MS: 86-1	1
Mr. W. L. Stewart, MS: 501-5	1
Mr. R. W. Schroeder, MS: 501-5	1
Mr. J. H. Povolny, MS: 60-6	1
Mr. E. W. Conrad, MS: 501-4	1
Mr. C. C. Ciepluch, MS: 501-4	1
Mr. D. N. Bowditch, MS: 86-1	1
Mr. R.J. Weber, MS: 86-1	1
Dr. E.J. Rice, MS: 501-5	1
Mr. J. F. Dugan, Jr., MS: 86-1	1
Mr. A. J. Glassman, MS: 77-2	1
Mr. R. R. Secunde, MS: 500-202	1
Mr. R. J. Rulis, MS: 501-2	1
Mr. A. A. Medeiros, MS: 501-4	1
Mr. M. J. Hartmann, MS: 5-9	1
Mr. S. S. Manson, MS: 49-1	1
Mr. J. B. Esgar, MS: 60-4	1
Mr. L. W. Schopen, MS: 500-206	1
Mr. R. J. Antl, MS: 501-4	43
Mr. L. M. Wenzel, MS: 100-1	1
Mr. N. T. Musial, MS: 500-311	1
Library, MS: 60-3	2
Report Control Office, MS: 5-5	1
National Aeronautics and Space Administration **Flight Research Center** **P. O. Box 273** **Edwards, CA 93523**	
Mr. Lee R. Scherer, Director, Code C	1
Mr. D. A. Deets, Code R	1
National Aeronautics and Space Administration **Langley Research Center** **Hampton, VA 23365**	
E. M. Cortright, Director, MS: 106	1
O. W. Nicks, Deputy Director, MS: 103	1
Dr. J. E. Duberg, Assoc. Dir., MS: 103	1
R. E. Bower, MS: 116	1
T. A. Toll, MS: 249-A	12
W. J. Alford, Jr., MS: 249-A	1
Air Transport Association of America **1000 Connecticut Avenue, NW** **Washington, DC 20036**	
Vern W. Ballenger	1
Department of Transportation **Federal Aviation Administration** **Washington, DC 20590**	
George P. Bates, Jr., Code RD-700	1
Grumman Aerospace Corporation **South Oyster Bay Road** **Bethpage, Long Island, NY 11714**	
Mark H. Siegel, Dept. 391, Plant 30	1
Headquarters **United States Air Force** **Washington, DC 20330**	
Lt. Col. Robert H. Blinn, Jr., AFRDQ	1

DISTRIBUTION LIST (Cont'd)

	Copies
Department of the Air Force AFML Wright-Patterson Air Force Base, OH 45433	
Bernard Chasman	1
Department of the Air Force AFFDL Wright-Patterson Air Force Base, OH 45433	
Maj. Joseph E. Graetch	1
Lawrence Kummeth	1
Cecil Wallace	1
Secretary of the Air Force/SAFRDD Washington, DC 20330	
Laurence K. Loftin, Jr.	1
Department of the Air Force AFAPL Wright-Patterson Air Force Base, OH 45433	
George E. Thompson	1
Department of the Navy Naval Air Systems Command Washington, DC 20360	
James C. Taylor, Code AIR 530141C	1
Trans World Airlines, Inc. 605 Third Avenue New York, NY 10016	
Edward A. Carroll	1
United Air Lines, Inc. San Francisco International Airport San Francisco, CA 94128	
Richard E. Coykendall	1
United Air Lines, Inc. P. O. Box 66100 Chicago, IL 60666	
Harry G. Lehr	1
American Air Lines, Inc. 633 Third Avenue New York, NY 10017	
M. B. Fannon	1
Pan American World Airways, Inc. Pan Am Building New York, NY 10017	
William F. Hibbs	1
Wright-Patterson Air Force Base AFAPL/TBP Wright-Patterson Air Force Base, OH 45433	
L. J. Obery	1
Eastern Air Lines, Inc. Miami International Airport Miami, FL 33148	
James E. McMillen	1
Delta Airlines Atlanta Airport Atlanta, GA 30320	
W. J. Overend	1
Gates Learjet Corporation P. O. Box 1280 Wichita, KS 67201	
Ronald D. Neal	1
National Aeronautics and Space Council Executive Office of the President Washington, DC 20502	
Richard D. Fitzsimmons	1
Department of Transportation Office of Secretary of Transportation Washington, DC 20590	
Lawrence P. Greene, Code TST-22	1

DISTRIBUTION LIST (Cont'd)

	Copies
Department of Transportation Joint DOT/NASA Noise Abatement Office Washington, DC 20590	
Louis J. Williams, Code TST-53	1
McDonnell-Douglas Corporation 3855 Lakewood Boulevard Long Beach, CA 90801	
Edward S. Rutowski	1
North American Rockwell Corporation 4300 East 5th Avenue Columbus, OH 43216	
Reid B. Lyford	1
William E. Palmer	1
Bell Aerospace Company Buffalo, NY 14240	
Alan Coles	1
LTV Aerospace Corporation Vought Missiles and Space Company 3221 North Armistead Avenue Hampton, VA 23366	
Charles W. Pearce	1
Northrop Corporation 1800 Century Park East Century City Los Angeles, CA 90067	
Sidney A. Powers	1
Joint DOT/NASA CARD Implementation Office 400 7th Street, SW Washington, DC 20590	
William N. Gardner, Code TST-31	1
Mr. S. M. Nehez Deputy for Development Planning Aeronautics System Division Directorate for General Purpose and Airlift Systems Planning (XRL) Wright-Patterson Air Force Base, OH 45433	1
Department of the Air Force AFSC Wright-Patterson Air Force Base, OH 45433	
Col. Francis J. McNamara, Jr.	1
Lt. Col. Alan M. Edwards Executive Office of the President National Aeronautics and Space Council Washington, DC 20502	1
Boeing Commercial Airplane Company A Division of The Boeing Company P. O. Box 3707 Seattle, WA 98124	
Glen W. Hanks, Advanced Transport Technology, MS: 4139	1
Lockheed-California Company Dept. 74-31 Plant 2, Bldg. 202 P. O. Box 551 Burbank, CA 91503	
T. Sedjwick	1
General Dynamics Corporation Convair Aerospace Division P. O. Box 748 Fort Worth, TX 76101	
A. J. K. Carline	1
Lockheed-Georgia Company 86 South Cobb Drive Marietta, GA 30060	
R. H. Lange, Zone 401, Dept. D/72-79	1

DISTRIBUTION LIST (Cont'd)

	Copies	Copies
Mr. C. J. Schueler, Chief Aerodynamics Division von Karman Gas Dynamics Facility Arnold Research Organization, Inc. Arnold Air Force Station, TN 37389	1	
NASA Scientific and Technical Information Facility P. O. Box 33 College Park, MD 20740		
Attn: Acquisitions Branch	10	